

Applications of Enzyme Induced Carbonate Precipitation (EICP) for Soil
Improvement

by

Nasser M. Hamdan

A Dissertation Presented in Partial Fulfillment
of the Requirements for the Degree
Doctor of Philosophy

Approved December 2014 by the
Graduate Supervisory Committee

Edward Kavazanjian Jr, Co-Chair
Bruce E. Rittmann, Co-Chair
Everett Shock

ARIZONA STATE UNIVERSITY

May 2015

ABSTRACT

In enzyme induced carbonate precipitation (EICP), calcium carbonate (CaCO_3) precipitation is catalyzed by plant-derived urease enzyme. In EICP, urea hydrolyzes into ammonia and inorganic carbon, altering geochemical conditions in a manner that promotes carbonate mineral precipitation. The calcium source in this process comes from calcium chloride (CaCl_2) in aqueous solution. Research work conducted for this dissertation has demonstrated that EICP can be employed for a variety of geotechnical purposes, including mass soil stabilization, columnar soil stabilization, and stabilization of erodible surficial soils. The research presented herein also shows that the optimal ratio of urea to CaCl_2 at ionic strengths of less than 1 molar is approximately 1.75:1. EICP solutions of very high initial ionic strength (i.e. 6 M) as well as high urea concentrations (> 2 M) resulted in enzyme precipitation (salting-out) which hindered carbonate precipitation. In addition, the production of NH_4^+ may also result in enzyme precipitation. However, enzyme precipitation appeared to be reversible to some extent. Mass soil stabilization was demonstrated via percolation and mix-and-compact methods using coarse silica sand (Ottawa 20-30) and medium-fine silica sand (F-60) to produce cemented soil specimens whose strength improvement correlated with CaCO_3 content, independent of the method employed to prepare the specimen. Columnar stabilization, i.e. creating columns of soil cemented by carbonate precipitation, using Ottawa 20-30, F-60, and native AZ soil was demonstrated at several scales beginning with small columns (102-mm diameter) and culminating in a 1-m^3 soil-filled box. Wind tunnel tests demonstrated that

surficial soil stabilization equivalent to that provided by thoroughly wetting the soil can be achieved through a topically-applied solution of CaCl_2 , urea, and the urease enzyme. The topically applied solution was shown to form an erosion-resistant CaCO_3 crust on fine sand and silty soils. Cementation of erodible surficial soils was also achieved via EICP by including a biodegradable hydrogel in the stabilization solution. A dilute hydrogel solution extended the time frame over which the precipitation reaction could occur and provided improved spatial control of the EICP solution.

ACKNOWLEDGMENTS

I am deeply grateful for the assistance and guidance provided by my committee members Dr. Edward Kavazanjian, Dr. Bruce Rittmann, and Dr. Everett Shock. Professor Kavazanjian has been instrumental to my success as a graduate student and I will always be indebted to him for his guidance and the knowledge he has imparted to me. In addition to his mentorship, Ed has become a good friend and I look forward to many more years of continued friendship. I would also like to thank Professor Rittmann for allowing me the opportunity to work and train in his laboratory. Professor Rittmann has provided me with guidance at critical junctures in my graduate career and I greatly appreciate all his efforts. I would also like to thank Professor Shock for his guidance and unique insights on all things geochemistry. In addition to being a great mentor, he has showed optimism and support throughout my graduate career.

I would like to thank my wife and best friend Abeer Hamdan, she has always been incredibly supportive and a source of unending happiness. I would also like to extend a special thanks to Brian Knorr and Jeff Fijalka for their excellent work and collaboration on various projects, their assistance was instrumental in various parts of this work. Sean O'Donnell and Angel Gutierrez have provided me great insight and have assisted on several projects, thank you. In addition, I am thankful for the technical assistance and use of ASU-NASA Planetary wind tunnel provided by Dr. David Williams and Amy Zink.

Last but not least, I would like to acknowledge support for this work that was funded by the Geomechanics and Geotechnical Systems, GeoEnvironmental

Engineering, and GeoHazards Mitigation program of the National Science Foundation (NSF) Division of Civil, Mechanical, and Manufacturing Innovation under grant number CMMI-1233658, "Collaborative Research: Enhancement of Vertical Elements for Foundation Support by Ureolytic Carbonate Precipitation". The author is whole-heartedly grateful for this support.

TABLE OF CONTENTS

	Page
LIST OF TABLES	x
LIST OF FIGURES	xii
CHAPTER	
1. INTRODUCTION	1
1.1 Background	1
1.2 Potential Applications of EICP	6
1.3 Scope of this Study.....	7
2. CARBONATE MINERAL PRECIPITATION FOR SOIL IMPROVEMENT.....	10
2.1 Introduction	10
2.2 Geochemical Basis for Carbonate Mineral Precipitation	12
2.3 Microbial Processes for Carbonate Mineral Precipitation	12
2.3.1 MICP Processes	13
2.3.2 Bacterial Ureolysis	15
2.4 Soil Improvement via MICP	16
2.5 Enzyme Induced Carbonate Precipitation	22
2.5.1 Introduction	22
2.5.2 Enzymes and the Urease Enzyme	25
2.5.3 Potential Advantages of EICP and Disadvantages of MICP.....	29
2.5.4 Potential Disadvantages to EICP	31

CHAPTER	Page
2.6 Summary and Conclusion	31
3. THE EFFECT OF INITIAL CHEMICAL CONDITIONS ON ENZYME INDUCED CARBONATE PRECIPITATION	33
3.1 Background	33
3.2 Methods	34
3.2.1 Test Tube Experiments.....	34
3.2.2 Chemical Analysis and Physical Characterization.....	39
3.3 Results and Discussion.....	42
3.3.1 The Effects of Initial Chemical Ratios and Initial Concentrations	42
3.4 Conclusion.....	77
4. THE EFFECT OF A STATIC SOIL ENVIRONMENT ON ENZYME INDUCED CARBONATE PRECIPITATION	81
4.1 Introduction.....	81
4.2 Methods.....	82
4.2.1 Soil Filled Acrylic Columns Set-up.....	85
4.2.2 Chemical Analysis and Physical Characterization.....	86
4.3 Results and Discussion.....	88
4.4 Conclusion.....	98
5. INFLUENCE OF SOIL TYPE AND PREPARATION METHOD ON CEMENTED SAND COLUMNS.....	100
5.1 Introduction.....	100

CHAPTER	Page
5.2 Set-up.....	101
5.2.1 Columns Improved by Percolation.....	101
5.2.2 Columns Improved by Mixing and Compacting.....	103
5.3 Treatment Methods.....	103
5.3.1 Mechanical Testing, Chemical Analysis and Physical Characterization.....	107
5.4 Results and Discussion.....	108
5.4.1 Percolation Type.....	108
5.4.2 Mix and Compact Type.....	116
5.5 Conclusion.....	119
6. COLUMNAR STABILIZATION USING EICP.....	122
6.1 Introduction.....	122
6.2 Set-up and Methods.....	123
6.2.1 Four-inch Diameter PVC Tubes.....	123
6.2.2 Five-gallon Bucket Tests.....	127
6.2.3 Large Soil Box Test (1 m ³).....	132
6.3 Results and Discussion.....	136
6.3.1 Four-inch Diameter PVC Tubes.....	136
6.3.2 Five-gallon Bucket Tests.....	140
6.3.3 Large Soil Box Test (1 m ³).....	144
6.4 Conclusion.....	149
7. SURFICIAL SOIL STABILIZATION USING EICP.....	153

CHAPTER	Page
7.1 Introduction.....	153
7.2 Methods.....	155
7.2.1 Soil Pan Set-up and Wind Tunnel Testing.....	155
7.2.2 Treatment Type, Application Method, and EICP Solution Formulation.....	160
7.2.3 Chemical Analysis and Physical Characterization.....	165
7.3 Results and Discussion.....	165
7.4 Conclusion.....	176
8. EICP WITH BIOMATERIALS.....	177
8.1 Introduction.....	177
8.2 Methods.....	179
8.2.1 Set-up.....	179
8.2.2 Sampling.....	183
8.2.3 Chemical Analysis and Physical Characterization.....	185
8.3 Results and Discussion.....	185
8.4 Conclusion.....	191
9. SUMMARY AND CONCLUSIONS.....	193
9.1 Overview.....	193
9.2 Summary.....	194
9.2.1 Chemical Ratios and Concentration Effects in Soil-less Test Tubes.....	194

CHAPTER	Page
9.2.2 Chemical Concentration Effects in Small Soil Filled Columns.....	196
9.2.3 Influence of Soil Type and Preparation Method on Cemented Sand Columns.....	198
9.2.4 Columnar Stabilization using EICP.....	201
9.2.5 Surficial Soil Stabilization.....	203
9.2.6 EICP in Biomaterials.....	207
9.3 Conclusions.....	208
9.4 Recommendations for Future Work.....	211
REFERENCES.....	214
 APPENDIX	
A- RELATIVE CONCENTRATIONS AND pH IN THE $\text{NH}_3\text{-NH}_4^+$ SYSTEM.....	222
B- SOIL PROPERTIES FOR OTTAWA F-60 SILICA SAND.....	225
C- SOIL PROPERTIES FOR OTTAWA 20-30 SILICA SAND.....	227

LIST OF TABLES

Table	Page
1. Chemical Compositions and Nomenclature for the Tests Conducted in 15-ml or 50-ml Test Tubes.....	36
2. Chemical Compositions of Control Tests.....	38
3. Qualitative Measures and General Observations from the L-series Tests.....	43
4. Qualitative Measures and General Observations from the H-series Tests.....	44
5. The Amounts of CaCO ₃ Precipitate Found in the L-series Experiments.....	48
6. The Amounts of CaCO ₃ Precipitate Found in the H-series Experiments.....	50
7. Summary of the Chemical Analysis Results for the L-series Tests.....	51
8. The L-series Nitrogen Balance in the NH ₃ -NH ₄ ⁺ System.....	52
9. Summary of the Chemical Analysis Results for the H-series Tests Containing.....	61
10. The H-series Nitrogen Balance in the NH ₃ -NH ₄ ⁺ System.....	65
11. Results Summary from the Tests (“HR”) Accounting for Protein Solubility.....	73
12. Concentrations, Test Type, and Numbering for the Sand-filled Columns.....	84
13. Results from Columns #1-15.....	89
14. Results from Unconfined Compressive Strength Testing and Acid Digestion of Mechanically Tested Specimens.....	91
15. Results of CaCO ₃ Quantification.....	94
16. Chemical Analysis Results from the Sand Column Tests.....	96
17. Summary of the Percolation Type Columns.....	106

Table	Page
18. Summary of the Mix and Compact Type Columns.....	107
19. Qualitative-general Observations for Percolation Acrylic Columns #1-3 and Triaxial Columns #1-3.....	109
20. Summary of Results from the Acid Digestion Tests for Percolation Acrylic Columns #1-3.....	111
21. Qualitative-general Observations for Mix-and-Compact Acrylic Columns #4-6.....	117
22. Results of UCS Testing and Acid Digestion for Acrylic Columns #4-5.....	118
23. pH Measurements of Pore and Head Fluid from the PVC Columns.....	140
24. Summary of pH Measurements from Head Fluid and the Pore Fluid.....	143
25. UCS Test Results of Five Cores from Bucket #2.....	144
26. Chemical Formulations for Type-1 Application (Pans #1-29).....	164
27. Chemical Formulations for Type-2 Application (Pans #30-56).....	164
28. Summary of the Chemical Formulations, Enzyme Activity (high/low), and Type of Hydrogel Used in the Soil Filled Paper Cups.....	182
29. Summary of the Chemical Formulations, Enzyme Activity (high/low), and Type of Hydrogel Used in the Soilless Filled Glass Beakers.....	183
30. Summary of the EICP Solution Penetration Depth, Crust Thickness, and the Perceived Hardness of the Crusts.....	189

LIST OF FIGURES

Figure	Page
1. Apparatus for Measuring CO ₂ Production via Acid Digestion of CO ₃ ²⁻ Minerals	41
2. Test Tubes Containing the Final Precipitate after Rinsing, Centrifugation, and Drying.....	45
3. Representative SEM Images of Calcite Crystals from Four Different L-series and H-series Test Tubes.....	47
4. Nitrogen Balance Plot in the NH ₃ -NH ₄ ⁺ System for the L-series.....	54
5. Net Increase in Alkalinity and the Final pH in Relation to Initial Ratios of Urea to CaCl ₂ for the L-series Tests.....	55
6. Comparison of the Net Alkalinity Increase and the General Trend in the Final pH in Relation to Initial Ratios of Urea to CaCl ₂ for the L-series Tests.....	59
7. Comparison of the Net Increases in Alkalinity and the Final pH in Relation to the Initial Ratios of Urea to CaCl ₂ for the H-series Tests.....	61
8. Urea Consumed and the Amount of Ca ²⁺ Precipitated Closely Follow in the H-series Tests.....	63
9. Nitrogen Balance Plot in the NH ₃ -NH ₄ ⁺ System for all H-series Tests.....	65
10. Relationship between Protein Solubility and the Ionic Strength of a Solution.....	69
11. Plot Demonstrating the Changes in Ionic Strength in the CaCl ₂ -NH ₄ ⁺ System.....	70

Figure	Page
12. Plots Comparing the Chemical Analysis Results from the Original H-series Tests and the (new) HR-series Tests.....	74
13. Sand-filled Acrylic Column before Adding the EICP Reaction Medium.....	86
14. Columns #1-2 (0.20 M) and #4 (0.5 M) before Extraction.....	90
15. Sand Column #2 before (left) and immediately after (right) UCS Testing.....	92
16. Percolation Acrylic Columns #1, #2 and #3.....	110
17. XRD Results from a Cemented Sand Sample.....	113
18. LV-SEM Images.....	113
19. p-q Plot Failure Envelopes for 20-30 Silica Sand.....	114
20. p-q Plot Failure Envelopes for F-60 Silica Sand.....	115
21. Triaxial sand Column #1 Standing without Support.....	116
22. SEM Images from Triaxial Sand Column #1.....	116
23. Acrylic Columns #4-5 Prior to and During UCS Testing.....	118
24. SEM Images from Mix-and-Compact Acrylic Column #4.....	119
25. PVC Injection Tube Used in the 19-L Bucket Experiments.....	128
26. Grain Size Distribution of Native AZ Soil.....	132
27. Soil-filled Box with Na-bentonite Seal around Injection Tube.....	135
28. Four-inch Diameter PVC Columns #1-3.....	137
29. CaCO ₃ Coating on and in-between Sand Grains in PVC Columns #1-3.....	139
30. Donut-shaped Cemented Soil Mass from Dry Bucket #2.....	141
31. Bulb-shaped Cemented Soil Masses from Wet Buckets #4-6.....	142
32. Soil Box after Disassembly.....	147

Figure	Page
33. SEM Images of CaCO ₃ and Particle Detachment Points from Soil Box.....	149
34. Grain Size Distribution for Native Sand.....	156
35. Grain Size Distribution for Mine Tailings Obtained from Southern AZ.....	156
36. Two Soil pans native Sand (left) and F-60 Sand (right) prior to Treatment.....	157
37. Wind Tunnel Stage Area.....	159
38. Treated Soil Pan Containing F-60 Silica Sand Loosely Covered in Plastic.....	161
39. Flowchart Summarizing the Soils Used and Application Type for the 56 Soil Pans.....	162
40. Type-1 Wind Tunnel Test Results of Native Sand, F-60 Soil and Mine Tailings.....	168
41. Type-2 Wind Tunnel Test Results of Native Sand, F-60 Soil and Mine Tailings.....	170
42. SEM Analysis of Type-2 EICP Treated F-60 Soils from Pan #32 and Pan #35 After Rinsing with DI Water.....	175
43. Paper Cups Cut Open Longitudinally to Provide a “Window” View of the Soil Profile.....	184
44. SEM Imaging of the Soil Crust Obtained from Cup #4 Using Xanthan-assisted EICP at High CaCl ₂ Concentration.....	191

CHAPTER 1

INTRODUCTION

1. Introduction

1.1 Background

This dissertation describes an investigation into the use of isolated urease enzyme and the hydrolysis of urea for ground improvement purposes. The urease and urea are combined in an aqueous solution with calcium chloride to induce the precipitation of calcium carbonate. The precipitated carbonate coats soil particles, cements soil particles together, and fills the void space between particles, thereby improving the mechanical properties of the soil. Ground improvement applications studied in this dissertation include columnar stabilization, mixing and compacting, and surficial soil stabilization. This dissertation also includes fundamental studies on the influence of chemical concentrations and chemical ratios on the EICP process.

Technological changes and advancements are driven by the needs and requirements of modern societies. The need to accommodate an ever-growing global population has taken center stage in many societies and has pushed human inventiveness to new levels. However, a rapidly growing global population has both increased the need for engineering technologies to improve the mechanical properties of the ground and has brought about concerns regarding the sustainability of engineering practices that rely heavily on energy intensive materials and techniques of the past. Sustainability concerns have

required new practices that have been drawn from advances in science and engineering.

One area of need that is taking on new practices is the development of civil infrastructure needed to accommodate expanding populations. In particular, civil infrastructure should be built on and within suitable ground that must reliably support it. Our search for suitable ground has become more challenging due to expanding populations move into previously undeveloped areas and into areas previously bypassed due to poor ground conditions. As a consequence of movement into these areas, engineers face new challenges in establishing suitable ground and developing environmentally sustainable approaches to make it suitable for civil infrastructure. Areas where seismic activity and geologic hazards affect ground conditions are of particular concern. Various techniques for ground improvement have been developed over the years to meet these challenges. Recently, efforts to develop new ground improvement techniques have focused on searching for sustainable methods to either supplement or replace conventional techniques while aspiring for lower costs with traditional practices.

Finding effective solutions to ground improvement challenges is becoming increasingly complex due to sustainability considerations. Established materials and methods often need to be either replaced or supplemented by innovative materials and environmentally-friendly practices to address sustainability considerations. One example of a nearly indispensable and common building material that poses significant sustainability concerns is

Portland cement. Portland cement is widely used in ground improvement applications. For example, direct treatment with Portland cement can be used in ground improvement applications where existing soils require strengthening through soil binding. Unfortunately, Portland cement production is extremely energy intensive and a major source of carbon dioxide (CO₂) emissions, as well as a significant source of sulfur and nitrogen oxides emissions. Cement production, most commonly Portland cement, accounts for the second largest source of global greenhouse gas emissions (18%) within the industry sector (World Resources Institute 2005). It is estimated that the cement industry is one of the top two manufacturing industries responsible for global CO₂ emissions constituting nearly 5% of the global CO₂ emissions (van Oss & Padovani 2003). Cement will mostly likely always be required for many construction projects. However, reductions in the use of Portland cement through either direct substitution or complementary use of environmentally-friendly methods and materials could contribute considerably towards meeting sustainability goals.

Microbially induced carbonate precipitation (MICP) has been explored as an alternative to Portland cement for ground improvement for well-over a decade (Whiffin 2004; DeJong et al. 2006; Karatas 2008; Kavazanjian and Karatas 2008; Dejong et al. 2010; van Paassen et al. 2010; Harkes et al. 2010; Chou et al. 2011; Burbank et al. 2012; Rebata-Landa & Santamarina 2012; He et al. 2013). Research suggests that cementation using MICP can address a number of important geotechnical problems in granular soils, including slope stability, erosion and scour, under-seepage of levees, the bearing capacity of

shallow foundations, tunneling, and seismic settlement and liquefaction (Kavazanjian and Karatas 2008; DeJong et al. 2010; Harkes et al. 2010; van Paassen et al. 2010). The MICP mechanism most often discussed in the literature and most advanced in terms of field application, hydrolysis of urea (or ureolytic hydrolysis), relies on microbes for the purpose of generating the urease enzyme, which then catalyzes the hydrolysis of urea for the carbonate precipitation reaction (DeJong et al. 2006; Whiffin et al. 2007; Chou et al. 2011; van Paassen et al. 2010).

The primary mechanism through which MICP attempts to create a cemented soil mass, improving strength and reducing compressibility, is by precipitating calcium carbonate from the pore fluid such that cementation bonds are formed at the interparticle contacts (Whiffin 2004; DeJong et al. 2006; van Paassen et al. 2010). Karatas et al. (2008) have identified several microbiological mechanisms for MICP, including hydrolysis of urea. Ureolytic MICP has typically been accomplished using a technique best described as biogrouting (Harkes et al. 2010; van Paassen et al. 2010), wherein bacteria and nutrients are mixed in a tank ex-situ and then injected into the soil followed by a fixation fluid to foster microbial attachment to soil particles and, finally, a calcium-laden cementation fluid. In this process, the enzyme urease (urea amidohydrolase) catalyzes the hydrolysis urea ($\text{CO}(\text{NH}_2)_2$) into carbon dioxide (CO_2) and ammonia (NH_3). In an aqueous solution, the CO_2 can speciate to carbonate. In the presence of calcium ions and a suitable pH, the carbonate precipitates as calcium carbonate.

Applications of the MICP technique on clean sands in both laboratory column tests and limited field tests have encountered practical difficulties, including bioplugging (permeability reduction accompanying the induced mineral precipitation) and generation of a toxic waste product (ammonium salt). Bioplugging not only limits the distribution of precipitation agents within the soil but also makes flushing of the waste product from the soil a difficult, energy intensive task. Furthermore, the microbes that produce the urease enzyme cannot readily penetrate the pores of soils smaller than fine sand, limiting the minimum grains size of soils amenable to MICP to clean medium-fine sands or coarser graded soils. Field application of this technology requires creating and maintaining the conditions required to cultivate urease producing microbes either in the ground or in an above-ground reactor of some sort. Due to these limitations, mass stabilization of soil using MICP can be challenging.

The use of plant-derived urease enzyme for ureolytic hydrolysis to induce CaCO_3 precipitation, or enzyme induced carbonate precipitation (EICP), eliminates the need for microbes in the CaCO_3 precipitation process. Since the EICP method does not consume or compete for the organic substrate (urea), EICP in itself is more efficient than processes that rely on microbial urease (i.e. ureolytic MICP). In addition to eliminating the need to nurture urease-producing microbes, EICP offers other advantages over ureolytic MICP. The small size (on the order of 12 nm) of the urease enzyme suggests that CaCO_3 precipitation by enzymatic ureolytic hydrolysis will be less susceptible to bio-

plugging and will be able to penetrate finer grained soils, perhaps into the silt-sized particle range, compared to MICP processes.

1.2 Potential Applications of EICP

Enzyme induced carbonate precipitation (EICP) potentially has the same applications as MICP over a wider range of soils due to the small size of the urease enzyme and water solubility of the EICP solution. These problems include slope stability, erosion and scour, under-seepage of levees, the bearing capacity of shallow foundations, tunneling in running or flowing ground, and seismic settlement and liquefaction. Research presented herein suggests that among the ground improvement techniques in which EICP can be employed to achieve these goals is formation of cemented columns of soil by infusing cementation solution through a perforated tube or pipe pushed into the ground. EICP-cemented columns can be installed in patterns similar to root piles (*pali radicii*) for slope stability, micro piles for foundation support, and stone columns or soil cement columns to support embankments and restrict lateral spreading in liquefiable soils. Furthermore, the ability to install EICP piles under existing structures without causing heave or settlement make them ideal for remediation of liquefaction potential beneath existing facilities. Columnar stabilization via EICP can also be employed through mix-and-compact methods.

Another area where EICP has potential applicability is for the surficial stabilization of soils against wind driven erosion in semi-arid to arid environments. Stabilization of erodible surficial soils, typically fine to medium grain soils, mitigates several important environmental and geotechnical

problems associated with soil erosion. In contrast to mass stabilization techniques, carbonate precipitation for surficial soil stabilization has received comparatively little attention in the literature.

Both EICP and microbially induced carbonate precipitation (MICP) can potentially be employed to stabilize erodible surficial soils. The rapid carbonate precipitation induced by the EICP process, in contrast to slower microbial methods, makes it well-suited for surface treatments that have a relatively short time frame within which they need to become effective. However, desiccation can limit the time an EICP reaction can proceed in semi-arid to arid environments and, thereby, reduce the efficiency of carbonate precipitation. Research presented herein also investigates the potential of EICP in a biodegradable hydrogel for rapid and efficient stabilization of surficial soils in rapidly desiccating environments. EICP applied in a hydrogel offers unique advantages that further improve efficiency by limiting the spatial extent of carbonate precipitation to the surface (or near surface) via the reduction of hydraulic conductivity associated with the ureolytic fluid. In addition, the hydrogel retains water (a necessary component of ureolysis) to extend the temporal frame of ureolysis, especially in semi-arid to arid environments, for greater substrate utilization and reaction time for carbonate precipitation.

1.3 Scope of this Study

Research on enzyme induced carbonate precipitation (EICP) presented herein is comprised of several components including:

- Chemical analysis of the EICP process in soil-less test tubes

- Enzyme solubility in an EICP solution at various initial concentrations
- Columnar stabilization of soil via EICP solution injection
- EICP in soil through mix-and-compact methods
- EICP for surficial stabilization of soils.

This thesis addresses these issues in the following manner:

- (a) Chapter 2 presents a review of the relevant literature on the applicability of carbonate mineral precipitation for soil improvement through MICP and EICP;
- (b) Chapter 3 present the results of an investigation into the chemical changes induced by the EICP process using soil-less test tubes and the impacts of the EICP solution on enzyme solubility;
- (c) Chapter 4 present the results of EICP experiments at various concentrations within soil-filled benchtop columns to evaluate the impact of soil on the EICP process;
- (d) Chapter 5 presents the results of EICP experiments performed in acrylic columns and membrane lined triaxial columns for mechanical testing and prepared by percolation of the EICP solution and the mix-and-compact method;
- (e) Chapter 6 presents the results of EICP experiments on columnar stabilization using a perforated tube;
- (f) Chapter 7 present the results of surficial stabilization of soils against wind erosion using EICP;

(g) Chapter 8 presents the results of preliminary experiments on hydrogel-assisted EICP for surficial stabilization of soils;

CHAPTER 2
CARBONATE MINERAL PRECIPITATION FOR SOIL
IMPROVEMENT

2. Carbonate Mineral Precipitation for Soil Improvement

2.1 Introduction

This dissertation studies the potential for improvement of the mechanical properties of granular soils using agriculturally derived urease enzyme. Recent research has demonstrated the potential for ground improvement through microbially induced carbonate precipitation (MICP) in granular soils (Whiffin 2004; DeJong et al. 2006; Karatas 2008; Kavazanjian and Karatas 2008; Dejong et al. 2010; Harkes et al. 2010; van Paassen et al. 2010; Chou et al. 2011; Hamdan et al. 2011; Burbank et al. 2012; Rebata-Landa & Santamarina 2012; He et al. 2013). The most frequently studied mechanism for MICP, hydrolysis of urea (ureolysis), relies on ureolytic microbes to produce membrane bound urease enzyme that catalyzes ureolysis. However, hydrolysis of urea can also be catalyzed using plant-derived urease, eliminating the need for microbes in the CaCO_3 precipitation process.

Carbonate precipitation may be able to help mitigate a number of serious geotechnical problems associated with cohesionless soils. Carbonate precipitation may be able to stabilize slopes, control soil erosion and scour, reduce under-seepage of levees and cut-off walls, increase the bearing capacity of shallow foundations, facilitate excavation and tunneling, and reduce the potential for earthquake-induced liquefaction and settlement (Whiffin 2004;

DeJong et al. 2006; Karatas 2008; Kavazanjian and Karatas 2008; Dejong et al. 2010; Harkes et al. 2010; van Paassen et al. 2010; Chou et al. 2011; Burbank et al. 2012). Due to its non-disruptive nature, carbonate precipitation is particularly attractive near or beneath existing structures, where traditional soil-improvement techniques are limited due to the ground deformations and/or high cost associated with these techniques. Furthermore, carbonate precipitation may reduce energy consumption and the generation of harmful emissions compared to conventional soil-improvement techniques.

In addition to eliminating the requirement to grow and sustain urease-producing microbes, plant-derived urease enzyme induced carbonate precipitation (EICP) offers several other advantages over ureolytic MICP. Applications of ureolytic MICP on clean sands in laboratory column tests and limited field tests have encountered significant practical difficulties, including biopugging (permeability reduction accompanying induced mineral precipitation via microbes), the production of ammonium (NH_4^+) waste product, and the added complexity of managing an on-site bioreactor prior to injection (van Paassen et al. 2008; Harkes et al. 2010). Biopugging limits the distribution of precipitation agents within the soil and also makes flushing of the NH_4^+ waste product from the soil (as employed by Harkes et. al, 2010) more difficult and more energy intensive. Furthermore, the microbes that contain the urease enzyme cannot readily penetrate the pores of soils smaller than medium to fine sand, limiting the minimum grain size of soils amenable to ureolytic MICP to clean fine sands or coarser graded soils. The small size of the urease

enzyme suggests that EICP will be less susceptible to bio-plugging, may be capable of forming uniformly shaped cemented soil columns, and will be able to penetrate finer grained soils, perhaps into the silt-sized particle range, compared to MICP processes. However, management of ammonium is a problem that must be dealt with whether ureolytic MICP or EICP is employed.

2.2 Geochemical Basis for Carbonate Mineral Precipitation

MICP and EICP both result in the formation of calcium-carbonate (CaCO_3) minerals, including calcite, that are common in the natural environment. Calcite is the most thermodynamically stable polymorph of CaCO_3 and the primary product in calcium carbonate rocks and cementing agents at or near the ground surface. Aragonite and vaterite are other less thermodynamically stable forms of CaCO_3 that may occur during EICP or MICP. The formation of aragonite is typically associated with marine environments where kinetic factors may favor the incorporation of Mg^{2+} ions in place of Ca^{2+} (calcium ions) in the carbonate lattice. Aragonite precipitation is also associated with biologically controlled processes such as those found in nearly all mollusk shells. Vaterite is a metastable phase of CaCO_3 that readily converts to the more stable phases, calcite or aragonite, in water at ambient conditions of temperature and pressure (approximately 25°C , 1 atm). The natural occurrence of vaterite is limited to extreme environments (temperature and pressure) and some biological tissues (Grasby 2003; Rodriguez-Navarro 2007). The thermodynamic stability of CaCO_3 polymorphs from most to least are: calcite, aragonite, vaterite.

2.3 Microbial Processes for Carbonate Mineral Precipitation

2.3.1 MICP Processes

Microbes can mediate the production of a wide variety of minerals in soils, including carbonates, oxides, phosphates, sulfides, and silicates (Fortin et al. 1997). In general, microbially *mediated* (or microbially induced) carbonate precipitation is distinctly different than biologically *controlled* carbonate precipitation. Whereas biologically controlled processes are tailored to form a particular polymorph, microbially mediated precipitation is an inorganic process in which microorganisms create the environment conducive to CaCO_3 precipitation without regard to a specific polymorph.

The complex interactions between microorganisms and minerals have been well documented by researchers attempting to understand the formation, dissolution, and alteration of minerals by microorganisms on geologic and engineering time scales (Ehrlich 2002; Karatas 2008; Phoenix and Konhauser 2008; Shock 2009). Bacteria in particular are associated with the formation of carbonate minerals and play a fundamental role in carbon cycling on the geologic timescale (Warthmann et al. 2000; Ehrlich 2002; Shock 2009). Many microbial processes can produce relatively strong geologic materials through carbonate minerals that result in inter-particle cementation. For example, caliche is a predominately calcium carbonate (CaCO_3) rock that can be formed by biological action (Dixon and McLaren 2009). Caliche can have an average uniaxial compressive strength of 12 MPa and an associated modulus of elasticity between 29-65 MPa (Zorlu and Kasapoglu 2009).

Carbonate precipitation is the most widely studied microbially mediated mineral precipitation phenomenon in soil. Many metabolic mechanisms create the essential geochemical conditions for carbonate precipitation by increasing the total carbonate content of the pore fluid, the pH, or both. For instance, anaerobic and aerobic oxidation of an organic compound results in production of carbon dioxide (CO₂) for the carbon fraction that is not incorporated into biomass. If the medium is a well-buffered alkaline environment, CO₂ acid-base speciation forms carbonate (CO₃²⁻), which can precipitate in the presence of a suitable cation, such as Ca²⁺.

A variety of microbial mechanisms can create the geochemical conditions for CO₃²⁻ precipitation. For instance, ureolysis (hydrolysis of urea) releases ammonia (NH₃), which protonates to NH₄⁺ and OH⁻, leading to an increase in pH: $\text{H}_2\text{O} + \text{NH}_3 \rightarrow \text{NH}_4^+ + \text{OH}^-$. However, ureolysis has an undesirable side effect, since NH₄⁺ is a water pollutant. A release of NH₃ can also occur during the microbial oxidation of a N-rich organic donor, resulting in the same adverse effect as ureolysis. Other metabolic pathways that produce OH⁻ are denitrification (dissimilatory reduction of nitrate) and sulfate reduction (Rittmann and McCarty, 2001).

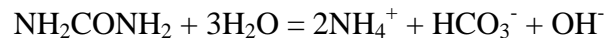
In principle, the geochemical conditions conducive to carbonate precipitation are not unique to any specific microorganism. Rather, carbonate precipitation can occur when carbonate forms in the vicinity of suitable cations under alkaline conditions, i.e., when a solution becomes supersaturated with respect to CaCO₃. MICP relies on the byproducts of bacterial metabolism (e.g.,

CO₂, alkalinity, and increased pH) to facilitate the formation of carbonate ions, which precipitate in the presence of divalent cations (e.g., Ca²⁺).

Candidate processes that can induce MICP include bacterial ureolysis, sulfate reduction, fermentation of fatty acids, and denitrification (Karatas 2008; Hamdan et al. 2011). Each of these processes produces a by-product and in three of four cases (bacterial ureolysis, sulfate reduction, fermentation of fatty acids) the by-product is undesirable (NH₃, H₂S, and CH₄, respectively). Only denitrification (dissimilatory reduction of nitrate) produces an end product (N₂) that does not have an undesirable side effect (Hamdan et al. 2011).

2.3.2 Bacterial Ureolysis

Bacterial ureolysis using *Sporosarcina pasteurii* is the most widely studied MICP process for ground improvement (Whiffin 2004; DeJong et al. 2006; van Paassen et al. 2008). Ureolysis, a form of ammonification (transformation of organic nitrogen into ammonia), produces ammonium (NH₄⁺), dissolved organic carbon in the form of bicarbonate (HCO₃⁻), and base (OH⁻) through the metabolism of urea (NH₂CONH₂), as illustrated in the reaction shown below.



Upon formation of a sufficiently saturated solution with respect to calcite, precipitation ensues and calcium carbonate is formed as shown in chemical reaction below.



The chemical reactions involved in bacterial ureolysis produce undesirable and potentially toxic end products: ammonia ($\text{NH}_{3(\text{g})}$) and ammonium (NH_4^+). Since ammonium speciation is highly pH dependent, the unionized form (NH_3) will be dominant in the elevated pH environment characteristic of bacterial ureolysis, but the dominant chemical species will rapidly shift to the ionized form (NH_4^+) with decreasing pH resulting from carbonate mineral precipitation.

The suppression of nitrifying organisms that produce acidic conditions via $\text{NH}_4^+ \rightarrow \text{NO}_3^-$ oxidation may be desirable in order to prevent the dissolution of carbonate mineral precipitation. A given fraction of ammonium may be converted to NO_3^- (nitrate) through bacterial nitrification, which may then be reduced to nitrogen gas (N_2) via bacterial denitrification in the presence of denitrifying bacteria with a suitable source of organic electron donor. But, it is unclear whether or not a substantial portion of NH_4^+ can be converted to nitrate in comparison to the amount produced since nitrifying bacteria are rate limited by the lack of subterranean dissolved oxygen. In addition, typical nitrifying organisms also experience severe inhibition at elevated ammonia concentrations (Anthonisen et al. 1976; Antoniou et al. 1990) and at high pH values (e.g. $\text{pH} > 9$) (Jones and Hood 1980; Antoniou et al. 1990; Ruiz et al 2003).

2.4 Soil Improvement via MICP

Whiffin (2004) studied the effects of MICP due to ureolysis on the physical properties of sands. Injecting an aerated solution of urea, calcium, and ureolytic bacteria into sand columns induced CaCO_3 precipitation that covered the sand particles and bridged inter-particle contacts. The compressional wave (P-wave) velocity of the sand columns increased with increasing concentration of hydrolyzed urea, an indication of an increase in soil cementation and shear strength. Whiffin (2004) subsequently performed triaxial shear strength tests on Dutch Koolschijn sand (sand grains are $<0.30\text{-mm}$ and contains some shale) injected with urea, calcium, and ureolytic bacteria. Whiffin (2004) reported that the shear strength increased by a factor of 8 and stiffness (secant modulus at 50% of peak shear stress) increased by a factor of 3.

Dejong et al. (2006) studied the effects multiple applications (flushes) of an aerated solution of urea, calcium, and ureolytic bacteria into sand columns filled with Ottawa 50-70 sand (a coarse silica sand). The shear wave velocity increased with the increasing number of flushes from approximately 180 m/s to 540 m/s after 10 flushes. Triaxial testing of the MICP improved sand columns showed a higher initial shear stiffness and higher ultimate shear capacity than untreated loose specimens.

Van Paassen et al. (2010) conducted a large-scale MICP test in a 100 m^3 ($8.0\text{m} \times 5.6\text{m} \times 2.5\text{m}$) concrete container filled with poorly graded fine to medium grained sand. Approximately 100-m^3 of an aerated solution of urea, calcium, and ureolytic bacteria was prepared ex-situ and flushed through the

soil using six wells, three each on opposite ends of the container (injection wells on one side, extraction wells on other side) over a 16 day period. The 100-m³ of solution was delivered using a sequential injection procedure to reduce clogging. Shear wave velocity increased by approximately three-fold in some areas of the cemented mass and unconfined compressive strengths of cored samples ranged from 0.7 MPa (12.6% CaCO₃ w/w) to 12.4 MPa (24.8% CaCO₃ w/w) depending on sampling location. Approximately 30-m³ of fresh water (approximately 2.3 pore volumes) was required to wash out the NH₄⁺ waste product from the soil mass at the conclusion of the experiment.

Chou et al. (2011) conducted direct shear tests on sand specimens subjected to treatment by growing, dormant (“resting”), and dead ureolytic bacterial cells prepared in well-mixed, stirred tank reactors. Treated specimens showed a peak shear strength that increased with increasing inoculum concentration, with a 13% increase from a solution containing 10³ colony forming units/ml and a 27% increase from a solution containing 10⁷ cfu/ml compared with the untreated sand at a normal stress 21 kPa. They found that microbial biomass, apart from CaCO₃ precipitation, provided small measurable increases in shear strength (i.e. friction angle) and that loose sand treated with bacteria exhibited dilatant behavior, presumably due to density increases resulting from both biomass and CaCO₃ precipitation. Significant bioclogging of the soil specimens was also observed in these tests.

Al Qabany et al. (2012) performed sand column experiments using medium coarse sands to assess the factors affecting the efficiency of MICP in

terms of calcium removal and distribution of CaCO_3 in a porous media. They found that for urea and CaCl_2 input rates below 0.042 Molar/h and at bacterial optical densities (OD_{600}) between 0.8 and 1.2, the reaction efficiency remained high for liquid medium input concentrations up to 1.0 M. However, they found that the precipitation patterns at the pore scale were affected by the liquid medium concentration. The use of lower chemical concentrations in the liquid medium resulted in better distribution of the CaCO_3 precipitate and less clogging than higher concentration mediums.

All the work on MICP discussed thus far involved bio-augmentation through the addition of externally grown ureolytic bacteria. Burbank et al. (2012) showed that native ureolytic bacteria could be enriched and stimulated to become viable for MICP in two alluvial sands obtained from the Snake River (Washington). An enrichment solution that contained one pore volume (each) of urea and CaCl_2 and 0.5% (v/v) molasses and 100 mM sodium acetate as additional carbon sources was used to stimulate ureolytic bacteria. After an enrichment period of four days, an additional 6.5 pore volumes of “biomineralization” solution that consisted of urea, CaCl_2 and 100 mM sodium acetate was delivered to the soils over 21 days. They found large increases in cone penetration tip resistance of MICP treated soils. The cone penetration results were used to infer an increase in the cyclic resistance ratio (cyclic stress ratio required to induce liquefaction) that were 2.6 times greater than the untreated soils for calcite precipitation in the range of 2.2% to 2.6% and 4.4 times greater for calcite precipitation between 3.8% to 7.4%. The researchers

also noted that the hydraulic conductivities were reduced in specimens with CaCO_3 contents greater than 4%, and that this may have resulted in the uneven distribution of CaCO_3 observed in these specimens.

Bang et al. (2009) studied the applicability of MICP for the surficial stabilization of soils against wind driven erosion, a major sustainability issue that is associated with air and water pollution. Bang et al. (2009) compared 3 biologically-based treatment options for surficial stabilization of cohesionless fine sand: (1) urease enzyme only, (2) enzyme mixed with ureolytic bacteria, and (3) ureolytic bacteria only. The outcome of the study was that the enzyme-only treatment produced the highest increase in strength and resistance to erosion. Meyer et al. (2011) used ureolytic bacteria for dust control and examined the effects of bacterial concentration, temperature and humidity, and the soil type (rinsed vs. unrinsed). They found that a higher fines content and higher temperature and humidity helped form a soil crust that resisted wind driven erosion. A study by Gomez et al. (2013) used ureolytic bacteria to stabilize loose overburden sands at a mine site in Canada. Although the researchers were able to successfully stabilize soil test plots, large quantities of nutrients were required and were delivered by 20 separate applications that spanned 20 days of treatment.

Construction Materials

The applicability of MICP has been investigated as a potentially sustainable method to produce bio-bricks (blocks formed using MICP to bind loose soil in a brick shaped mold) and related construction materials and to improve existing

construction materials (De Muynck et al. 2010; Dhami et al. 2012; Bernardi et al. 2014). De Muynck et al. (2008) presented an in-depth review of the current state-of-the-art of MICP in construction materials. They concluded, among other things, that MICP has many practical applications for the production of new construction materials and for the improvement of existing construction materials, e.g. sealing cracks in concrete, restorative plasters for statues, and protective coatings for erodible mortar surfaces. Dhami et al. (2012) used the ureolytic microorganism *Bacillus megaterium* to induce CaCO_3 precipitation for improving the properties of conventional fly ash bricks and rice husk ash bricks. The treated 228 mm x 107 mm x 169 mm bricks showed a 21% to 24 % increase in compressive strength, a significant reduction in water absorption, and better frost resistance. The improved bricks were treated by immersion in 20-L of MICP solution for four days and then topically treated for an additional four weeks.

Bernardi et al. (2014) used the ureolytic microbe *Sporosarcina pasteurii* to make bio-bricks from silica rich masonry sand. The bio-bricks showed increases in P-wave velocity, stiffness, strength, and CaCO_3 content with increasing number MICP treatments. Bio-bricks were treated for 28 days (84 treatments) by repeated percolation and reached strength values between 934 kPa to 2286 kPa with CaCO_3 contents of approximately 10% to 18%, with the higher strengths corresponding to higher CaCO_3 content. They authors note that their bio-bricks were comparable in strength and stiffness to bricks prepared using conventional cement and hydraulic lime additives.

2.5 Enzyme Induced Carbonate Precipitation (EICP)

2.5.1 Introduction

The chemical pathway of EICP is essentially the same as that for ureolytic MICP. Enzymatic ureolysis is catalyzed by the urease enzyme (EC 3.5.1.5) which hydrolyzes urea ($\text{CO}(\text{NH}_2)_2$) into carbon dioxide (CO_2) and ammonia (NH_3) as previously discussed. The use of plant-derived free urease enzymes for ureolysis offers several advantages over microbially bound enzymes. As previously noted the free enzymes eliminate the need for microbes and thereby increase the efficiency of ureolytic carbonate precipitation. The free enzyme is several orders of magnitude smaller than the typical ureolytic microbes and is not capable of producing biofilms or extra polymeric substances. This greatly reduces bioplugging (permeability reduction accompanying the induced mineral precipitation) and should extend the range of EICP applicability to finer grained soils. The water soluble free enzyme allows for greater flexibility in its method of application and potential uses.

The practical advantages of EICP afforded by the small water soluble free enzyme are bolstered by the ubiquity of the plant enzyme. The work discussed in this dissertation uses both high activity and low activity laboratory grade urease derived from the beans (embryo) of the Jack Bean plant. But urease is also found in the beans and seeds (embryos) of many other plants that span across several families of plants (Hogan et al. 1983; Jones & Mobley 1989; Hirayama et al. 2000; Das et al. 2002). In addition, leaf urease (also known as

“ubiquitous urease”) can be found in the leaves and litter of most plants including non-farmed vegetation.

The applicability of the urease enzyme for soil improvement purposes has received little attention in the literature. Whiffin (2004) compares the strength of CaCO₃ sand cemented using plant urease enzyme to sand cemented using a microbe with high urease activity. The results indicated that greater strength and penetration was attained in sands cemented using the enzyme than sand cemented using microbially mediated ureolysis. Whiffin concluded that the most likely reason for the difference was that lower enzyme activity yielding more effective cementation crystals.

Nemati and Voordouw (2003) and Nemati et al. (2005) compared the permeability profile reduction of porous soils treated using bacterially formed calcium carbonate and using enzyme only. The focus of these studies was on facilitating oil recovery using Jack Bean urease and ureolytic microbes to seal porous non-oil bearing formations in the borehole. These researchers noted that the free urease enzyme had greater activity than the ureolytic microbes used in their work and that increased applications of the enzyme and urea-CaCl₂ solution resulted in progressively greater decreases in permeability. Harris and McKay (2004) and Kotlar and Haavind (2005) discussed mineral precipitation in oil-bearing sediments and water reservoirs using isolated urease enzyme to control sand production and seal the bottom of the reservoir against leakage (respectively). Gustavsen et al. (2010) discuss the precipitation of calcite using the urease enzyme as a method to stabilize surficial soils against erosion. While

focusing on microbially mediated calcite precipitation, Van Meurs (2006) and Al-Thawadi (2011) noted that plant derived urease is capable of CaCO_3 precipitation.

Yasuhara and Kazayuki (2011) discussed the use of urease enzyme as a ground improvement method. Yasuhara et al. (2012) employed urease enzyme induced carbonate precipitation to cement soil in 50-mm x 100-mm molds and assessed its applicability to reduce soil permeability. Dry enzyme powder was mixed with dry Toyoura sand and then pluviated into a test column. The test column was then evacuated to facilitate saturation with an equimolar CaCl_2 -urea solution under a confining pressure of 50 kPa. No specific data was provided on the enzyme used or the enzyme activity. Depending on the column, four to eight additional treatments of CaCl_2 -urea were applied to each column. These treatments results in unconfined compressive strengths ranged from 400 kPa (CaCO_3 content $\approx 4\%$) to 1600 kPa (CaCO_3 content $\approx 5\%$). The columns were rinsed with distilled water prior to testing. The carbonate contents for these columns ranged from approximately 4% to 8% (500 kPa). The authors also noted a reduction in hydraulic conductivity by approximately an order of magnitude after four injections of CaCl_2 -urea solution.

Neupane et al. (2013a, 2013b) produced bulb-shaped cemented sand specimens approximately 84-mm in diameter by injecting a urea- CaCl_2 and enzyme solution into 100-mm x 200-mm dry, sand-filled PVC columns. Each of the columns received two treatments at 0.75 pore volumes each that was delivered over several hours through a bulb-shaped soil mesh attached to the

end of the injection tube. The columns were allowed to slowly drain through a porous stone at the bottom of the columns during the injections. A similar set of experiments were performed in steel drum containers that were 56 cm x 85 cm that received between one to four treatments per drum. Two major differences between the PVC column and steel drum experiments are that the steel drums were (1) aerated with CO₂ gas and (2) that the top of the drum was sealed with mortar. The authors did not address the potential of externally added CO₂ as source of inorganic carbon that may have contributed to CaCO₃. The carbonate contents and shear strengths were not reported.

2.5.2 Enzymes and the Urease Enzyme

Enzymes are highly selective biopolymeric macromolecules that catalyze chemical reactions without being consumed in the reactions. Enzymes have complex 3-dimensional structures based on chemical bonding and electrostatic interactions that can be reversibly or irreversibly altered (denatured) under certain environmental and chemical conditions. Enzymes have been described as the workhorses of all living organisms and are involved in nearly every biological process including chemical reactions, DNA synthesis, and metabolic reactions. The net effect of enzymes is to increase reaction rates. Enzymes accomplish this by lowering the activation energy of reactions between reactants and the transition state. Specifically, the difference in energy between the enzyme-substrate complex (ES) and the enzyme-transition state (EX) is lower than the difference between the substrate (S) and the uncatalyzed transition state (X). The *net* thermodynamic properties of chemical reactions

such as the change in Gibb's energy of the reaction (ΔG_r) are not affected by enzymes, although enzymes do lower the Gibb's energy of activation (i.e., the difference between S and X).

The catalytic power of enzymes lies in their ability to greatly alter reaction kinetics. For example, urea is spontaneously hydrolyzed in the absence of the urease enzyme at a rate of approximately 3×10^{-10} particles/sec (20°C) and is hydrolyzed at a rate of approximately 3×10^4 particles/sec (14 orders or magnitude faster) when the urease enzyme is present (Alberts et al. 2002).

There are a number of thermodynamic and chemical mechanisms that contribute to the catalytic power of enzymes. One of the major thermodynamic mechanisms is the decrease in entropy upon formation of the enzyme-substrate complex. The binding of a substrate to its enzyme results in the molecular organization of these two chemical units reducing their ability to freely interact within their chemical environments. A decrease in entropy results in a positive addition to ΔG , a thermodynamically unfavorable condition which promotes the destabilization of the ES complex to EX and thereby pushes the reactants to products, or decouples the ES complex. Desolvation is another mechanism that destabilizes the ES complex. Binding of a substrate removes its waters of hydration which can increase the enthalpy of solvation ($+\Delta H$) and make the substrate more reactive.

There are several chemical mechanisms that strongly affect the catalytic power of enzymes that include: (1) structural strain, (2) covalent catalysis, (3) general acid-base catalysis, and (4) metal ion catalysis. Structural strain is a

common destabilization mechanism that induces bond strain in the substrate, the enzyme, or both. Covalent catalysis is the formation of covalent bonds between the enzyme and the substrate and is typically driven by a nucleophilic attack of the enzyme by the substrate. General acid-base catalysis is common to nearly all enzyme reactions and can mediate the formation of the ES complex, drive covalent catalysis, and induce structural strains. Metal ion catalysis is especially important to the metalloenzyme urease that requires two Ni atoms to stabilize the enzyme's native state. Metal ions serve as electrophilic centers that activate the substrate by stabilizing increased electron density during a reaction and also assist in coordinating the ES complex.

The urease enzyme (urea amidohydrolase) is a widely occurring protein found in many microorganisms, higher order plants and some invertebrates. Urease is a nickel-dependent metalloenzyme with a molecular weight of approximately 590kDa +/- 30kDa for the Jack Bean variety (Dixon et al. 1980). The urease enzyme is a hexameric protein that is approximately 12 nanometers by 12 nanometers (Blakely & Zerner 1984). The best known and most studied urease enzyme is that extracted from the jack-bean (*Canavalia ensiformis*) plant (Jones & Mobley 1989; Jabri et al. 1992). The jack-bean plant is a commonly occurring drought-resistant legume of the Fabaceae (or Leguminosae) family. Plant derived urease is not unique to the jack bean, it is synthesized by many plants including the pigeonpea (*Cajanus cajan* L.). Several families of common plants including Fabaceae (beans), Cucurbitaceae (melons and squash e.g.) and

Pinaceae (pine family) are very rich in urease (Kayastha & Das 1999; Das et al. 2002).

Urease is also found in the leaves of some plants listed above and many more including some non-farmed plants common to semi-arid environments such as the *Callistemon viminalis* (weeping bottlebrush) (Hirayama et al. 1983; Hogan et al. 1983). Hogan et al. (1983) showed that simply chopping the leaves of several urease containing plants, rather than chemically extracting the enzyme, was sufficient to induce urease activity in urea solutions. Recent preliminary work by the author of this dissertation (unpublished) using coarsely chopped leaves from *Parkinsonia florida* (palo verde, Fabaceae family) indicates that urease is present in the leaves of this drought resistant tree common to U.S. Southwest. In addition to their broad availability, extraction of the urease enzyme from some crops has been shown to be very simple requiring only basic laboratory equipment (Kayastha & Das, 1999; Srivastava et al, 2001). The fruits, seeds, and beans of most urease containing plants can be readily obtained from local markets and the enzyme can then be isolated following well-established protocol. The leaves of urease containing plants can be obtained as plant litter and enzyme extraction may be pursued through several methods including crude and inexpensive leaf extractions methods. The enzyme can also be acquired from laboratory suppliers since urease has many uses including biomedical applications.

Hydrolysis of urea via urease is initiated by a nucleophilic attack by the urea carbonyl oxygen atom on one of the two nickel atoms in the urease active

site (Blakeley and Zerner 1984). Urea is further coordinated through hydrogen-bonding interactions that result in binding of one of the urea amino groups with the other Ni atom. Once urea is firmly coordinated in the enzyme active site, conformational changes result in acid-base reactions between certain amino acid residues and urea that form and stabilize a carbon tetrahedral intermediate. In this transition state, the central carbon atom is bonded to two amino groups, the original carbonyl oxygen, and a hydroxide ligand coordinated with one of the enzyme nickels (Benini et al. 1999; Zambelli et al. 2011). Other urease amino acid residues initiate acid-base reactions with one of the amino groups bonded to the tetrahedral intermediate resulting in the release of NH_3 which weakens the urea-urease coordination and releases a carbamate group (NH_2COO^-) from its coordination with Ni, which then decomposes to CO_2 and another NH_3 (Blakeley and Zerner 1984).

2.5.3 Potential Advantages of EICP and Disadvantages of MICP

It is well-established that urease can occur as both an intra- and extra-cellular enzyme (Ciurli et al. 1996; Marzadori et al. 1998). Free soil urease (i.e. urease not bound to a living organism) readily occurs apart from the host microorganism and is generally derived from dead and decaying microorganisms and from plant sources. A major consequence of absorptive association of free soil urease with soil particles is that the absorbed urease can persist for very long periods of time without proteolytic degradation or loss of function (Pettit et al. 1976). In fact, the longevity of urease-soil colloids is of significant agricultural importance in nitrogen regulation to plants provided via

urea fertilization (Pettit et al. 1976; Krogmeier et al. 1989; Ciurli et al. 1996). By contrast, exogenously added urease, as a free enzyme, has a limited lifespan as its activity and function decrease with time (Pettit et al. 1976; Marzadori et al. 1998). A potential advantage to short-lived urease activity may be in engineering applications where a desired goal may be achieved over a limited time, after which the enzyme naturally degrades thereby eliminating long term impacts to the ecosystem.

The small size of a solubilized urease enzyme affords it a distinct advantage over microbial urease for engineering applications that require penetration into very small pore spaces, e.g. in finer-grained soils. Nearly all known bacteria are greater than 300 nm in diameter, with the majority in the range of 500-5000 nm, limiting their ability to penetrate soils finer than fine sand and facilitating bioclogging. The free urease enzyme is water soluble and, therefore, is expected to reach any space that water based solutions can penetrate. Another potential advantage of using urease enzyme for CaCO_3 precipitation, in contrast to slower microbial methods, is that carbonate precipitation induced by the free enzyme is rapid (since ureolysis begins immediately upon contact of the enzyme with urea), which makes it well-suited for applications where rapid desiccation of the cementation solution is a concern. Furthermore, unlike MICP, the free enzyme method does not consume or compete for the organic substrate (urea) and therefore is more efficient with respect to utilization of the urea than similar processes that rely on microbial urease. In addition, although ureolytic microbes are common in many natural

soils, most current MICP studies have relied on bio-augmentation (i.e., introduction of microbes grown ex-situ) to achieve soil stabilization goals, and the effectiveness of bio-augmentation in highly processed mined soils (i.e, mine tailings) is uncertain.

2.5.4 Potential Disadvantages to EICP

Disadvantages of using free enzyme rather than microbial urease include that the use of the free enzyme does not provide nucleation points on the soil surface for CaCO₃ precipitation. In the microbially-mediated approach, the microbes typically attached themselves to the soil particle surface and may provide nucleation points for mineral precipitation. Furthermore, the rapid precipitation of carbonate minerals induced by free urease enzyme may be a disadvantage in that it leads to smaller and less-structured (more amorphous) crystals and may hinder penetration into the soil in some cases. Other disadvantages of using the free enzyme include the higher cost of procuring the free enzyme and solubility limitations in high ionic strength mediums.

2.6 Summary and Conclusion

Recent research has demonstrated the potential for ground improvement through carbonate precipitation. Almost all of the work to date has employed microbially induced carbonate precipitation (MICP). However, carbonate precipitation for ground improvement can also be accomplished by enzyme induced carbonate precipitation (EICP). EICP uses plant derived urease enzyme to induce carbonate precipitation without the need for microbes.

Laboratory tests have shown that significant increases in soil strength and stiffness can be obtained using MICP. MICP has been employed for mass stabilization in a large (100-m³) container test. MICP has been used to form bricks of cemented sand for potential applications related to construction materials. Both MICP and EICP have been used for the surficial stabilization of soil against wind erosion.

The use of plant-derived free urease enzymes for ureolysis has several advantages over microbially bound enzymes. The free enzymes eliminate the need for microbes and thereby increase the efficiency of ureolytic carbonate precipitation. The free enzyme is several orders of magnitude smaller than ureolytic microbes and is not capable of producing biofilms or extra polymeric substances. This greatly reduces biopugging and should extend the range of EICP applicability to finer grained soils. EICP uses a water based solution that allows for greater flexibility in its method of application and potential uses. However, both MICP and EICP via ureolysis must deal with management of the ammonium by product of the chemical reaction.

CHAPTER 3

THE EFFECT OF INITIAL CHEMICAL CONDITIONS ON ENZYME INDUCED CARBONATE PRECIPITATION

3.1 Background

This chapter presents experiments performed in closed 15-ml and 50-ml test tubes without soil to assess the impacts on the EICP process of (1) the initial ratios of urea to CaCl_2 , (2) the initial concentrations of urea and CaCl_2 , and use the knowledge gained from these experiments to (3) estimate a “benchmark range” of urea to CaCl_2 ratio for use in EICP. Understanding the geochemical changes induced by the EICP process is one of the first steps in assessing the potential uses of EICP for geotechnical purposes.

The primary geochemical changes associated with the EICP process include increases in pH, alkalinity, and inorganic carbon. Ideally, the EICP process should yield sufficiently large increases in pH and alkalinity in order to shift carbonate equilibria from CO_2 to HCO_3^- to CO_3^{2-} and then precipitate CaCO_3 in the presence of Ca^{2+} . But, the precipitation of CaCO_3 has the effect of reducing both pH and alkalinity, while simultaneously removing inorganic carbon and Ca^{2+} from solution (necessary components for CaCO_3 precipitation), which inhibits sustained precipitation of CaCO_3 . CaCO_3 precipitation cannot occur without sufficiently high pH and alkalinity. However, decreasing amounts of inorganic carbon and Ca^{2+} in an actively precipitating system will require even higher pH and alkalinity to reach CaCO_3 saturation (and thus induce precipitation).

The geochemical changes associated with the EICP process are dynamic and reflect interdependent changes in the chemical constituents involved. One question that may arise in trying to better understand these interdependent changes is related to the impact of the initial chemical conditions on CaCO_3 precipitation. More specifically, what effect, if any, do the initial *ratios* of the chemical constituents used in the EICP process have on net changes in pH, alkalinity, carbon and nitrogen balance, Ca^{2+} , and CaCO_3 precipitation? Also, *if* the differences in initial chemical constituent ratios are found to have an effect on the EICP process, one may ask whether or not these differences hold at different initial concentrations (e.g., high vs. low) since the amount of CaCO_3 precipitation desired (and rate of formation) may be concentration specific. So, an important question is what effect(s) do initial chemical *concentrations* have on the EICP process? A final question is whether it possible to establish a “benchmark range” of the urea to CaCl_2 ratio that induces a substantial rise in pH and sufficiently buffers the EICP system against rapid declines in pH during CaCO_3 precipitation?

3.2 Methods

3.2.1 Test Tube Experiments

The following experiments were conducted to evaluate the effects of initial chemical conditions on the EICP process: (1) the effects of the *initial ratio* of urea to CaCl_2 and (2) the effects of the *initial concentrations* of urea. All tests were performed in sterile Falcon brand 15-ml (or 50-ml) polypropylene (PP) test tubes. The clear, conical style test tubes were approximately 12 mm ID x

120 mm long with screw-caps (or 30 mm x 115 mm for 50-ml tubes). The reagents that were used in these experiments are as follows: reagent grade urea (Sigma Aldrich, $\geq 99\%$), reagent grade $\text{CaCl}_2 \cdot 2\text{H}_2\text{O}$ (Sigma Aldrich, $\geq 99\%$), urease enzyme (Sigma Aldrich Type-III lyophilized powder, Jack Bean Urease, specific average activity = 32,400 units/g), stabilizer (nonfat dry milk), and stock solutions of 0.5 M NaOH and 0.5 M HCl.

Two series of tests were performed: (1) a low concentration series designated the “L-series,” and a high concentration series designated the “H-series.” Within each test series (L and H), five different initial chemical ratios were employed, starting from a minimum urea to CaCl_2 ratio of 1:2 and then gradually increasing this ratio to a maximum value of 3:1 (urea to CaCl_2). The highest initial chemical concentration in the L-series tests had a maximum urea and $\text{CaCl}_2 \cdot 2\text{H}_2\text{O}$ concentration of 0.60 M and 0.20 M (respectively), and a lowest concentration of 0.10 M and 0.20 M (respectively). The highest initial chemical concentration in the H-series tests had a maximum urea and $\text{CaCl}_2 \cdot 2\text{H}_2\text{O}$ concentration of 6.0 M and 2.0 M (respectively), and a lowest concentration of 1.0 M and 2.0 M (respectively).

Table 1 presents the Urea- CaCl_2 concentrations employed in the L and H series tests. Within each of the two test series, each unique chemical ratio was given a number between 1 and 5. The minimum urea to CaCl_2 ratio (1:2) was designated number “1” and maximum ratio (3:1) was designated number “5;” for example, the test tube with the minimum chemical ratio in the “L” series

was identified as “1L” (“1H” in the “H” series), while the maximum ratio was “5L” (“5H” in “H” series).

Table 1 Chemical compositions and nomenclature for the tests conducted in 15-ml or 50-ml test tubes. High concentration is defined as the “H-series” and low concentration is the “L-series.” Note that CaCl_2 concentrations are fixed at either 0.20 M for the L-series or 2.0 M for the H-series. All tests were conducted in triplicate.

	Test Tube Set	Urea (M)	CaCl_2 (M)	Initial Ratio (Urea:CaCl_2)	Initial pH
L-Series (“L”)	1L	0.10	0.20	1:2	8.0
	2L	0.20	0.20	1:1	8.0
	3L	0.30	0.20	1.5:1	8.0
	4L	0.40	0.20	2:1	8.0
	5L	0.60	0.20	3:1	8.0
H-Series (“H”)	1H	1.00	2.0	1:2	8.0
	2H	2.00	2.0	1:1	8.0
	3H	3.00	2.0	1.5:1	8.0
	4H	4.00	2.0	2:1	8.0
	5H	6.00	2.0	3:1	8.0

Solutions containing the ratios and concentrations of urea and $\text{CaCl}_2 \cdot 2\text{H}_2\text{O}$ indicated in Table 1 were prepared in sterile 50-ml PP test tubes using Nanopure deionized (DI) water (18.2 $\text{M}\Omega \cdot \text{cm}$). The urea and $\text{CaCl}_2 \cdot 2\text{H}_2\text{O}$ solutions in the 50-ml tubes were adjusted to an initial pH of approximately 8.0. Ten milliliters (10-ml) of the urea- CaCl_2 solution was then transferred from the 50-ml PP tubes to the appropriate 15-ml PP test tube set. All tests were conducted in triplicates, which left approximately 20-ml of urea- CaCl_2 solution in the 50-ml test tubes. The remaining fluid in the 50-ml test

tubes was sampled to determine initial values of (1) total alkalinity, (2) ion concentrations, and (3) carbon profile (i.e., organic, inorganic, total).

A concentrated urease enzyme solution was prepared using 1.51 g of enzyme powder and 0.82 g of stabilizer in 200-ml of 18.2 MΩ of sterilized DI water at pH≈7.0 (enzyme rate = 7.55g/L) in a sterile 250-ml glass bottle. Fluid samples of the enzyme solution were analyzed for initial values of total alkalinity and ion concentrations. The enzyme solution was stored in a refrigerator until the start of the experiment (approximately 12-hours), but was allowed to reach room temperature before use.

The 15-ml test tube experiments were started by adding 0.666-ml of enzyme solution to each test tube using an adjustable 1000-μL single channel Eppendorf pipette. Enzyme solution was added to one test tube at a time, and each test tube was then immediately capped, gently shaken and inverted, and allowed to stand for approximately 9 days at room temperature. The total volume in each test tube was approximately 10.67-ml and was composed of 10-ml of urea-CaCl₂ solution plus 0.666-mL of urease solution, equating to 0.47 g/L of enzyme per test tube. The test tubes were gently shaken and inverted once more on day 5, but were otherwise undisturbed during the 9 days.

Controls were also set-up using the same reagents, equipment, and procedures as for the tests described above. The following controls were set-up: (1) 10-mL solution containing 0.20 M each urea and CaCl₂ (identical to the “2L” test tubes) with 0.666-μL sterile DI water added instead of enzyme solution (no enzyme added); (2) 10-mL solution containing 2.0 M each urea and

CaCl₂ (identical to the “2H” test tubes) with 0.666-μL sterile DI water (no enzyme added); (3) 10-mL sterile DI water with 0.666-μL of enzyme solution.

The details pertaining to the control experiments are presented in Table 2.

Table 2 Chemical compositions of control tests. Chemical ratios and concentrations are identical to the “2L-series” and “2H-series” tests. All controls were done in duplicate.

Control Test Tubes	Urea (M)	CaCl₂ (M)	Initial Ratio (Urea:CaCl₂)	Enzyme Added
2L-C	0.20	0.20	1:1	No
2H-C	2.0	2.0	1:1	No
Water +Enzyme	0	0	n/a	Yes

After 9 days, the experiment was terminated by opening the test tubes (including the control test tubes) and drawing nearly the entire fluid volume (approximately 9-mL) using different sterile syringes and needles for each test tube. The test tubes were opened and sampled one-at-time. Test tubes were also qualitatively assessed for the presence of ammonia by carefully wafting and smelling the headspace gases in the test tubes. The fluid samples were filtered through sterile 0.2-μm syringe filters (Pall Acrodisc) into sterile 50-mL PP test tubes and were then immediately tested for pH and alkalinity. The pH probe was alcohol sterilized (70% EtOH v/v) and rinsed between samplings. The 50-ml test tubes were transferred to a freezer (-20°C) immediately after pH and alkalinity measurements were taken to prevent any further potential reaction by the urease enzyme. The low temperature in the freezer should have denatured the enzyme and prevent further (potential) ureolysis if urea was present. The test tubes remained in the freezer until further chemical analysis was performed

several days later. The control test tubes were treated in the same manner upon termination of the experiment.

3.2.2 Chemical Analysis and Physical Characterization

Total alkalinity was determined by HACH colorimetric Method 10239 (TNT plus 870, range 25-400 mg/L as CaCO₃) using a HACH DR-2800 spectrophotometer. Fluid samples that initially tested outside the total alkalinity detection range (25-400 mg/L) were diluted with 18.2 MΩ DI water and retested (the total alkalinity of 18.2 MΩ DI water was approximately 0 mg/L CaCO₃). Final alkalinity dilutions ranged from 0 to 100-fold and were performed 2-3 times for specimens that initially tested outside of the detection range to assess repeatability. Chemical analysis of ions was performed through ion chromatography (IC) using a Dionex ICS-3000. Standard ICS-3000 operating procedures were followed for all ion analyses. Anion and cation calibration standards were made using Dionex 7-Anion and Dionex 6-Cation IC standards. Nanopure DI water was used in all dilutions and for any case where water was required for testing. A typical batch run included the following: 2 DI water blanks to make sure the column was clean before starting; 5 standards (cation or anion) from lowest to highest concentration; test samples; test sample of known concentration (check standard); and an additional DI water blank every 3-4 test samples.

IC analysis depends on alternating pH conditions between the ion column, suppressor, and detector. It is generally recognized that IC analysis of NH₄⁺ can be misleading since NH₃-NH₄⁺ speciation is highly pH dependent and

is subject to alternating pH conditions (Dionex Application Note 141, 2001; Shimadzu Lab Note 42). In general, NH_4^+ analysis via IC is non-linear, especially at low concentrations. Nitrogen-ammonium (N-NH_4^+) detection and quantification is especially important for the work described in this dissertation, therefore additional IC analyses were required for more accurate detection and quantification due to the complex nature of NH_4^+ analysis via IC. The details of the additional IC analysis are not presented here, but generally involve testing regimes to develop a basic 2 part calibration curve: (1) a nonlinear section and (2) a mostly linear section. The final NH_4^+ results presented here are considered to be good estimates with some variability.

The chemical carbon profile was determined via a Shimadzu TOC-V Series Total Organic Carbon Analyzer. A typical batch run included the following: 2 DI water blanks before starting; test samples; test sample of known concentration (check standard); and a DI water blank every 4 test samples. A standard calibration curve was established and used for the analyses of unknown specimens.

Wet laboratory techniques were used to confirm the presence of precipitated carbonate minerals in specific test tubes at the end of testing. Acidification with warm 1 M HCl acid was employed to test for carbonate minerals. A small amount of precipitate from test tube replicate #2 was taken from each set of three test tubes and subject to acidification. As a result of this procedure, replicate #2 in each set of test tubes could not be used for CaCO_3 quantification. Quantification of CaCO_3 for the remaining, undigested

specimens, replicates #1 and #3, was performed via the gasometric method using a small, clear chamber that measures CO₂ gas pressure generated from carbonate dissolution. Essentially, gas pressure is correlated to CaCO₃ content through a 5-point calibration curve that is established using known amounts of a CaCO₃ standard and associated gas pressures measured upon dissolution of the standard. The apparatus is shown in Figure 1 and the quantification method is detailed in ASTM D4373. The ASTM procedure was followed as much as possible with the following exceptions: two water-filled sealed 50-ml PP vials were placed in the chamber during calibration and testing to reduce the internal volume for (a) better resolution and (b) higher sensitivity.



Figure 1 Apparatus for measuring CO₂ production via acid digestion of CO₃²⁻ minerals.

Electron microscopy and X-ray diffraction were used for analysis and characterization of the unused portion of the precipitate from test tube replicate #2. A PANalytical Powder X-Ray Diffractometer (XRD) was used to determine the mineral phase. Samples were ground in an agate mortar & pestle

and powdered coated onto a standard glass slide. A FEI/Philips XL-30 Field Emission Environmental Scanning Electron Microscope (ESEM) was used to investigate morphological features on coated (gold-palladium, 50-50) pieces of the precipitate.

3.3 Results and Discussion

3.3.1 The Effects of Initial Chemical Ratios and Initial Concentrations

General Observations and Morphology

Experiments were performed in closed 15-ml test tubes without soil to assess the impacts on the EICP process of (1) the *initial ratios* of urea to CaCl_2 and (2) the *initial concentrations* of urea and CaCl_2 . The results of subjective, qualitative measures of NH_3 gas and direct observations of the mineral precipitates are presented in Tables 3 and 4. All test tubes in the low concentration series (“L-series”) experiments contained CaCO_3 precipitate, while all except for the highest concentration test tube (“5H”) in the “H-series” contained CaCO_3 . The CaCO_3 precipitates formed in the L-series tests had different textural characteristics than the H-series. The L-series precipitates were generally loose with a granular texture, while the H-series precipitates were compact with solid intact pieces that required significant effort to dislodge from the test tubes (except that precipitate did not form in set “5H”). The directly observable textural characteristics of the CaCO_3 precipitate (e.g., firmness and texture) seemed to be independent of initial ratio of urea to CaCl_2 in both L-series and H-series tests, since the characteristics were approximately same *within each series*.

Table 3 Qualitative measures and general observations from the L-series tests. The amount of NH₃ was based on odor strength and subjectively assessed as follows: - - = no odor detected, + = faint, ++ = strong, +++ = very strong, ++++ = extremely strong.

Qualitative-General Observations				
0.20 M CaCl₂-dihydrate				
Test Tube	NH ₃ Odor	Mineral Precipitate		
		Present	Formation	Features
1L-1	--	Yes	slow, 2-3 days	Loose, granular
1L-2	--	Yes	slow, 2-3 days	Loose, granular
1L-3	--	Yes	slow, 2-3 days	Loose, granular
2L-1	+	Yes	slow, 1-2 days	Loose, granular
2L-2	+	Yes	slow, 1-2 days	Loose, granular
2L-3	+	Yes	slow, 1-2 days	Loose, granular
3L-1	++	Yes	slow, 1-2 days	Loose, granular
3L-2	++	Yes	slow, 1-2 days	Loose, granular
3L-3	++	Yes	slow, 1-2 days	Loose, granular
4L-1	+++	Yes	med., 1-2 days	Loose, granular
4L-2	+++	Yes	med., 1-2 days	Loose, granular
4L-3	+++	Yes	med., 1-2 days	Loose, granular
5L-1	++++	Yes	med., 1-2 days	Loose, granular
5L-2	++++	Yes	med., 1-2 days	Loose, granular
5L-3	++++	Yes	med., 1-2 days	Loose, granular

The test tubes were also monitored for precipitate “formation” several times per day in the first week through direct visual observation. It should be noted that the subjective non-quantitative visual estimation of precipitate “formation,” as used here, is not the same as precipitation rate, a well-defined chemical-quantitative measure of CaCO₃ production with time. The observed precipitate formation varied markedly in the L-series tests, as described in Table 4. The formation of precipitation was slowest in set “1L,” requiring 2-3 days before a visible white precipitate collected at the bottom of the test tubes, while sets “2L,” “3L,” “4L,” and “5L” produced precipitates within the first 1-2 days. It should be noted that the *absence* of an obvious white precipitate does not

mean that active mineral precipitation was not occurring in the EICP solution. Rather, the absence of visible precipitate only means that it was not immediately detectable through visual observation. Representative test tubes (one from each set) containing the final rinsed, centrifuged, and dried precipitates are shown in Figure 2.

Table 4 Qualitative measures and general observations from the H-series tests. The amount of NH₃ was based on odor strength and subjectively assessed as follows: - - = no odor detected, + = faint, ++ = strong, +++ = very strong, ++++ = extremely strong.

Qualitative-General Observations				
2.0 M CaCl₂-dihydrate				
Test Tube	NH ₃ Odor	Mineral Precipitate		
		Present	Formation	Features
1H-1	--	Yes	Very fast, 1 day	Compact, solid
1H-2	--	Yes	Very fast, 1 day	Compact, solid
1H-3	--	Yes	Very fast, 1 day	Compact, solid
2H-1	--	Yes	Very fast, 1 day	Compact, solid
2H-2	--	Yes	Very fast, 1 day	Compact, solid
2H-3	--	Yes	Very fast, 1 day	Compact, solid
3H-1	--	Yes	Very fast, 1 day	Compact, solid
3H-2	--	Yes	Very fast, 1 day	Compact, solid
3H-3	--	Yes	Very fast, 1 day	Compact, solid
4H-1	--	Yes	Very fast, 1 day	Semi-compact, solid
4H-2	--	Yes	Very fast, 1 day	Semi-compact, solid
4H-3	--	Yes	Very fast, 1 day	Semi-compact, solid
5H-1	--	No	n/a	n/a
5H-2	--	No	n/a	n/a
5H-3	--	No	n/a	n/a

Precipitate formation in the H-series tests, described in Table 4, was different than the L-series. With the exception of set “5L” that did not form CaCO₃, the rate of precipitation was fast in all the test tubes and was visible on the same day the experiments were started. Indeed, precipitation was so rapid that small pieces of CaCO₃ grew on the inside walls of the test tubes as illustrated in

Figure 2. Although unconfirmed by quantitative testing, it appeared that the white precipitates which collected at the bottom of the test tubes reached their maximum (and final) amounts within 2 days. This is in sharp contrast to the L-series, wherein precipitation appeared to continue for several days into the experiment, as noted above.

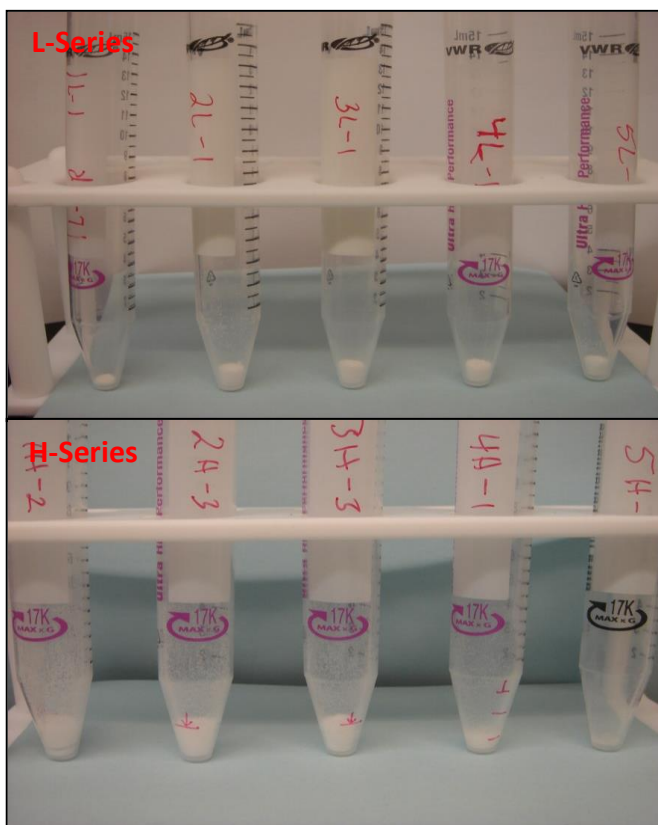


Figure 2 Test tubes containing the final precipitate after rinsing, centrifugation, and drying. Note the mineral precipitation along the inside walls of the first 4 tubes in the H-series (“1H” to “4H”). No precipitate was formed in set “5H.”

Based upon the visual observations made in these tests, the rate of precipitate formation appeared to be sensitive to the initial ratio of urea to CaCl_2 in the L-series tests as evidenced by the shorter precipitation times with

increasing ratios. In contrast, the rate of precipitate formation in the H-series tests seemed to be insensitive to the initial ratio of urea to CaCl_2 since the precipitation formation was approximately the same across all concentration ratios (for the four test tubes where precipitation occurred).

The test tubes were checked for the presence of NH_3 at the end of the experiment. Subjective detection of NH_3 gas in the headspace of the test tubes indicates that $\text{NH}_{3(\text{g})}$ ranged from non-detectable to extremely strong, as noted in Table 4. An odor of ammonia was detected in all L-series tests except for the test set containing the lowest initial urea to CaCl_2 ratio of 1:2 (set “1L”). Ammonia odor was only faint in set “2L” (1:1 ratio) and progressively increased in strength to a level of “extremely strong” in set “5L” (3:1). Ammonia odor was not detected in the headspace of any H-series test. These observations suggest that the presence of NH_3 gas in the headspace of the test tubes depended on the initial ratio of urea to CaCl_2 at low initial concentrations of these constituents (L-series), but this does not seem to be the case for the high initial concentration tests (H-series).

In the test tubes that contained a mineral precipitate, the precipitate was identified as calcite phase CaCO_3 via XRD analysis. SEM analysis of the precipitate also indicated that the crystal morphology was consistent with calcite, as shown in Figure 3. The calcite crystals in the L-series tests are larger and appeared generally more uniform in shape than the H-series calcite. Larger crystals and more uniform crystal size distributions are consistent with slower mineral precipitation and are generally due to lower levels of supersaturation

(Kile et al. 2000). This is significant, as crystal morphology and size distribution may play a role in the mechanical properties of soil cemented using EICP.

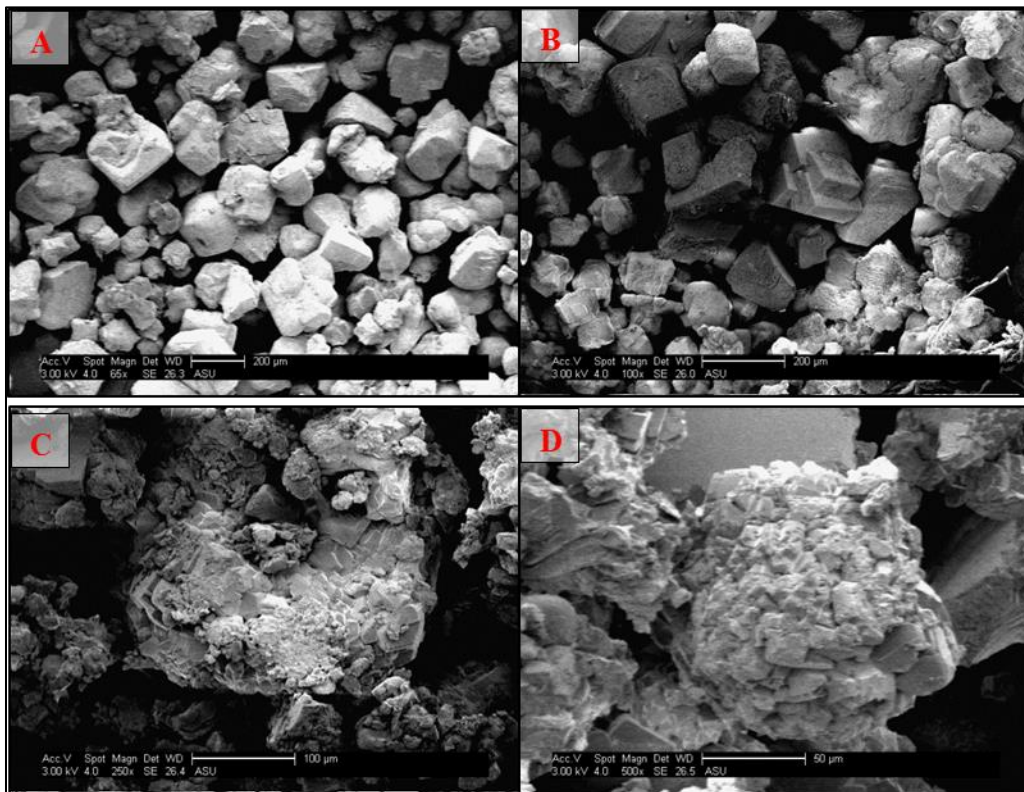


Figure 3 Representative SEM images of calcite crystals from 4 different L-series and H-series test tubes (2 each). Images “A” and “B” are representative CaCO_3 crystals from the L-series, and images “C” and “D” are from the H-series. Note the generally larger and more uniform crystals in the L-series, and the smaller and more variable crystals in the H-series.

Quantification of CaCO_3 Precipitate

The CaCO_3 precipitated in the test tubes was quantified and the amounts are presented in Tables 5 and 6 for the L-series and H-series tests (respectively).

The CaCO_3 precipitate was quantified by (1) acid digestion and (2) by calculation based on the IC-measured Ca^{2+} concentration changes. The

stoichiometric maximum amount of CaCO_3 that could form was also determined; this is the amount that would form if 100% of the available Ca^{2+} (0.2 M) precipitated as CaCO_3 . The stoichiometric maximum serves as a theoretical upper bound for comparison to the other CaCO_3 quantification methods.

Table 5 The amounts of CaCO_3 precipitate found in the L-series experiments. The “*Stoichiometric maximum*” is the amount of CaCO_3 if 100% of the Ca^{2+} precipitated as CaCO_3 ; the “*Amount based on ΔCa^{2+}* ” was calculated from IC-measured changes in Ca^{2+} concentrations; “*acid digestion*” is from acid digestion of recovered precipitate. Asterisk indicates that C is the limiting reagent (0.10 M) in set “1L” not Ca^{2+} (0.2 M).

	Test	Calcium	CaCO_3 (grams)		
	Test Tube	ΔCa^{2+} (g/L)	Stoichiometric maximum based on limiting reagent	Amount based on ΔCa^{2+}	Amount via <i>acid digestion</i> of precipitate
0.20 M CaCl_2-dihydrate	1L-1	-4.21*	0.10	0.11	0.10
	1L-2	-4.25*	0.10	0.11	n/a
	1L-3	-4.14*	0.10	0.10	0.10
	2L-1	-7.76	0.20	0.19	0.20
	2L-2	-7.79	0.20	0.19	n/a
	2L-3	-7.76	0.20	0.19	0.19
	3L-1	-8.00	0.20	0.20	0.20
	3L-2	-8.00	0.20	0.20	n/a
	3L-3	-8.00	0.20	0.20	0.20
	4L-1	-8.00	0.20	0.20	0.20
	4L-2	-8.00	0.20	0.20	n/a
	4L-3	-8.00	0.20	0.20	0.19
	5L-1	-7.92	0.20	0.20	0.20
	5L-2	-8.00	0.20	0.20	n/a
	5L-3	-8.00	0.20	0.20	0.20

The limiting reagent in the L-series sets “2L” through “5L” is Ca^{2+} , so the maximum amount of CaCO_3 possible is 0.20 grams for the total fluid volume in the test tubes (10 ml). The limiting reagent in first set of test tubes (“1L”) is carbon (0.10 M), so the maximum amount of CaCO_3 is 0.10 grams. This point is illustrated in subsequent plots and tables (using an asterisk) for set

“1L” where values of “% Ca^{2+} used” are doubled to illustrate that a Ca^{2+} removal of 50% requires 100% of the available carbon from urea, so this equates to 100% of the maximum Ca^{2+} removal. The amounts of CaCO_3 that were precipitated in the L-series tests were either at or very near the maximum possible amounts.

As with the L-series, the limiting reagent in the H-series sets “2H” through “5H” is Ca^{2+} , so the maximum amount of CaCO_3 possible is 2.0 grams for the total fluid volume in the test tubes (10-ml). The limiting reagent in the first set of test tubes (“1H”) is carbon (1.0 M), so the maximum amount of CaCO_3 is 1.0 gram. This point is illustrated in subsequent tables and plots as indicated above for the “1L” series tests. Unlike the L-series tests, the amounts of CaCO_3 that were precipitated in the H-series tests were far less than the maximum possible. The range of CaCO_3 precipitate in the H-series tests was between 0% and 54% of the maximum possible. Note that 54% of the maximum CaCO_3 precipitate was obtained from doubling the highest “% Ca^{2+} used” value in set “1H” (27%) in Table 6. In summary, the absolute amounts of CaCO_3 produced in the H-series tests are much greater than in the L-series, but far less as a percentage of the maximum amount possible.

Table 6 Table showing the amounts of CaCO₃ precipitate found in the H-series experiments. The columns have the same meaning as described above in Table 5 for the L-series tests. * = carbon is the limiting reagent in set “1H.”

	Test	Calcium	CaCO ₃ (grams)		
	Test Tube	ΔCa ²⁺ (g/L)	Stoichiometric Maximum based on limiting reagent	Amount based on ΔCa ²⁺	Amount via <i>acid digestion</i> of precipitate
2.0 M CaCl₂-dihydrate	1H-1	-18.79*	1.0	0.47	0.47
	1H-2	-21.59*	1.0	0.54	n/a
	1H-3	-21.17*	1.0	0.53	0.52
	2H-1	-30.38	2.0	0.76	0.74
	2H-2	-24.39	2.0	0.61	n/a
	2H-3	-23.60	2.0	0.59	.59
	3H-1	-18.33	2.0	0.46	0.48
	3H-2	-19.83	2.0	0.49	n/a
	3H-3	-17.90	2.0	0.45	0.46
	4H-1	-2.69	2.0	0.07	0.09
	4H-2	-8.73	2.0	0.22	n/a
	4H-3	-6.33	2.0	0.16	0.19
	5H-1	-0.07	2.0	0.00	0
	5H-2	-1.46	2.0	0.04	n/a
	5H-3	-1.81	2.0	0.05	0

The results from the L-series tests indicate that the amount of precipitate formed at low initial concentrations does not appear to depend on the initial ratio of urea to CaCl₂ for the ratios tested here unless there is a limiting reagent. But, this observation does not hold at high initial concentrations indicating that there are factors other than the initial ratio of urea to CaCl₂ that are influencing CaCO₃ precipitation.

L-Series Chemical Analysis

A summary of the chemical analysis results from the L-series tests is presented in Table 7. Alkalinity measurements show a net increase in all L-series tests and the measured alkalinity increases were progressively greater with increasing initial ratios of urea to CaCl₂. The net increases in alkalinity ranged from approximately 81 mg/L (as CaCO₃) in set “1L” (1:2 urea to CaCl₂) to

approximately 25,000 mg/L in set “5L” (3:1). Net pH measurements show that pH decreased by approximately 1.0 and 0.36 units from a starting pH=8.0 in sets “1L” and “2L” (respectively), but this trend reversed and pH increased sharply with increasing initial ratios of urea to CaCl₂ in sets “3L” to “5L.” The net increases in pH ranged from approximately 0.8 units in set “3L” to 1.0 unit in set “5L,” which yielded final pH-values between 8.8 and 9.1. It is worth noting that these net increases in alkalinity and pH are occurring in actively precipitating carbonate systems, but that carbonate precipitation has the effect of reducing both alkalinity and pH. The results from the control specimens (not shown here) indicated no appreciable changes or patterns in any of the chemical parameters monitored other than Ca²⁺ (\approx 5% loss).

Table 7 Summary of the chemical analysis results for the L-series tests. Initial [NH₄⁺]=0 and pH \approx 8.0, and fluid volume \approx 10-ml. Asterisk on Ca²⁺ indicates that urea (0.10 M) is the limiting reagent, as such 50% removal equates to maximum possible.

	Test	Urea		NH ₄ ⁺	Alkalinity	pH	Calcium		Inorganic Carbon
	Test Tube	Net Δ (mol/L)	% Used	Net Δ NH ₄ ⁺ (g/L)	Net Δ (mg/L CaCO ₃)	Net Δ pH	Δ Ca ²⁺ (g/L)	% of total Ca ²⁺ used	Net Δ (mol/L)
0.20 M CaCl₂-dihydrate	1L-1	-0.10	100	3.78	81	-1.02	-4.21	53*	0.10
	1L-2	-0.10	100	3.83	94	-1.03	-4.25	53*	0.10
	1L-3	-0.10	100	3.83	89	-1.07	-4.14	52*	0.10
	2L-1	-0.20	100	6.61	464	-0.35	-7.76	97	0.20
	2L-2	-0.20	100	6.63	510	-0.36	-7.79	97	0.20
	2L-3	-0.20	100	6.70	485	-0.36	-7.76	97	0.20
	3L-1	-0.30	100	10.69	9187	0.80	-8.00	100	0.30
	3L-2	-0.30	100	10.44	9618	0.75	-8.00	100	0.30
	3L-3	-0.30	100	10.68	7930	0.75	-8.00	100	0.30
	4L-1	-0.40	100	13.48	15925	0.95	-8.00	100	0.40
	4L-2	-0.40	100	13.57	16049	0.96	-8.00	100	0.40
	4L-3	-0.40	100	13.35	16171	0.95	-8.00	100	0.40
	5L-1	-0.60	100	14.85	24297	1.06	-7.92	99	0.60
	5L-2	-0.57	95	16.47	25269	1.07	-8.00	100	0.57
	5L-3	-0.58	96	15.48	24137	1.07	-8.00	100	0.58

Urea utilization (via ureolysis) was between 95%-100% in the L-series tests, with the majority (13 out of 15 tests) showing utilization of approximately 100%. The inorganic carbon (provided as CO_3^{2-}) for CaCO_3 comes primarily from urea-derived CO_2 , with urea utilization of 1 mole of CO_2 per mole of urea under the proper geochemical conditions. However, it is also likely that some inorganic carbon was present in the water used in the experiments.

Table 8 The L-series nitrogen balance in the $\text{NH}_3\text{-NH}_4^+$ system comparing the differences between **IC-measured**, stoichiometrically **maximum possible** (based on amount of urea consumed), and **calculated** (pH-dependent) concentrations of NH_4^+ . The column “*pH after 100x dilution*” refers to sample dilution for IC analysis.

Test Conditions			Nitrogen Balance as $\text{NH}_3\text{-NH}_4^+$				
Test Tube	Final pH	pH after 100x dilution	Max possible NH_4^+ based on urea balance (g/L)	Measured via IC NH_4^+ (g/L)	Calculated NH_4^+ as a function of pH (g/L)	% Difference b/w maximum possible and measured	% Difference b/w calculated and measured
1L-1	7.0	7.3	3.61	3.68	3.57	2.0	-3.1
1L-2	7.0	7.3	3.61	3.73	3.57	3.4	-4.4
1L-3	6.9	7.3	3.61	3.73	3.57	3.5	-4.4
2L-1	7.7	7.5	7.21	6.61	7.08	-8.4	7.2
2L-2	7.6	7.5	7.21	6.63	7.08	-8.0	6.8
2L-3	7.6	7.5	7.21	6.70	7.08	-7.2	5.8
3L-1	8.8	7.9	10.82	10.69	10.35	-1.2	-3.2
3L-2	8.8	7.9	10.82	10.44	10.35	-3.5	-0.9
3L-3	8.8	7.9	10.82	10.68	10.35	-1.3	-3.1
4L-1	9.0	8.3	14.42	13.48	12.94	-6.6	-4.0
4L-2	9.0	8.3	14.42	13.57	12.94	-6.0	-4.6
4L-3	9.0	8.3	14.42	13.35	12.94	-7.4	-3.1
5L-1	9.1	8.8	21.64	14.85	15.8	-31.4	6.3
5L-2	9.1	8.8	20.57	16.47	15.0	-19.9	-8.8
5L-3	9.1	8.8	20.85	15.48	15.2	-25.7	-1.7

Depending on the pH, the production of NH_4^+ should closely follow urea utilization. The results shown below in Table 8 indicate that IC measured NH_4^+ concentrations were within approximately +/-8% of the stoichiometrically

estimated maximum concentrations (i.e., based solely on the amount of urea consumed) with the notable exception of set “5L.” The measured NH_4^+ concentrations were closest to the stoichiometric maximum concentrations at pH values below 8, but began to rapidly diverge with increasing pH. The IC measured NH_4^+ concentrations in the “5L” series tests (pH=9.1) were between 20-31% less than the stoichiometrically estimated maximum, but the measured and estimated amounts were very similar (+/-8%) in sets “1L” to “3L” (pH 7.3-7.9).

Noting that the equivalence point in the $\text{NH}_3\text{-NH}_4^+$ system occurs at pH=9.24 (at STP) and that rapid changes in speciation occur within a relatively narrow pH range, most of the differences between the IC-measured concentrations and stoichiometric maximum NH_4^+ concentrations seen in Table 8 can be explained by pH effects. The stoichiometric maximum assumes that nearly all NH_3 will be in the ionic form (NH_4^+), which would require a pH \leq 6.90; at pH \leq 6.90 (STP), 99.6% NH_3 will occur as NH_4^+ (pH and relative concentrations taken from the $\text{NH}_3\text{-NH}_4^+$ speciation table in Appendix A). The pH of most test specimens was significantly greater than 6.90 even after dilution, as shown in Table 8, therefore, the measured NH_4^+ concentrations should be lower than the stoichiometric maximum. The pH values of the test specimens presented in Table 8 range from approximately 7.3 to 8.8 after 100x dilution with DI water, which correlates to relative NH_4^+ concentrations ranging from 98.8% to 73.3% (respectively) based on the $\text{NH}_3\text{-NH}_4^+$ speciation table (Appendix A). Again, the measured NH_4^+ concentrations should be lower than

the maximum and this difference should become greater as pH increases above 6.90, as shown in Table 8, column 7 (titled “% Difference b/w maximum possible and measured”). The general trend within column 7 shows an increase in the absolute difference between the maximum possible NH_4^+ and the amount measured as a function of increasing pH. In other words, as pH increases, the difference between the IC measured and the maximum possible also increases. The pH dependence of NH_4^+ concentration is graphically illustrated below in Figure 4. Note that set “5L” (pH=8.8 after 100x dilution) has a calculated relative NH_4^+ concentration of only 73.3% of the maximum possible at pH=8.8, which illustrates the strong pH-dependence of NH_4^+ concentration.

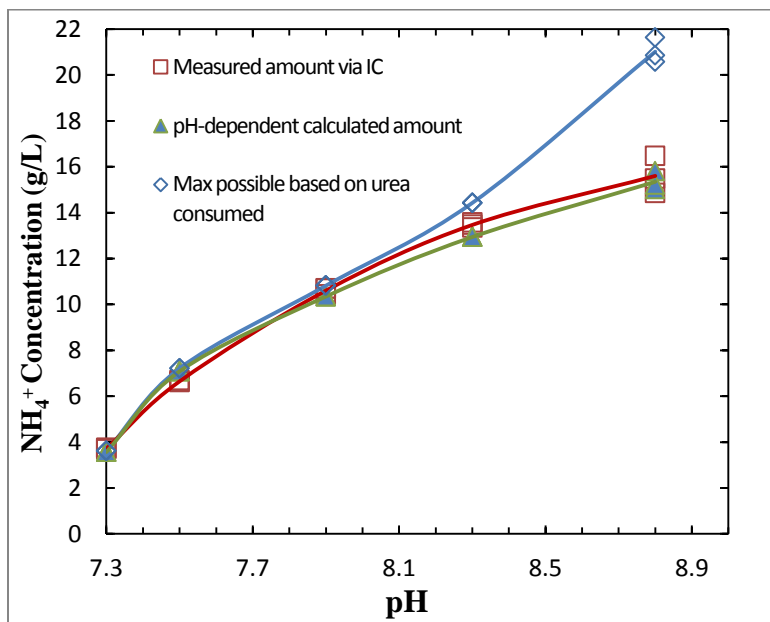


Figure 4 Nitrogen balance plot in the $\text{NH}_3\text{-NH}_4^+$ system for the L-series comparing the differences between IC measured, stoichiometrically predicted (based on the actual amount of urea consumed), and calculated (pH-dependent) concentrations of NH_4^+ .

The IC-measured NH_4^+ concentrations are reasonably close to the concentrations obtained via pH-dependent calculations that account for speciation. Based on the strong pH-dependence of the $\text{NH}_3\text{-NH}_4^+$ system, one would also expect that the qualitative odor detection of NH_3 also depends on pH; that is, NH_3 odor should be present at high pH, but should be faint to non-detectable at lower pH values since the ionic form (NH_4^+) predominates. The qualitative (and subjective) determinations of NH_3 based on odor and described in Tables 3 and 4 support this assessment. The odor of NH_3 in the test tube headspaces ranged from non-detectable in set “1L” (pH=7.0) to extremely strong in set “5L” (pH=9.1). Figure 5 illustrates the trends in pH and alkalinity in relation to the initial ratio of urea to CaCl_2 in the L-series tests. The net alkalinity increased for all ratios tested, but increased sharply as the initial ratios of urea to CaCl_2 increased beyond 1.0:1.

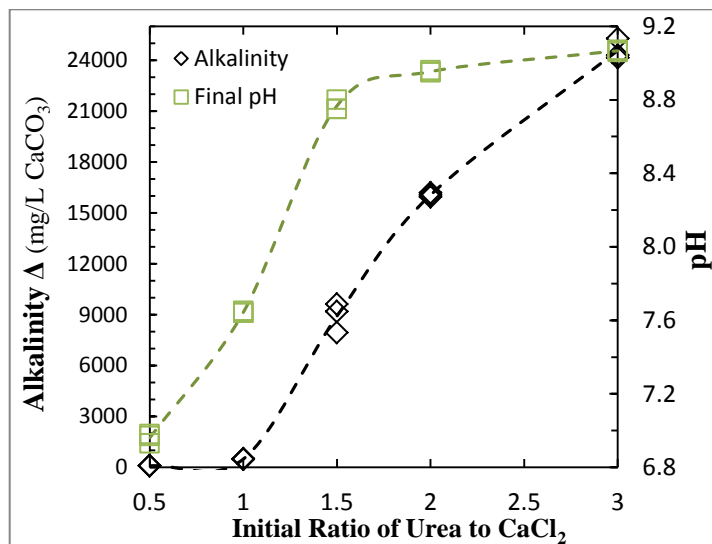


Figure 5 Net increase in alkalinity and the final pH in relation to initial ratios of urea to CaCl_2 for the L-series tests. Initial pH=8, alkalinity increased in every test.

The reason for the sharp increase in alkalinity after 1.0 is that all available Ca^{2+} was removed as CaCO_3 by this point, which resulted in a stoichiometric rise in alkalinity with further NH_3 release (via ureolysis). In contrast to alkalinity, the final pH declined rapidly at urea to CaCl_2 ratios of 0.5:1 to 1.0:1, but then the pH increased sharply by 1.5 units and rose modestly thereafter.

The final pH of a closed ureolytic system undergoing active carbonate mineral precipitation depends on several factors including: the initial conditions of alkalinity and pH, CO_2 production, NH_3 production that increases the pH and alkalinity, and Ca^{2+} mineral precipitation which decreases pH and alkalinity. The pH-dependence of the $\text{NH}_3\text{-NH}_4^+$ is evident as discussed above and illustrated in Table 8 and Figure 4. The primary benefits of inducing and maintaining sufficiently high pH in an EICP environment (e.g., $\text{pH}>9$) are as follows: (1) increased saturation with respect to CaCO_3 drives the EICP reaction further towards completion; (2) $\text{NH}_3\text{-NH}_4^+$ speciation will shift towards NH_3 which limits the acidic form (NH_4^+) and reduces the potential for reaction reversal; (3) suppression of typical nitrifying organisms that produce acidic conditions via $\text{NH}_4^+\rightarrow\text{NO}_3^-$ oxidation since these organisms are typically inhibited at high pH (e.g. $\text{pH}>9$). Therefore, it is desirable to establish a urea to CaCl_2 ratio that induces and maintains a high pH environment but minimizes the amount of excess nitrogen introduced into the surround environment and the costs associated with EICP. The initial ratio of urea to CaCl_2 strongly affected pH and alkalinity and, thereby, the ratio of NH_3 and NH_4^+ in the low concentration tests. The results show that pH and alkalinity, the two primary

geochemical factors driving EICP, are higher at greater initial ratios of urea to CaCl_2 .

As previously discussed, calcium removal in the form of CaCO_3 was nearly complete for all L-series tests (i.e., across all initial ratios of urea to CaCl_2), indicating that the geochemical conditions were at least sufficient for precipitation but offering little insight for estimating optimal ratios. As seen in Figure 5, the increase in alkalinity from set “1L” to “2L” is comparatively modest as the initial urea- CaCl_2 ratio increases from 0.5:1 to 1.0:1 (from 88 to 486 mg/L as CaCO_3 , average), but the small decline in pH for set “2L” is significantly less than occurs in “1L” (-0.36 vs. -1.06 pH units). This indicates that the solution in “2L” (urea- CaCl_2 ratio=1.0:1) was substantially more buffered than “1L” and, therefore, more capable of resisting the pH decline associated with CaCO_3 precipitation. Greater levels of buffering capacity and resistance to pH decline are further illustrated at higher urea- CaCl_2 ratios shown in Figure 5. As the ratio of urea to CaCl_2 increased from 1.0:1 to 1.5:1, alkalinity increased from 486 to 8912 mg/L (as CaCO_3) and pH increased by 1.2 units (pH=7.6 to 8.8). The pH at a urea to CaCl_2 ratio of 1.5:1 is approximately 8.8, an increase of 0.8 units above the pH at the start of the experiment in an actively precipitating CaCO_3 system. At higher ratios of urea to CaCl_2 (2.0, 2.5, and 3.0:1), alkalinity climbs rapidly while pH increases at a slower yet substantial rate in increments of approximately 0.1 pH units.

Further consideration of Figure 5 and the relevant data tables indicates that there is a “benchmark range” of urea to CaCl_2 ratio that induces a

substantial rise in pH, albeit at a decreasing rate of increase with urea-CaCl₂ ratios, and sufficiently buffers the EICP system against rapid declines in pH during CaCO₃ precipitation. The benchmark range should be chosen so that a minimum pH ≥ 9 is maintained in order to maintain high NH₃ levels and the associated benefits previously discussed. Incremental increases in urea-CaCl₂ ratios beyond this benchmark range will yield little increase in pH with unnecessarily large increases in alkalinity. Although the rise in alkalinity is stoichiometrically correlated with NH₃ production after all the Ca²⁺ is removed, the rise in pH from a weak base (NH₃) is not. It should also be noted that there are others factors that strongly affect pH changes and extend beyond simple addition or removal of a weak base (NH₃) in a chemical system such as acid-base chemical complexes and high ionic strengths.

Using the L-series tests as an approximation to estimate a proposed benchmark range of urea to CaCl₂ ratios for the EICP process, Figure 6 was created as a revised version of Figure 5 with pH trend arrows illustrating the benchmark range.

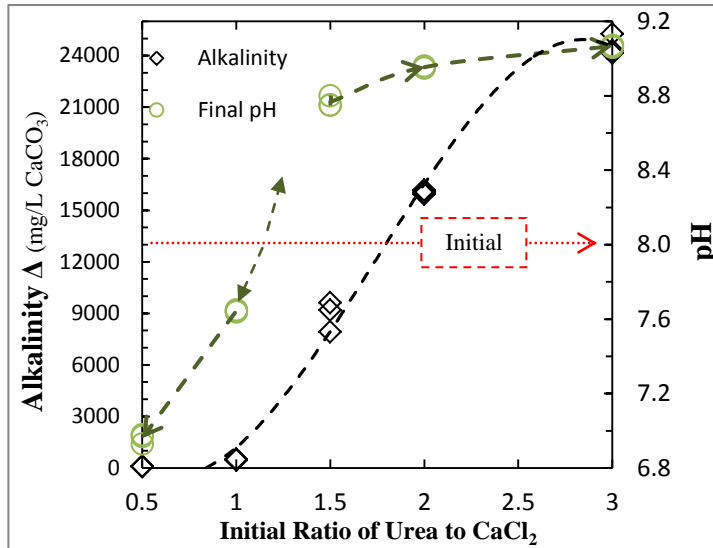


Figure 6 Comparison of the net alkalinity increase and the general trend in the final pH in relation to initial ratios of urea to CaCl₂ for the L-series tests. Initial pH=8

Inspection of Figure 6 indicates that at low concentrations a urea to CaCl₂ ratio 1.5:1 and 2.0:1 induces a substantial rise in pH. Referencing Figure 6 and Table 7, there appears to be room for significant increases in pH at urea to CaCl₂ ratios below of 1.5:1, but the pH rise is nearly flat for ratios greater than 2.0:1. Alkalinity continues to rapidly climb at urea to CaCl₂ ratios of 2.0:1 and greater, but possibly at a slower rate and to no immediately obvious advantage in terms of pH rise. As such, the data imply that a urea to CaCl₂ ratio of 2.0:1 is the upper limit of the proposed “benchmark range” that substantially increases pH after the removal of Ca²⁺ and sufficiently buffers the EICP system against a rapid decline in pH. Therefore, it may be concluded that at low concentrations the benchmark range for the initial urea to CaCl₂ ratio that may be most effective with the least amount of residual nitrogen production (as discussed above) is between approximately 1.75:1 and 2.0:1.

H-series Chemical Analysis

The chemical analysis results from the H-series tests are summarized in Table 9. Unlike the L-series tests, the H-series tests showed only small alkalinity increases in some cases and net decreases in other cases. The largest decline in alkalinity was approximately -109 mg/L (as CaCO₃) and the greatest increase was 90 mg/L. There was a slight trend towards increasing alkalinity with initial ratios of urea to CaCl₂ from test tube set “1H” to “4H” (-102 to 72 mg/L), but the highest ratio set, set “5H,” did not follow this trend and showed the largest average alkalinity drop of -106 mg/L. The net pH decreased in all tests, with the decrease ranging from approximately -2.3 to -1.5 units. There was a general trend towards a smaller pH decline with increasing initial ratio of urea to CaCl₂ from set “1H” to “4H” (-2.3 to -1.8 units, respectively), but the highest ratio set, set “5H,” did not follow this trend and had an average pH drop of 2.30 units. The alkalinity and pH trends are plotted in Figure 7. The control specimens (not shown here) showed no appreciable changes or patterns in any of the chemical parameters monitored other than Ca²⁺ (4-9% losses).

Table 9 Summary of the chemical analysis results for the H-series tests containing 2.0 M CaCl₂. Initial [NH₄⁺]=0, initial pH ≈8.0, and fluid volume ≈10-ml. Alkalinity = total alkalinity and inorganic carbon is moles of carbon liberated as CO₂ from urea. Asterisk on Ca²⁺ indicates that urea (1.0 M) is the limiting reagent in set “1H.”

Test	Urea		NH ₄ ⁺	Alkalinity	pH	Calcium		Inorganic Carbon
	Net Δ (mol/L)	% of total used	Net ΔNH ₄ ⁺ (g/L)	Net Δ (mg/L CaCO ₃)	Net ΔpH	ΔCa ²⁺ (g/L)	% of total used	Net Δ (mol/L)
1H-1	-0.50	50.0	14.66	-106	-2.32	-18.79	23.5*	0.50
1H-2	-0.50	49.5	17.30	-106	-2.22	-21.59	27.0*	0.50
1H-3	-0.47	46.9	12.56	-94	-2.29	-21.17	26.5*	0.47
2H-1	-0.70	35.0	24.06	-66.6	-2.20	-30.38	38.0	0.70
2H-2	-0.62	31.0	19.32	-58	-2.11	-24.39	30.5	0.62
2H-3	-0.60	30.2	17.91	-66	-2.13	-23.60	29.5	0.60
3H-1	-0.49	16.3	15.47	40	-1.46	-18.33	22.9	0.49
3H-2	-0.42	14.1	16.11	50	-1.73	-19.83	24.8	0.42
3H-3	-0.50	16.5	13.96	59	-1.69	-17.90	22.4	0.50
4H-1	-0.18	4.5	5.30	90	-1.77	-2.69	3.4	0.18
4H-2	-0.19	2.3	5.25	40	-1.85	-8.73	10.9	0.19
4H-3	-0.19	2.3	5.43	85	-1.72	-6.33	7.9	0.19
5H-1	0.00	0.0	0	-109	-2.28	-0.07	0.1	0.00
5H-2	-0.01	0.2	0	-108	-2.26	-1.46	1.8	0.01
5H-3	-0.03	0.4	0	-102	-2.21	-1.81	2.3	0.03

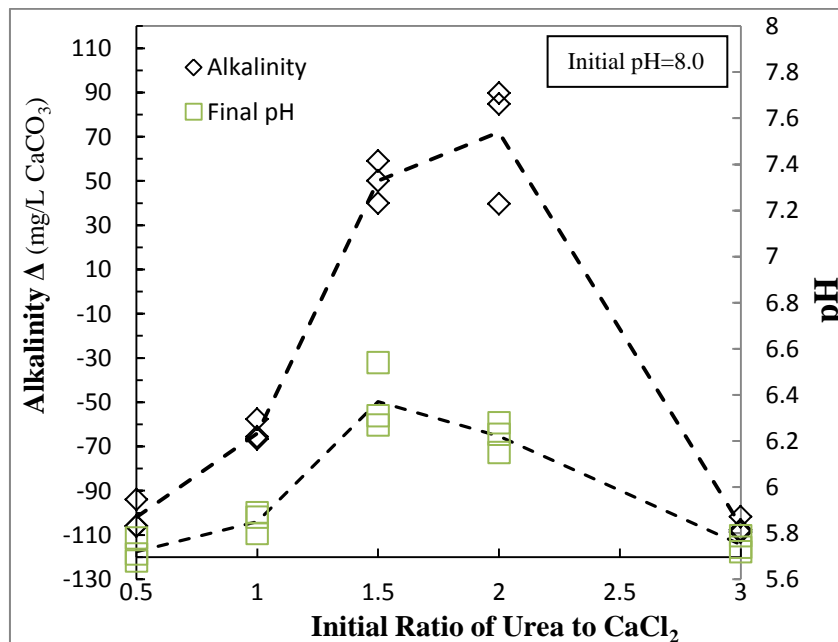


Figure 7 Comparison of the net increases in alkalinity and the final pH in relation to the initial ratios of urea to CaCl₂ for the H-series tests. Initial pH=8.0.

As shown by the data in Tables 5 and 6, the absolute amounts of CaCO_3 precipitated in the H-series tests (when precipitation occurred) were much greater than in the L-series. But, in terms of the maximum amount of precipitate possible, the H-series tests only yielded a precipitation efficiency between 0% and 54% of the maximum possible based on the total available Ca^{2+} vs. an efficiency of nearly 100% for all of the L-series tests; the maximum possible Ca^{2+} removal for set “1H” is only 40 g/L out of the 80 g/L available and since 21.5 g/L (27%) was removed then $21.5/40 \text{ g/L} = 54\%$ (Table 6). The low CaCO_3 yield in the H-series tests indicates that the geochemical conditions for CaCO_3 precipitation were largely unfavorable to non-existent. Indeed, the final pH values in the H-series tests ranged from 5.71 to 6.54 and the buffering capacities were very low across all tests even though most of the available Ca^{2+} was not precipitated. These results suggest that the effects of initial urea to CaCl_2 ratio observed in the low concentration tests do not hold at the higher concentrations discussed here. One implication of these results is that the higher chemical concentration in the H-series tests has a negative effect on the agent *inducing* the changes in the EICP system.

Recall that both the L-series and H-series tests were intended to evaluate the impacts of the “initial chemical *ratios* used in the EICP process” on the geochemical changes induced via ureolysis at low and high concentrations. Ureolysis is the fundamental underlying process driving the EICP reaction via changes in pH, alkalinity, carbon and nitrogen balance. The L-series experiments showed that initial chemical ratios had a significant impact on pH

and alkalinity, the primary factors affecting CaCO_3 precipitation. Urea consumption (via ureolysis) was complete in nearly every L-series test, which provided inorganic carbon for CO_3^{2-} formation and $\text{NH}_3\text{-N}$ for increases in pH and alkalinity. The results from the H-series tests in Table 9 indicate that very little ureolysis occurred in the high concentration tests which, among other things, limited the amount of inorganic carbon available for precipitation. The total consumption of urea and production of inorganic carbon ranged from 0% for set “5H” to 50% for set “1H.” The amount of urea consumed and the amount of Ca^{2+} precipitated closely follow each other in the “H” series tests, as shown in Figure 8, strongly indicating that CaCO_3 precipitation was limited by the amount of available inorganic carbon.

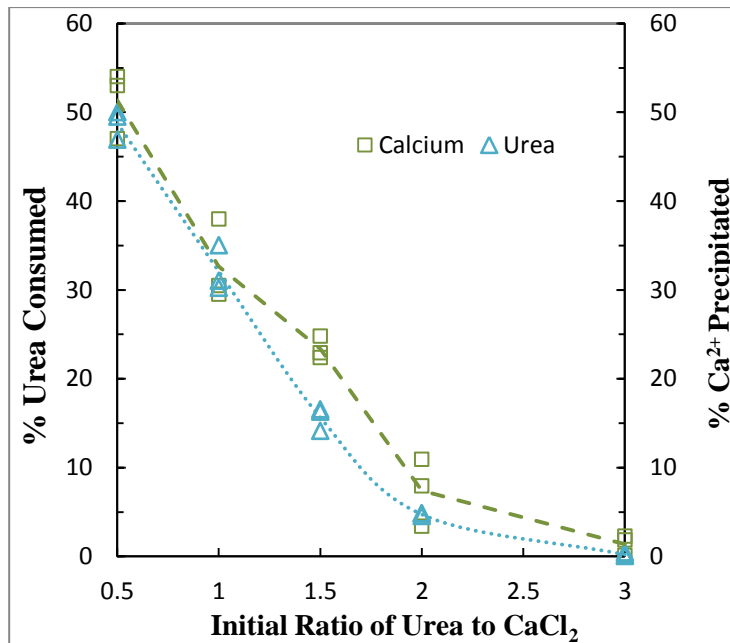


Figure 8 Urea consumed and the amount of Ca^{2+} precipitated closely follow in the H-series tests.

It appears that all other chemical parameters for the H-series tests were affected by the incomplete or total lack of ureolysis. Table 10 and Figure 9 show the results of analysis of the H-series nitrogen balance in the $\text{NH}_3\text{-NH}_4^+$ system. The small amounts of nitrogen produced in these tests are an indication that ureolysis was incomplete and NH_3 was almost entirely in the ionic form (NH_4^+) due to the consistently low pH and alkalinity across all tests. This point is well-illustrated by the similarities in the stoichiometric maximum based on urea utilization where all NH_3 is in the NH_4^+ form, and the pH-dependent concentrations of NH_4^+ (low pH in this case). The stoichiometric maximum and the pH-dependent concentrations show more NH_4^+ (and less NH_3) than the IC-measured amounts because sample dilution for IC testing resulted in a pH increase of the original samples (recall, increase in pH shifts NH_4^+ to NH_3).

Table 10 The H-series nitrogen balance in the $\text{NH}_3\text{-NH}_4^+$ system comparing the differences between IC measured, stoichiometric maximum predicted (based on actual amount of urea consumed), and calculated (pH-dependent) concentrations of NH_4^+ .

Test Conditions			Nitrogen Balance as $\text{NH}_3\text{-NH}_4^+$				
Test Tube	Final pH	pH after dilution	Max possible NH_4^+ based on urea balance (g/L)	Measured NH_4^+ (g/L)	Calculated NH_4^+ as a function of pH (g/L)	% Difference b/w measured and maximum possible	% Difference b/w measured and calculated
1H-1	5.68	7.3	18.03	14.66	17.81	-18.7	21.5
1H-2	5.78	7.3	17.85	17.30	17.64	-3.1	2.0
1H-3	5.71	7.3	16.91	12.56	16.71	-25.7	33.0
2H-1	5.80	7.3	25.26	24.06	24.96	-4.7	3.7
2H-2	5.89	7.3	22.36	19.32	22.09	-13.6	14.3
2H-3	5.87	7.3	21.81	17.91	21.54	-17.9	20.3
3H-1	6.54	7.3	17.61	15.47	17.40	-12.2	12.5
3H-2	6.27	7.3	15.27	16.11	15.08	5.5	-6.4
3H-3	6.31	7.3	17.90	13.96	17.69	-22.0	26.6
4H-1	6.23	7.3	6.48	5.30	6.40	-18.2	20.8
4H-2	6.15	7.3	6.84	5.25	6.76	-23.2	28.7
4H-3	6.28	7.3	6.84	5.43	6.76	-20.6	24.4
5H-1	5.72	7.3	0.07	0	0.07	-100	--
5H-2	5.74	7.3	0.40	0	0.39	-100	--
5H-3	5.79	7.3	0.91	0	0.90	-100	--

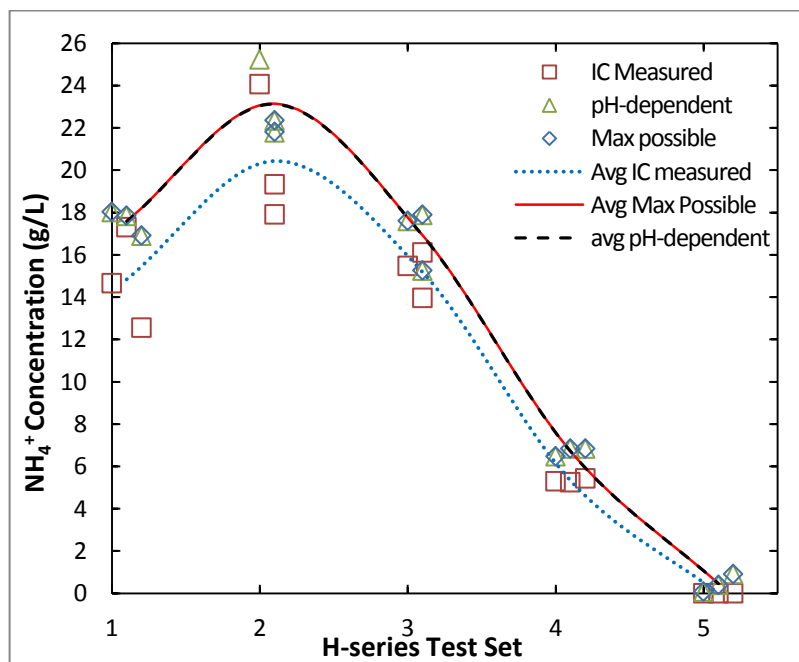


Figure 9 Nitrogen balance plot in the $\text{NH}_3\text{-NH}_4^+$ system for all H-series tests comparing the differences between IC measured, stoichiometrically predicted (based on actual amount of urea consumed), and calculated (pH-dependent) concentrations of NH_4^+ . The pH ≈ 7.3 for after dilution for IC testing.

It is clear from the H-series test results and well-established in the literature (Kile et al. 2000; Zuddas and Mucci 1998) that CaCO_3 does in fact occur in highly supersaturated systems (i.e., high concentrations at sufficiently high pH) and at very high ionic strengths (Zang and Dawe 1998), so a high concentration alone should not be a negative factor in CaCO_3 precipitation. The results from the H-series tests show that the geochemical parameters of interest and the amounts of CaCO_3 produced were negatively affected by the limited extent of ureolysis that occurred. But, these results open the door for a different question concerning the impact of high chemical concentrations on the mechanism that induces ureolysis in an EICP system. This question can be understood using the chemical analysis data in this chapter and by broadly identifying the different chemical stages encountered during ureolysis and solubility properties of enzymes.

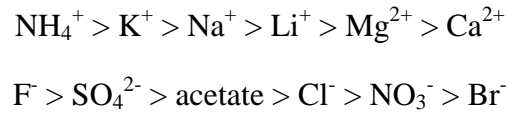
H-series Tests and Protein Solubility

Enzyme solubility depends on several factors including the nature of the enzyme (extent of hydrophobicity e.g.), the pH, and the ionic strength of the solvent. With the exception of denaturation processes, the general mechanism by which proteins precipitate is through agglomeration induced by electrostatic interactions associated with the protein structure and composition. Processes that maintain or increase repulsion or shield attractive charge interactions between proteins will improve solubility, whereas increased protein-to-protein interactions result in protein aggregation and subsequent precipitation. Proteins

are generally least soluble at their isoelectric point, the pH at which the sum of their negative and positive electric charges is approximately zero, which reduces repulsion between proteins. The isoelectric point of urease is at approximately pH=5.0-5.2, so pH values in this range will tend to precipitate urease enzyme.

Enzyme solubility is also highly dependent on the ionic strength of the solvent as well as the charge and the type of ion. Enzyme solubility is generally greater at low salt concentrations (ionic strengths < 1M) compared to pure water, a phenomena known as “salting-in.” But, this behavior reverses sharply at ionic strengths greater than 1 M and leads to protein precipitation, also known as “salting-out.” Ions in solution begin to compete with the proteins and other ions for waters of solvation at high ionic strength (> 1M) and the ions eventually dominate the organization of water leading to protein insolubility. The effects due to control of waters of solvation is not limited to ions; any solute that requires solvation will compete with other solutes including proteins. For example, the urea solute is dissolved in the water-based EICP solution (solvent) and, therefore, also competes with the ions and urease protein for water. Therefore, even non-ionic solutes such as urea can strongly affect protein solubility.

The impacts of charge and the type of ion on protein precipitation are described by the lyotropic series (or Hofmeister series). The following is a partial list of ions in the lyotropic series arranged in decreasing order of effect:



The salting out process can be further understood by the Cohn equation, an equation that represents the relationship between protein solubility and ionic strength of a solution:

$$\log S = B - K_s I_s$$

where S = solubility of the protein, B = protein-dependent theoretical solubility in salt free water, K_s = salt specific constant, and I_s = ionic strength.

The Cohn equation is only valid for the salting-out region of the protein precipitation process. An example of the Cohn equation superimposed against a characteristic protein solubility curve is shown in Figure 10.

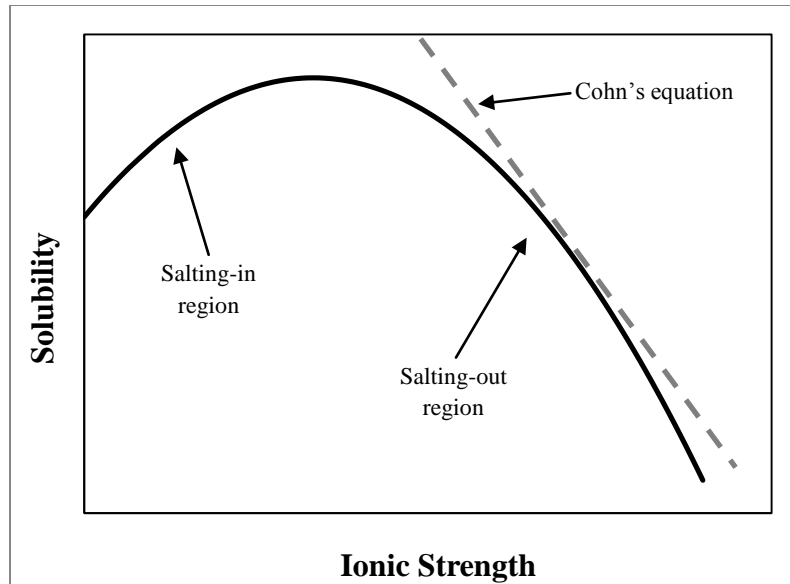


Figure 10 Relationship between protein solubility and the ionic strength of a solution. The Cohn equation (linear), valid for only the salting-out region, is superimposed against a characteristic protein solubility curve (\approx parabolic).

Referencing the data from the H-series tests, the initial stage chemical environment in these tests has an ionic strength of approximately 6.0 Molar due to 2.0 M CaCl_2 and a $\text{pH} = 8.0$. The primary salt at this stage is CaCl_2 with only a very minor contribution from the stabilizer used in the urease solution. At an ionic strength of 6.0M, CaCl_2 alone is sufficiently capable of salting out the urease enzyme and, thereby, stopping ureolysis once all of the enzymes have been precipitated from solution. The pH of the bulk solution (5.7-6.5) in the H-series tests is well-above the isoelectric point of urease, so pH is unlikely to drive protein precipitation here. During the limited time when ureolysis is occurring and CaCO_3 is precipitated, the decline in ionic strength due to the loss of Ca^{2+} (which should reduce salting-out) is countered by the production of NH_4^+ , a much more capable precipitating agent. In addition, two moles of NH_3

are produced for every mole of inorganic carbon produced (needed for CaCO_3) and the rate of NH_3 production (as NH_4^+) is very rapid ($32,500$ enzyme units/g \times 0.47 g/L \times 1.0 $\mu\text{mole NH}_3/\text{unit-minute} = 0.0325$ moles- $\text{NH}_3/\text{L} - \text{minute}$). Figure 11 presents a plot demonstrating the overall changes in ionic strength in the $\text{CaCl}_2\text{-NH}_4^+$ system based upon the following simplifying assumptions: (1) Ca^{2+} is removed (as CaCO_3) at about the same rate NH_4^+ is generated from urea; (2) CO_3^{2-} is immediately removed upon generation and therefore has negligible impact on ionic strength; (3) the bulk solution pH is predominately below 7.5 so that effectively all NH_3 occurs in the ionic form (NH_4^+).

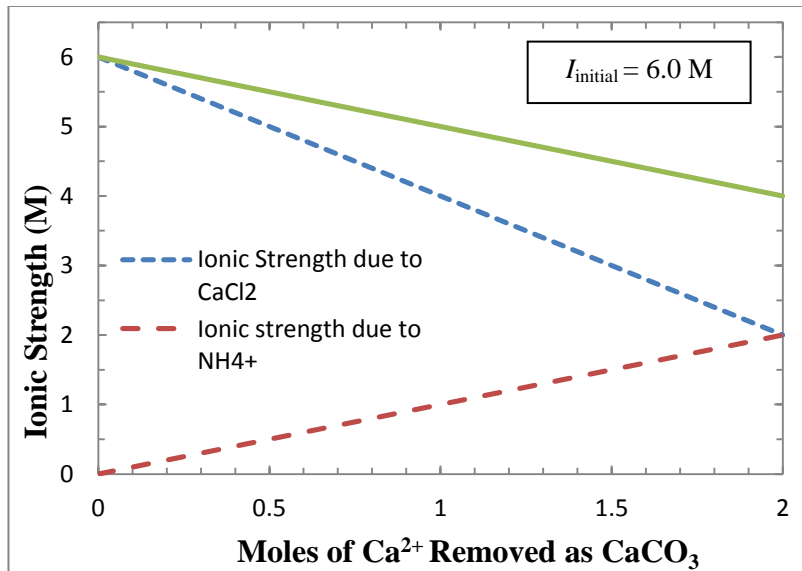


Figure 11- Plot demonstrating the changes in ionic strength in the $\text{CaCl}_2\text{-NH}_4^+$ system. It is assumed that bulk solution $\text{pH} \leq 7.5$, Ca^{2+} is removed as soon as inorganic carbon (CO_2) becomes available via ureolysis, and contributions from CO_3^{2-} are negligible.

The salting-out process takes time, ureolysis can occur during this time, and the amount of urea consumed may serve as an approximate proxy measure for the time the enzyme was still soluble. The tests in sets “1H,” “2H,” and

“3H” consumed very similar amounts of urea (range of 0.42 to 0.70 moles/L, average =0.53 m/L), so one could conjecture that the salting-out time was very similar across these three test sets. If CaCl_2 alone was the driving force behind protein precipitation, we would expect all sets to consume approximately the same amount of urea since the initial ionic strength was the same across all sets. But, this is not the case for test tube sets “4H” and “5H” where extremely little to no ureolysis occurred. An average of approximately 0.19 mole/L of urea was consumed (range of 0.18 to 0.19 m/L) across all tests in set “4H,” while no measurable change in urea was detected in set “5H.” The urea concentrations in sets “4H” and “5H” were 4.0 and 6.0 molar (respectively), while the first three tests sets were 1.0, 2.0, and 3.0 molar (respectively). Although calculation of activity of coefficients were not performed at the experiment endpoints, it suffices to say that solvation of increasing concentrations of urea has a significant impact on water activity; i.e., the activity of water is lowered with increasing amounts of dissolved solute. The thermodynamics of salting-out favor greater protein precipitation in highly concentrated solvents. From the Gibbs energy equation $\Delta G = \Delta H - T\Delta S$, the energy required to dissolve more solute (proteins e.g.) would further decrease the entropy (S) of the system and possible decrease enthalpy (H) leading to a thermodynamically unfavorable positive ΔG . The reverse process (i.e., precipitation) increases entropy and would yield a negative ΔG which favors precipitation.

The salting-out phenomenon, whether due to ionic solutes (e.g., CaCl_2 and NH_4^+) or non-ionic solutes such as urea, effectively terminates ureolysis. It

is generally understood that precipitated proteins can be re-dissolved once the ionic strength of the solvent is reduced or when waters of solvation are available, as in the case of non-ionic solutes. The experiments in sets “1H,” “3H,” and “4H” were rerun to verify the salting-out phenomenon. The new tests were conducted in duplicates and in larger 50-ml PP vials using the same initial volume as before (≈ 10 -ml), but were otherwise identical to the original test tube sets “1H,” “3H,” and “4H.” The tests were allowed to run for the same total time (9 days) and under the same conditions as the initial tests, e.g. in sealed test tubes at room temperature. The new tests were designated “1HR,” “3HR,” and “4HR” and were directly comparable to the original tests.

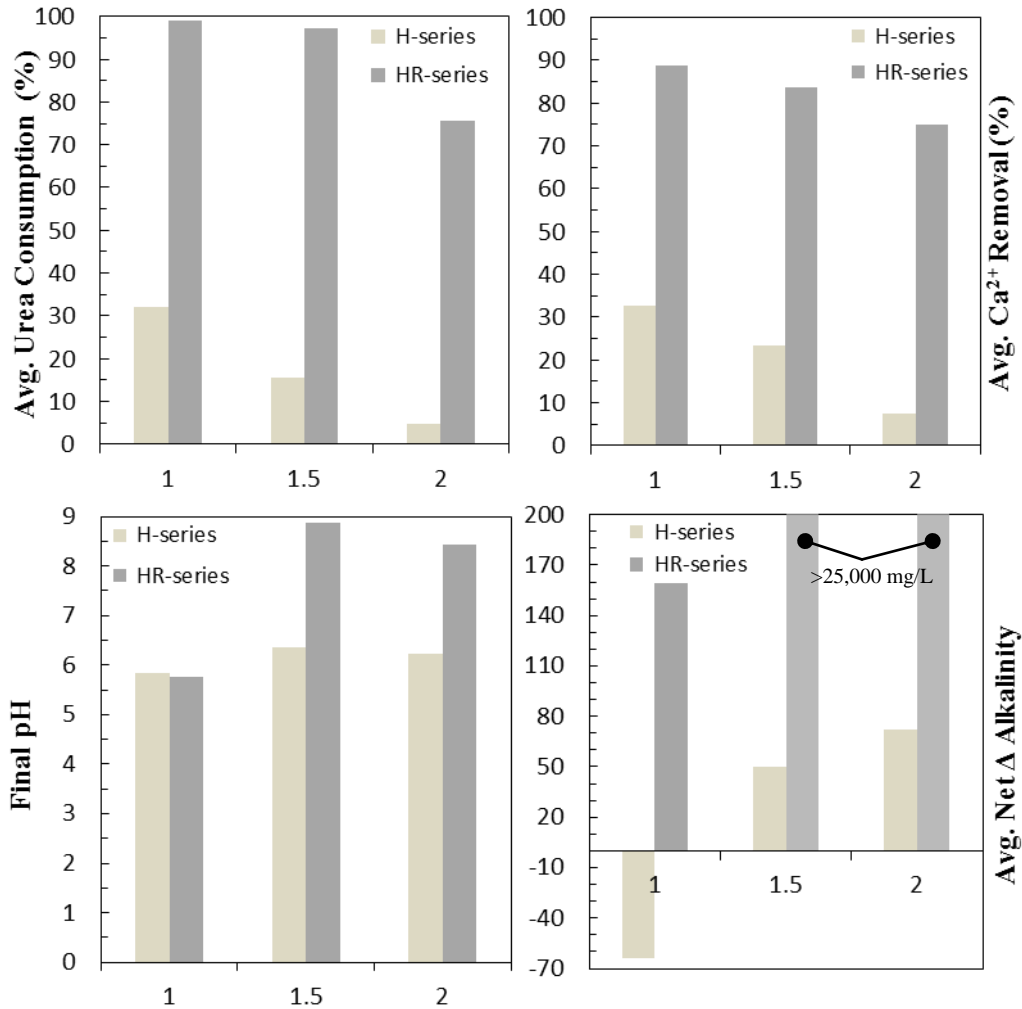
The new high concentration tests (“1HR,” “3HR,” and “4HR”) were allowed to run for two days and then, rather than drawing samples for analysis, approximately 40-ml of 18.2 M Ω DI water was added to the 50-ml vials and then quickly resealed. The tests were then allowed to run for seven more days during which time no analyses were performed and no fluid or solid was removed from the 50-ml vials. The tests were analyzed in the same manner as previously described in the Methods Section above (3.2.2) except for CaCO₃ quantification and electron microscopy, which were not performed.

The chemical analysis results from the second set of H-series tests (the “HR-series”) are presented in Table 11 and plotted in Figures 12 along with data from the original H-series tests. The results shown in Table 11 were corrected for dilution (i.e., 40-ml of DI water added on day 2) and can be compared to the information in Tables 4, 6, and 9. The results from the HR-series tests are very

different than the original comparable H-series tests, but appear to follow a trend similar to the L-series test results: increasing pH, alkalinity, and Ca^{2+} removal with increasing ratios of urea to CaCl_2 . The final pH for test set “1HR” (avg. pH=5.75) was approximately the same as test set “1H” (avg. pH=5.70), but the final average pH values for sets “3HR” and “4HR” were 8.87 and 8.43 compared to pH = 6.38 and 6.22 for sets “3H” and “4H” (respectively).

Table 11 Results summary from the new tests (“HR”) accounting for protein solubility. Initial $\text{NH}_4^+=0$, initial pH ≈ 8.0 . Asterisk on Ca^{2+} indicates that urea (1.0 M) is the limiting reagent in set “1HR” so that 50% Ca^{2+} used = max. possible. “n/a”= too high for detection method, “- -”=no odor, “++”=strong, & “++++”=extremely strong.

2.0 M CaCl_2	Test & Observation		Urea Utilization			NH_4^+	Alkalinity	pH	Calcium		Inorganic Carbon
	Test Tube	NH_3 Odor	Initial Conc. (mol/L)	Net Δ (mol/L)	% Used	Net ΔNH_4^+ (g/L)	Net Δ (mg/L CaCO_3)	Net ΔpH	ΔCa^{2+} (g/L)	% Ca^{2+} Used	Net Δ (mol/L)
	1HR-1	--	1.00	-0.99	99.2	35.2	157	-2.30	-36.2	45.3*	0.99
	1HR-2	--	1.00	-0.99	99.0	34.6	161	-2.20	-34.7	43.4*	0.99
	3HR-1	++++	3.00	-2.99	99.7	88.7	n/a	0.91	-65.7	82.1	2.99
	3HR-2	++++	3.00	-2.85	95.0	81.4	n/a	0.83	-68.4	85.5	2.85
	4HR-1	++	4.00	-3.01	75.3	92.7	n/a	0.47	-60.6	75.8	3.01
	4HR-1	++	4.00	-3.03	75.9	90.3	n/a	0.39	-59.1	73.9	3.03



Initial Ratio of Urea to CaCl₂

Figure 12 Plots comparing the chemical analysis results from the original H-series tests and the (new) HR-series tests. The HR-series tests were corrected for 40-ml of H₂O added on day 2 to reverse salting-out. Alkalinity is in mg/L as CaCO₃ & initial pH=8.0.

The net alkalinity change for set “1HR” was approximately 159 mg/L (avg., as CaCO₃) compared to -102 mg/L for set “1H” (avg.). The alkalinity changes for sets “2HR” and “4HR” were too far outside of the test detection range for reliable determination even after 500x dilution. Although the alkalinity was too high to be quantified in sets “2HR” and “4HR” using the

HACH test kit, the alkalinity was at a minimum greater than the highest previously tested value of 25,000 mg/L (set “5L” diluted 100x). The original test sets “3H” and “4H” had average alkalinity changes of 50 and 72 mg/L, respectively. Carbonate mineral precipitation occurred in all vials of all three test sets (1HR, 3HR, and 4HR) and was verified via acid test.

Calcium removal was almost twice as high in set “1HR” than in “1H” (35.5 g/L vs. 20.5 g/L), over four-times greater in set “3HR” than in “3H” (85.1 g/L vs. 18.6 g/L), and approximately ten-times greater in set “3HR” than in “3H” (59.8 g/L vs. 5.9 g/L). Sets “1HR” and “3HR” removed significantly more Ca^{2+} as a percentage than set “4HR,” approximately 88-84% of the maximum possible vs. 75%, respectively (avg. 35g out of 40g max possible due to carbon limitation = 88% for set “1HR”).

Urea consumption was nearly complete in sets “1HR” and “3HR” at approximately 95-99%, but only about 75% of the total available urea was used in set “4HR.” Urea consumption in the comparable test sets, “1H,” “3H,” and “4H,” was approximately 50%, 15%, and 5% (respectively). Ammonium concentrations were below the stoichiometric maximum, but appeared to be in line with pH-corrected values seen in previous tests shown above. Overall, the extent of ureolysis and CaCO_3 precipitation was far greater in these water diluted tests than in the original H-series tests.

The greatest improvement in CaCO_3 precipitation efficiency was seen in set “1HR” followed closely by set “3HR” and then “4HR,” which implies that greater dilution improved the extent of ureolysis. But, set “1HR” did not yield

the best conditions for the EICP process when considering pH and alkalinity. In fact, the relatively low pH environment (≈ 5.75) and the lack acid neutralizing capacity (avg. alkalinity = 159 mg/L) in set “1HR” promotes conditions for both short and long term CaCO_3 dissolution. Set “3HR” on the other hand yields much more favorable pH (avg. 8.87) and alkalinity ($\gg 25,000$ mg/L) conditions for the EICP process. As seen with the L-series tests, these results indicate that an initial urea to CaCl_2 ratio of 0.5:1 is also too low at high concentrations and that a ratio between 1.75:1 and 2.0:1 may be an optimal range for the EICP process *at high concentration*.

Clearly, water dilution of the HR-series tests on day two greatly improved the EICP process across all three HR test sets compared to the original H-series tests. The improvement in ureolysis and CaCO_3 precipitation seen in the HR-series tests suggest that the protein salting-out effect can be reversed. The salting-out effect appears to be mostly reversible. However, the data also suggest that it is probably not fully reversible under the given test conditions. For example, although ureolysis in sets “1HR” and “3HR” appeared to recover greatly after water dilution compared to the original tests, ureolysis in set “4HR” was far from complete and yielded the least amount of CaCO_3 as a percentage of the maximum possible amount. All three test sets started at the same ionic strength (6.0 M), so the main difference was the initial urea concentration (1.0 M, 3.0 M, and 4.0 M). The impact of the 40-ml water dilution resulted in effective urea concentrations that were approximately only 20% of the initial amounts: 0.2, 0.6, and 0.8 Molar compared to 1.0, 2.0, and 4.0

Molar. However, this assumes that ureolysis did not occur in the first two days of the experiment, an unlikely assumption since the results from the H-series tests show that some ureolysis did occur before protein salting-out. This would presumably reduce the effective concentrations of urea and CaCl_2 even further below 20% of their initial amounts after the 40-ml dilution. In this case, the effective concentrations would be even lower than estimated above, possibly lower than some of the L-series tests where ureolysis was complete without dilution. The fact that ureolysis and CaCO_3 precipitation in set “4HR” was incomplete and coupled with the high likelihood that effective concentrations were lower than the estimated 20% after dilution implies that the salting-out effect may not be fully reversible in solutions equal to or more concentrated than “4H” (6.0 M ionic strength as CaCl_2 and 4.0 M urea).

3.4 Conclusion

The physical characteristics of CaCO_3 (e.g., firmness and texture) seemed to be independent of the initial ratio of urea to CaCl_2 , but the higher initial concentrations in the H-series tests appeared to form more compact precipitates than the low concentration L-series. The calcite crystals formed in the L-series tests were larger and appeared generally more uniform in shape than the H-series calcite. The presence of NH_3 gas in the test tube headspace is a pH-dependent $\text{NH}_3\text{-NH}_4^+$ speciation process where higher pH conditions (e.g. pH >8) favor NH_3 .

The primary benefits of inducing and maintaining a sufficiently high pH EICP environment (e.g., pH>9) include: (1) increased CaCO_3 saturation that

drives the EICP reaction further towards completion; (2) $\text{NH}_3\text{-NH}_4^+$ speciation that shift towards NH_3 which limits the acidic form (NH_4^+) and reduces the potential for reaction reversal; (3) suppression of typical nitrifying organisms that produce acidic conditions via $\text{NH}_4^+ \rightarrow \text{NO}_3^-$ oxidation since these organisms are typically inhibited at high pH (e.g. $\text{pH} > 9$). Therefore, it is desirable to estimate a urea to CaCl_2 ratio that induces and maintains a high pH environment, but minimizes the amount of excess nitrogen introduced into the surround environment and the costs associated with EICP.

Low concentration tests with an initial ionic strength of 0.5M and urea concentrations less 0.6M show that pH and alkalinity both increase with an increasing initial ratio of urea to CaCl_2 . Nearly all available Ca^{2+} and urea was consumed in the low concentration tests. In the low concentration tests, the greatest increases in pH and alkalinity occurred at the greatest initial ratio of urea to CaCl_2 , which yielded $\text{pH} > 9$ and alkalinity $> 25,000$ mg/L in an actively precipitating CaCO_3 system. Urea to CaCl_2 ratios at or below 1.5:1 showed limited increases in pH and alkalinity, but ratios greater than 2.0:1 showed a slower increase in pH and alkalinity as well as unnecessarily high N-NH_3 production. As such, the data imply that a ratio of 2.0:1 is the upper limit of the range of urea- CaCl_2 ratio that substantially increases pH after the removal of Ca^{2+} and sufficiently buffers the EICP system against a rapid decline in pH. Therefore, the range of initial urea to CaCl_2 ratio that may be most effective with the least amount of residual nitrogen production is between 1.75:1 and 2.0:1 for *low concentrations*.

The first stage high concentration tests (H-series) with an ionic strength of 6.0M and urea concentrations up to 6.0M, produced very different results than the L-series tests. The results from the H-series tests ranged from partial ureolysis and CaCO₃ precipitation of up to 50% of maximum possible, down to no measurable ureolysis or CaCO₃ precipitation. Follow-up tests were performed on the high concentration mixtures at three different initial ratios of urea to CaCl₂ to assess the impact of enzyme precipitation (“salting-out”) as a causative factor in limited ureolysis and CaCO₃ precipitation at high initial concentrations. The results from follow-up tests show large improvements in both ureolysis (75% to 99% urea consumption) and CaCO₃ precipitation (74% to 88% Ca²⁺ removal). In addition, the follow-up tests indicate that enzyme precipitation can be mostly reversed by water dilution to allow for a “restart” of EICP, but that enzyme dissolution at higher initial concentrations may be limited. Enzyme solubility is strongly affected by the presence of NH₄⁺, which is highly capable of driving enzyme precipitation, and further illustrates the need for high pH and alkalinity in the EICP process to keep NH₄⁺ levels low in order to limit salting-out. As seen with the L-series tests, these results indicate that an initial urea to CaCl₂ ratio of 1.5:1 may be too low and that a ratio between 1.75:1 and 2.0:1 may be an optimal range for the EICP process at high concentration.

Finally, the enzyme solubility results from the high concentration follow-up tests imply that the EICP process may be very limited at high initial concentrations unless enzyme precipitation can be addressed. On the other

hand, controlled enzyme precipitation may open the possibility to a controlled EICP process that can be initiated upon water dilution of an enzyme-CaCl₂-urea matrix.

CHAPTER 4

THE EFFECT OF A STATIC SOIL ENVIRONMENT ON ENZYME INDUCED CARBONATE PRECIPITATION

4.1 Introduction

This chapter presents the results of experiments to assess the EICP process in soil-filled acrylic columns rather than the soil-less test tubes employed in the previous chapter. Soil was included in this experiment to (1) determine the impact of a static and partially open soil environment on the chemical changes in the EICP process and (2) to assess the impact of CaCO_3 precipitation on the soil properties. The column tests were performed at equimolar ratios of urea and CaCl_2 at increasing initial concentrations.

The successful application of EICP for soil improvement will likely depend on several factors including temperature, soil characteristics and composition, soil chemistry, pH, and the composition of the EICP medium. This chapter aims to gain insight on the application of EICP in a soil environment and therefore focuses only on a few immediate factors that directly affect CaCO_3 precipitation: (1) increases in pH and alkalinity, and (2) the precipitation of free Ca^{2+} as CaCO_3 .

An important question to be addressed in order to help advance the understanding of the EICP process is determining the necessary concentrations of urea and CaCl_2 required to form CaCO_3 . Specifically, how much urea is needed to precipitate a given amount of available calcium as CaCO_3 ? The primary guiding principle in trying to answer this question is to develop an

EICP formulation that uses all or nearly all of the chemical reagents in the medium, i.e. to maximize the efficiency of chemical constituent usage. In other words, the successful application of EICP should minimize the amount of unused reagents and unnecessary byproducts that are potentially harmful to the EICP process and the environment. Results from the previous chapter indicate that an equimolar initial urea to CaCl_2 ratio (i.e. a ratio of 1:1) produces the least amount of excess nitrogen (stoichiometrically with urea) while consuming approximately 97% of the available Ca^{2+} (as CaCO_3) and approximately 100% of the urea. But, these high reagent utilization results were obtained for tests carried out at relatively low equimolar urea and CaCl_2 concentrations of 0.2 M. Tests conducted at much high equimolar urea and CaCl_2 concentrations of 2.0 M (ten times greater) did not produce similar results: stoichiometrically more NH_4^+ was produced, but only about 1/3rd of the total available Ca^{2+} and urea were consumed. The question addressed in this chapter is will the same results in the chemical changes be seen in a soil-filled environment? Also, how does the resultant calcium carbonate precipitation impact the mechanical properties of the soil? For example, will CaCO_3 precipitation yield inter-particle soil cementation or will it lead to precipitation of CaCO_3 in the pore space instead?

4.2 Methods

Tests were performed to evaluate the EICP process in clear, soil-filled acrylic columns in order to assess (1) the impact of a semi-open and static soil-filled environment on the chemical changes in the EICP process and (2) to assess the outcome of EICP on soil properties such as mechanical strength. The column

tests were performed at equimolar ratios of urea and CaCl_2 (i.e. a 1:1 ratio) and at increasing initial concentrations. The reagents, enzyme type, and methods of preparation used here are the same as those used for the test tube experiments described in Section 3.2.1 with the following exception: the initial pH of the EICP medium used in the acrylic column was approximately 8.75 compared to 8.0 for the test tube experiments. There was no particular reason for adjusting to a higher initial pH, rather this initial pH value (8.75) was due to the unintentionally rapid addition of 1M NaOH under low stir. Other EICP tests (not shown here) show that an initial pH in the range of 7.0 -8.8 has no obvious impacts on the final pH or the EICP process.

All tests were conducted in duplicates with one control column. A total of 15 sand-filled acrylic columns were prepared for these tests: one control column and 14 test columns at 7 different initial concentrations. The columns contained equimolar urea and CaCl_2 concentration ranging from 0.20 M for Columns #1-2 to 2.20 M for Columns #13-14.

A 1-L batch of 3.0 M of urea and CaCl_2 solution was prepared and the pH was adjusted to approximately 8.75. For each concentration employed in the columns, 200-ml aliquots of 3.0 M urea and CaCl_2 solution were diluted to the desired concentrations in glass beakers. Approximately 10-ml of fluid was sampled from the glass beakers to determine initial values of (1) total alkalinity, (2) ion concentrations, and (3) organic carbon. The remaining fluid in the glass beakers received small aliquots of enzyme solution (H_2O for the control) and then the EICP medium was immediately added to the columns. Only one two-

column test set at a time was prepared in this manner and each column then received approximately 70-ml of the EICP reaction medium, which was enough fluid to fill the columns approximately 5-6 mm (0.25”) above the soil line. The tops of the columns were loosely closed-off using clear plastic wrap and laboratory tape and allowed to stand undisturbed for 15 days at room temperature. The details regarding concentrations, test type, and numbering are shown in Table 12.

Table 12 Concentrations, test type, and numbering for the sand-filled columns

Column #	Urea-CaCl₂ (M)	Enzyme Solution	Initial Ratio	Initial pH
1-2	0.20	Yes	1:1	8.75
3-4	0.50	Yes	1:1	8.75
5-6	0.80	Yes	1:1	8.75
7-8	1.10	Yes	1:1	8.75
9-10	1.30	Yes	1:1	8.75
11-12	1.60	Yes	1:1	8.75
13-14	2.20	Yes	1:1	8.75
15	1.10	No	1:1	8.75

The experiment was ended after 15 days by piercing several small holes in the bottom rubber cap of the sand columns using a 16-gauge needle and then removing the plastic wrap that covered the tops. The pore fluid was allowed to drain into a 50-ml glass beaker with a probe in place to measure pH as soon as the fluid height covered the probe tip. Drainage was slow for all 14 test columns, requiring several minutes to drain approximately 15 to 20-ml of pore fluid into the beakers. Note that this was approximately only one-third of the initial total fluid volume, possibly because of the fluid loss observed in all

columns (as discussed below). The columns were drained one at a time and were evaluated for the presence of NH_3 odor while draining. The control column drained slightly more pore fluid over a shorter time than the test columns, but the drained fluid volume was still less than the total fluid volume. Immediately after pH measurements were recorded, the pore fluids were filtered ($0.2 \mu\text{m}$) and alkalinities were determined. Note that some fluids required the use of a second filter to filter the entire fluid volume due to rapid clogging. Approximately 10-ml of filtered pore fluid from each column was poured into a 15-ml PP vial and then sealed and transferred to a freezer (-20°C) until further testing. The columns were allowed to air dry for 7 days before disassembly and further testing.

4.2.1 Soil Filled Acrylic Columns Set-Up

The tests were conducted in clear acrylic columns with an inside diameter of 48 mm x 101 mm long (1.9"x4.0"). The columns were lined with a thin, clear polypropylene (PP) liner to allow for easy soil extraction at the end of the experiment. The bottoms of the columns were closed off with flexible rubber caps that were sealed into place using black silicon tape. The acrylic and rubber components of the sand columns were alcohol sterilized (70% v/v ethanol), while the sand was autoclaved. Small circular sheets of polypropylene (PP) mesh with a $400\text{-}\mu\text{m}$ opening size were placed inside the columns (at the bottom) to reduce soil loss upon draining at the end of the experiment. Each empty column was filled with 275 grams of Ottawa 20-30 sand (US Silica Company), a uniform quartz sand with a mean grain size of 0.6 mm, by pouring

the sand from a drop height of approximately 127 mm (\approx 5-inches). A prepared sand-filled acrylic column is shown in Figure 13 prior to the addition of the EICP reaction medium. The sand-filled columns were then placed in a holding rack and the EICP solution was added and the columns were allowed to stand as described above.



Figure 13 Sand-filled acrylic column before adding the EICP reaction medium.

4.2.2. Chemical Analysis and Physical Characterization

The following analyses and characterizations performed on the test columns and recovered fluid were previously described in Section 3.2.2: total alkalinity via HACH colorimetric Method 10239; chemical analysis of ions through ion chromatography (IC) using a Dionex ICS-3000; chemical carbon profile via a Shimadzu TOC-V Series Total Organic Carbon Analyzer; wet laboratory techniques to confirm the presence of precipitated carbonate minerals. Quantification of CaCO_3 was performed by the method of mass loss after acid digestion as follows: the soil specimens are (1) rinsed with >5 pore volumes of 18.2 M Ω deionized water (DI), (2) oven dried and then weighed to establish a

baseline dry soil weight, (3) acid washed in warm 1.0-2.0 M HCl acid, (3) rinsed with >5 pore volumes of DI water, (4) oven dried and then weighed to obtain the acid digested dry soil weight, and (5) the difference weight before and after acid digestion it is assumed to be the mass loss due CaCO₃ dissolution. Note that in steps #1 and #3 an additional step of several extra DI water rinses of the drained soil column was taken to further assist in the removal of unused salts (e.g Ca²⁺) prior to CaCO₃ quantification. In this step, the soil columns were slowly rinsed using approximately 5 pore volumes of DI water (≈100-ml) while still in the acrylic columns (the rinse water was allowed to drain through a hole pierced the bottom rubber cap). The presence of NH₃ in the soil columns was qualitatively monitored by the odor of NH₃ over the columns and in the extracted pore fluids.

Unconfined compressive strength testing was conducted in a GCTS brand triaxial load frame on the rinsed and drained columns. The intact cemented columns were trimmed to make them flat at the top and bottom before testing. The dimensions of the cemented columns were either very close to or slightly less than the height to width ratio of 2 typically recommended to reduce potential impacts due to edge effects. To mitigate potential edge effects in testing of the relatively short columns, the top and bottom of the specimen were lubricated using a thin sheet of wax paper placed between the cemented soil columns and the pedestal and top-cap. The interfaces between the (a) pedestal and wax paper and (b) top-cap and wax paper were lubricated with a thin layer of petroleum jelly prior to testing.

4.3 Results and Discussion

General Observations

Experiments were performed to evaluate the EICP process in clear, soil-filled acrylic columns, rather than soilless test tubes, in order to assess (1) the impact of a static soil-filled environment on the chemical changes in the EICP process and (2) to assess the outcome of EICP on soil properties such as mechanical strength. The results of subjective, qualitative measures of NH_3 gas and color changes in the sand columns (presumably due to mineral precipitates) are presented in Table 13 as well as tests for the presence of carbonate minerals and other general observations. A significant but unquantified observation not included in Table 13 is the loss of fluid from columns that did not leak. It appears that fluid evaporated from the columns over the 15 days of the experiment and in some cases resulted in enough fluid loss to expose soil at the top of some columns. The loss of fluid resulted in salt deposits that coated the inside upper portions of several acrylic columns where fluid once was. These salt deposits readily dissolved when the columns were rinsed with DI water. The loss of fluid appears to have had an adverse impact on the EICP for soil cementation. For example, the fluid loss in Column #2 resulted in depletion of approximately the top 13-mm of pore fluid where loose (uncemented) soil was found in the area of fluid depletion upon disassembly, the soil below this point was cemented and strongly intact.

Table 13 Results from Columns #1-15. Note that Column #15 is the control column. -- = no odor detected, + = faint, and ++ = strong.

Qualitative-General Observations						
Column #	Test (mol/L)	NH ₃ Odor	Color Change	Carbonate Present	Leak Developed	Column Intact
1	0.20	++	Cloudy	Yes	No	Yes
2	0.20	++	Cloudy	Yes	No	Yes
3	0.50	++	Cloudy	Yes	No	Yes
4	0.50	++	Cloudy	Yes	No	Yes
5	0.80	+	Cloudy	Yes	No	Partially
6	0.80	+	Cloudy	Yes	Yes	Partially
7	1.10	--	No	Yes	Yes	No
8	1.10	--	No	Yes	Yes	No
9	1.30	--	No	Yes	Yes	No
10	1.30	--	No	Yes	Yes	No
11	1.60	--	Cloudy	Yes	Yes	No
12	1.60	--	Cloudy	Yes	Yes	No
13	2.20	--	No	No	Yes	No
14	2.20	--	No	No	No	No
15	1.10	--	No	No	No	No

Most columns did develop leaks at different times within 2-5 days after the start of the experiment. Leaks were sealed as best as possible from the outside using vacuum grease. Collection and/or analysis of lost fluid was not possible since the fluids leaked into a common secondary catchment where they mixed, partially evaporated, and sat for up 24 hours before detection.

The odor of ammonia was detected over Columns #1-6 and subjectively ranged from strong to faint, while no odor was detected over Columns #7-15. But, recalling that the sand columns were only loosely covered and taped at the start of the experiment, some NH₃ may have escaped from these columns if it was present. The initially clear walls of the acrylic test columns #1-6 and #11-12 gradually became cloudy over the duration of the experiment while no color change was observed in Columns #7-10, #13-14, and #15. Columns #1-12

tested positive for the presence of carbonate, while Columns #13-14 and the control column (#15) tested negative. The level of effervesce observed upon acidification was strongest in Columns #1-6, and was variable with no distinctive pattern in the other columns. Columns #1-4 were mostly to entirely intact upon extraction and were tested for carbonate using a single small fragment from either the top or the bottom of the column. Columns #5-6 broke into several pieces upon extraction and the chunks were acid tested in various spots. Columns #7-12 had small randomly occurring intact chunks soil that appeared to be held together by a cementing agent that was subsequently confirmed to be a carbonate. Images from Columns #2 and #4 before extraction are shown in Figure 14.



Figure 14 Columns #1-2 (0.20 M) and #4 (0.5 M) before extraction. Soil exposure due to evaporation was most notable in Column #1.

Although carbonate was detected in most of the test columns (#1-12), the observations described above suggest that EICP may have been more effective in the columns with the lowest concentration of urea and CaCl_2 in the

cementation fluid (#1-6), as evidenced by the strong to faint presence of NH_3 and continuous inter-particle cementation observed in Columns #1-6 (0.20 M to 0.80 M).

Mechanical Testing

The results of unconfined compressive strength (UCS) testing for intact sand Columns #1-4 are shown in Table 14. The trimmed specimens that were used for UCS testing were shorter (64 mm, 2.5”) than the original columns (102 mm, 4”). The % CaCO_3 in shown Table 14 for the shorter mechanically tested specimens were based upon the mechanically tested sections and is not the same as the amount obtained for the overall columns that is shown later in this study in Table 15, which was based upon the average of the mechanically tested sections and the remainder of the soil in the columns and trimmed fragments. The shorter specimens were a consequence of trimming prior to testing and represent the most intact sections of any individual column.

Table 14 Results from unconfined compressive strength testing and acid digestion of mechanically tested specimens. ND = no data.

Column #	Peak strength (kPa)	% CaCO_3	Axial Strain (%)
1	38	0.82	3.55
2	192	0.81	2.20
3	220	ND	3.28
4	210	1.44	2.81

The four sand columns that were tested for UCS were not completely symmetrical along their circumferences. Figure 15 shows Column #2 prior to

and immediately UCS testing. The left image of Figure 15 shows a vertical groove that ran the entire length of the column prior to the start of testing (the groove is indicated by the red arrows). Stress concentrations due to this groove may have led to premature failure. Note the image on the right side of Figure 15 shows a vertical failure plane that appears to follow the vertical gap.

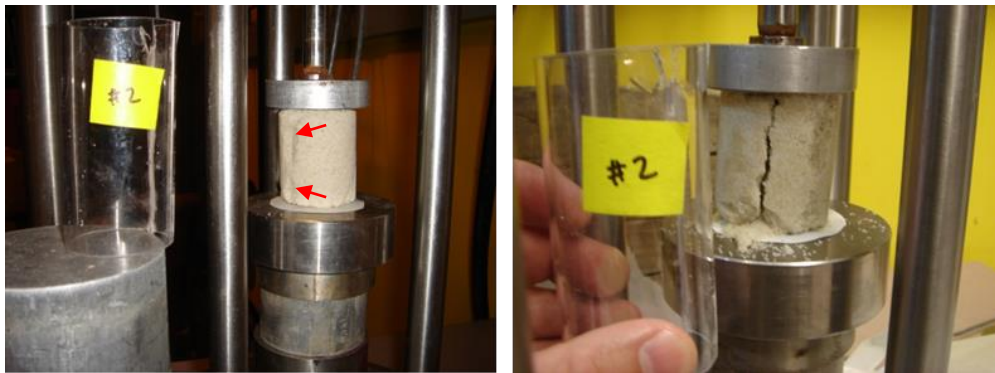


Figure 15 Sand Column #2 before (left) and immediately after (right) UCS testing. The red arrows show a vertical gap along the length of the column where the failure plane occurred.

All of the cemented columns that were tested for UCS exhibited vertical to nearly vertical failure planes. Vertical failure planes are typical in cemented soils with zero confining stress and likely represent tensile splitting that occurs because there is a cohesive component to the shear strength.

Quantification of CaCO_3 Precipitate

The column tests were conducted at equimolar concentrations, so theoretically neither Ca^{2+} nor urea was a limiting reagent. As noted in the

methods sections of this section, a small amount of fluid was sampled from each column to determine initial values of alkalinity, organic carbon, and ion concentrations. Prior to the end of the experiment, it was found via IC and TOC testing that the initial target concentrations of urea and CaCl_2 for test columns #5,6, and 9-14 were between 5-11% *lower* than the target concentrations. For example, Columns #5-6 were expected to have a target concentration of 0.80 M urea and CaCl_2 , but tested values indicated that the actual concentrations were closer to 0.74 M ($\approx 7.5\%$ lower). The tested values for Columns #1-2 were approximately 6.3% *higher* than the target concentration. Columns #3-4, #7-8, and #15 were within reasonable limits of their target concentrations ($\pm 4\%$). As such, the stoichiometric quantification of CaCO_3 was based on the *tested* values rather than the *target* concentrations and the results are shown in Table 15.

Table 15 Results of CaCO₃ quantification. ND = no data, -- = values are not possible since they exceed input parameters of initial concentration.

Test	Calcium				CaCO ₃ (g) Calculated for 70-mL			CaCO ₃ in sand column
	Column #	Target CaCl ₂ -Urea (mol/L)	Tested Initial Conc. (g/L)	Δ Ca ²⁺ (g/L)	% Ca ²⁺ Used	Max. based on Tested Conc.	Amount based on Δ Ca ²⁺	Amount via acid digestion
1	0.20	8.5	-7.4	87.6	1.49	1.30	1.58	0.57
2	0.20	8.5	-5.4	63.1	1.49	0.94	1.55	0.56
3	0.50	19.1	-16.8	87.9	3.35	2.94	ND	ND
4	0.50	19.1	-16.2	84.9	3.35	2.84	3.17	1.15
5	0.80	29.6	-0.9	3.0	5.18	0.15	2.88	1.05
6	0.80	29.6	1.6	--	5.18	--	ND	ND
7	1.10	44.9	0.1	--	7.85	--	ND	ND
8	1.10	44.9	3.2	--	7.85	--	1.07	0.39
9	1.30	48.4	7.4	--	8.47	--	ND	ND
10	1.30	48.4	6.8	--	8.47	--	0.83	0.30
11	1.60	69.3	-2.3	3.3	12.13	0.40	2.80	1.02
12	1.60	69.3	-3.6	5.2	12.13	0.63	ND	ND
13	2.20	86.8	9.2	--	15.19	--	0.31	0.11
14	2.20	86.8	4.1	--	15.19	--	ND	ND
15	1.10	44.9	-1.7	3.7	7.85	0.29	0.19	0.07

Due to the cumbersome nature of CaCO₃ quantification via weight loss through acid digestion and the uncertainties associated with salt removal and soil loss, the whole-specimen carbonate content of only one specimen from each column pair was quantified by acid digestion (except Columns #1-2). The unquantified specimens are indicated as “ND” for no data. The previous section on mechanical testing used a smaller subsection of the overall sand column for CaCO₃ quantification. The last column in Table 15, *weight % of sand column*, represents the average % CaCO₃ of the entire column obtained from the digestions of the mechanically tested specimens (Table 14) and the trimmed/left over soils. The whole-specimen amounts of CaCO₃ (obtained via acid

digestion) are within the maximum amounts possible based on tested concentrations (stoichiometric upper limit), as expected. The maximum amounts of CaCO_3 range from 1.49 grams for Columns #1-2 up to 15.19 grams for Columns #13-14. The estimated amounts of CaCO_3 based on the change in Ca^{2+} concentration (7th column of Table 15) is within the theoretical upper bound as expected. But, in several cases, the changes in Ca^{2+} concentrations are outside of the range calculated using input parameters of initial concentration. For example, Columns #6-10 and #13-14 show net *increases* in Ca^{2+} concentrations that are beyond a reasonable margin of error (\approx 6-15% increases).

One possible explanation for the relatively large net increases in measured Ca^{2+} is that dehydration of pore fluid will concentrate dissolved salts in the bulk fluid. Fluid samples drawn from columns where leakage and/or evaporation occurred may reflect concentration environments near the bottoms of the columns where most of the bulk fluid is expected. Referencing Tables 13 and 15, Columns #6-13 developed a leak at some point in addition to evaporative losses, and these are also the same sand columns where there is no agreement in CaCO_3 quantification data.

One possible explanation for some of the differences between the maximum amount of CaCO_3 based on the tested concentration (6th column, Table 15) and the amounts determined via acid digestion may be due to the loss of small (<0.40 mm) CaCO_3 particles. CaCO_3 precipitates form in a wide range of sizes and may not necessarily be bound to soil particles or other larger CaCO_3 crystals. One example of this phenomenon is mineral precipitation in

the soil pore fluid that does not nucleate onto soil particles but rather precipitates, and possibly grows, as a discrete particle in the soil pore space. The PP mesh placed at the bottom of the sand columns had openings of 0.40 mm that may have allowed loss of pore space calcite during initial draining and subsequent rinse cycles.

Chemical Analysis

The chemical analysis results from the sand column tests are shown in Table 16, but calcium data which can be found in Table 15 was excluded from this table.

Table 16 Chemical analysis results from the sand column tests. Calcium data can be found in Table 15. -- indicates that values are not possible since they exceed input parameters of initial concentration.

Test Column #	Urea Utilization			NH ₄ ⁺		Alk.	pH	Inorganic Carbon
	Tested Initial Conc. (mol/L)	Net Δ (mol/L)	% Used	Stoich. Max. (g/L)	IC-Measured (g/L)	Net Δ (mg/l CaCO ₃)	Net ΔpH	Net Production (mol/L)
1	0.19	-0.19	100	6.85	7.22	398	-1.21	0.19
2	0.19	-0.19	100	6.85	6.87	738	-1.05	0.19
3	0.40	-0.40	100	14.42	15.92	679	-0.98	0.40
4	0.40	-0.40	100	14.42	14.14	447	-1.31	0.40
5	0.71	-0.01	1.4	0.36	4.06	113	-1.61	0.01
6	0.71	0.08	--	-2.88	3.46	161	-1.77	--
7	1.05	0.00	0.0	0.00	1.20	99	-1.99	0
8	1.05	0.03	--	-1.08	1.12	109	-2.23	--
9	1.04	0.19	--	-6.85	0.00	101	-2.03	--
10	1.04	0.18	--	-6.49	0.58	161	-2.46	--
11	1.29	0.20	--	-7.21	0.00	180	-2.25	--
12	1.29	0.01	--	-0.36	0.00	232	-2.45	--
13	1.96	-0.31	15.8	11.18	0.00	82	-3.32	0.31
14	1.96	-0.31	15.8	11.18	0.00	82	-3.32	0.31
15	1.05	-0.03	2.9	1.08	0.00	10	0.15	0.03

The chemical analysis results from Columns #1-4 show a logical and recognizable pattern of urea consumption, alkalinity increases, Ca^{2+} removal (Table 16), and subsequent pH reduction. IC-measured NH_4^+ concentrations also correlated well with urea consumption and the stoichiometric maximums. These are the same columns (#1-4) that were continuously cemented and intact for UCS testing.

Columns #6 and #8-12 (which were not strongly cemented) showed *increases* in urea concentrations implying that ureolysis did not occur, but alkalinity rose by 99-232 (mg/L as CaCO_3) in these columns. Most of these same columns showed increases in Ca^{2+} concentrations, but with large pH decreases implying that CaCO_3 precipitation had occurred. In fact, all columns except for #13-14 and the control tested positive for the presence of a carbonate mineral. The IC-measured NH_4^+ concentrations do not correlate well with urea consumption and the stoichiometric maximums and indicate that ureolysis leading to the production NH_4^+ did not occur. While most of these columns (#7-14) were not continuously cemented or intact (except for Columns #5-6 that broke into several pieces upon extraction), all of the specimens showed some signs of cementation and indicated the presence of carbonate upon acid digestion. The source of this discrepancy is unknown.

It was expected from the work in the previous chapter that Columns #13-14 may undergo very limited to no ureolysis due to protein salting-out effects. It is difficult to draw any logical assessments from the chemical analysis results for Columns #5-12. This is especially challenging when

considering the physical observations and positive results of acid spot testing (Columns #1-12), odor of NH_3 (#1-6), color changes (#1-6, #11-12), intact columns (#1-6), and digestion data. Concentration increases in urea and Ca^{2+} from the initial values may be due to solute concentration effects as previously discussed and discrepancies in CaCO_3 quantification may be due particle loss during pore fluid draining. But, the absence of NH_4^+ in Columns #5-14 is difficult to understand. Many of the columns developed a leak at one point in addition to evaporative losses over the 15 days of the experiment. Ammonium is an exceptionally soluble and mobile substance, and although highly speculative, some NH_4^+ may have been lost to salt deposits that coated parts of the columns or ammonium carbonate $((\text{NH}_4)_2\text{CO}_3)$ precipitates.

4.4 Conclusion

The chemical analysis results from Columns #1-4 show a logical and recognizable pattern that for the most part is generally typical of what was anticipated for the EICP process. This logical pattern was not the case for the 10 sand columns (#5-14) that exhibited large variability and seemingly unexplainable increases in Ca^{2+} and urea from the initial values. Although it is uncertain what the actual reasons are for the large discrepancies in the chemical analysis data, poorly mixed environments that concentrate solutes can complicate the EICP process considerably. For example, concentrated Ca^{2+} may actually improve EICP by increasing CaCO_3 saturation and thereby precipitation (assuming sufficient CO_3^{2-} is available). But, this may also lead to discontinuous carbonate precipitation or precipitation that proceeds too rapidly

for large continuous crystal growth. Dehydration can also compound the effects of poorly mixed environments that concentrate solutes and complicate the EICP process and may also become location specific. For example, the effective concentration of a dehydrating bulk solution may be much greater than the initial value, but this could be even greater along dehydration fronts. It should be noted that all of the results obtained herein were also affected by the limitations involved with obtaining representative pore fluid samples and controlling for the potential mineral and pore fluid losses.

The effects of CaCO_3 precipitation on the soil properties of Columns #1-4 indicate that EICP treated soils show an increase in shear strength due to inter-particle cementation. There were four columns that were continuously cemented and capable of UCS testing. UCS testing results show that the shear strength of cemented specimens ranged from approximately 38 kPa (0.20 M initial concentration) to 220 kPa (0.50 M) and likely increased with increasing CaCO_3 content. Columns #5-6 were partially cemented and broke into large fragments upon extraction and were therefore not amendable to UCS testing. The other sand columns (#7-14) in which testing indicated that CaCO_3 precipitation had occurred were discontinuously cemented and composed of mostly small chunks of weakly cemented soil.

CHAPTER 5

INFLUENCE OF SOIL TYPE AND PREPARATION METHOD ON CEMENTED SAND COLUMNS

5.1 Introduction

This chapter includes the results of additional unconfined compression tests and triaxial compression tests conducted on columns of sand improved using EICP. In Chapter 4, mechanical testing of EICP improved soil columns was performed via unconfined compression testing. Although the unconfined compressive strength (UCS) is an informative strength measure, triaxial compression testing is more useful with respect to characterizing the strength of EICP-improved soil for most geotechnical engineering purposes. Triaxial testing allows for characterization of the impact of overburden stress on the strength of EICP-improved soil via the Mohr-Coulomb failure criterion (e.g., p - q plot). In addition, the EICP tests in Chapter 4 used only Ottawa 20-30 silica sand, a medium coarse quartz sand, improved by percolation of the EICP solution through the specimen. In this chapter, the effects of EICP on the mechanical strength of fine grained soils and the method used to improve the soil via EICP are investigated.

Experiments were performed in six soil-filled acrylic columns to evaluate the effect of the method of sample preparation on the strength of EICP improved soil. Experiments were also conducted in three columns formed in split molds to facilitate triaxial compression testing to evaluate (1) the influence of application of a confining pressure on EICP improved soil and (2) the

effectiveness of the EICP process on the mechanical strength properties of two different soil types (medium and fine sand).

The experiments performed in the six soil-filled acrylic columns were conducted to evaluate the effect of the sample preparation method on EICP soil improvement as follows: three columns were prepared using the percolation method (Columns #1-3), and three columns were prepared using a mix-and-compact method (Columns #4-6). Experiments performed on the EICP columns formed in split molds used the percolation method of preparation. The results of these tests demonstrate the effect of the method of sample preparation on the unconfined strength of EICP-improved sand, the effects of EICP on the mechanical strength properties of two different soil types (medium and fine sand), the influence of a confining pressure on the behavior of EICP-treated sand, and highlight the morphological features of EICP in sand via SEM analysis.

5.2 Set-up

5.2.1 Columns Improved by Percolation

Sand column tests were conducted to induce CaCO_3 precipitation in five columns of Ottawa 20-30 medium-coarse sand and one column of Ottawa F-60 medium grain sand through percolation of the EICP solution into the sand. Three of these tests were carried out in 152 mm x 51 mm (6"x 2") clear acrylic columns closed-off at the bottom with a rubber cap similar to the acrylic columns used in previous chapter. Unlike the acrylic columns in the previous

chapter, the rubber caps used here were sealed with silicone glue rather silicone tape and a PP liner was not used.

Three sand columns were prepared by percolation in rubber membrane-lined 71 mm x 152 mm (2.8" x 6") aluminum split molds (jackets) designed for forming specimens for triaxial testing. The membrane liner for the split mold was attached to the pedestal using two conventional (round/oval) o-rings and supported by the aluminum jacket for the duration of the EICP portion of the experiment.

The three acrylic columns, labeled Acrylic Columns #1-3, were filled with 20-30 Ottawa silica sand (mean grain size 0.6 mm, coefficient of uniformity 1.1) as follows: in Acrylic Columns #1 and #2 the sand was dry pluviated via funnel at 76 mm (3") drop height; in Acrylic Column #3, the lower-third of column was filled with a sand and dry enzyme (\approx 3g) mixture, and the remainder of the column contained dry pluviated sand without enzyme. The two first two triaxial columns were filled with Ottawa sand in the same manner as described for Acrylic Column #1 and labeled Triaxial Columns #1-2. One additional triaxial column was prepared using Ottawa F-60 silica sand (mean grain size 0.275 mm, coefficient of uniformity 1.74) to investigate EICP in a finer grained material. The sand was placed in the same manner as described above for the triaxial columns that used the Ottawa 20-30 sand. This column was designated Triaxial Column #3.

5.2.2 Columns Improved by Mixing and Compacting

In addition to the six tests described above, three additional column tests were set-up in 152-mm x 51-mm acrylic cylinders using Ottawa 20-30 (2 columns) and F-60 sand (1 column). The EICP process used to improve these columns was a mix-and-compact method. In the mix-and-compact method, the EICP solution was added to an empty column followed by addition of the sand. The solution and sand were thoroughly mixed using a polypropylene (PP) stir rod and then compacted by tamping the soil using a compaction rod that was approximately 25 mm (1") in diameter. These tests were carried out in the same type of clear acrylic columns as described above, but with the use of a PP liner. These columns were designated Acrylic Columns #4-6.

5.3 Treatment Methods

Percolation Type

After the first three acrylic sand columns (Acrylic Columns #1-3) were set-up and assembled, they were treated as follows: Acrylic Columns #1-3 each received approximately 100-ml of pH=7.8 EICP solution (described below) on the first application. The solution applied to Columns #1 and #2 included urease, while urease was omitted from the solutions applied to Acrylic Column #3. The amount of solution that Acrylic Columns #1-3 would accept was notably reduced in subsequent applications when, following gravity drainage of the columns, less than 75-ml was required to fill the columns to ≈ 12 mm (0.5") above soil line. Acrylic Column #1 ultimately received five applications of the EICP solution for a total solution volume of approximately 350-ml; Column #2

ultimately received two applications of the same EICP solution for a total solution volume of approximately 150-ml; Column#3 ultimately received two applications of the EICP solution *without enzyme added* for a total volume of approximately 150-ml. The EICP solution used in the first application to Acrylic Columns #1-2 contained approximately 383 mM urea (reagent grade, Sigma-Aldrich), 272 mM CaCl₂-2H₂O (laboratory grade, Alfa Aesar), 1.4 g/L of low-grade urease powder (Fischer Chemical, jack bean urease powder, typical activity = 200 units/g), and stabilizer (4.0 g/L). Acrylic Column #3 initially received a similar EICP solution, but without enzyme added.

Subsequent applications in these acrylic columns employed approximately 50-ml of a pH=7.6 solution containing approximately 416 mM urea and 289 mM CaCl₂-2H₂O without enzyme. Solution concentrations, while variable, were formulated within a reasonably similar range as a matter of convenience. In each application, the solution was poured into the top of the acrylic column. The columns were allowed to stand loosely covered for at least 24 hours and then drained through the bottom cap. Drainage was accomplished by puncturing the plastic caps at the base of the columns with a 20-gauge needle. When drainage was complete, the needle was removed and the puncture was plugged with a dab of silicone. Occasionally, the needle became plugged and an additional needle was inserted through the base to fully drain the specimen. The next application followed immediately after drainage was complete.

Each of the two triaxial columns that contained the Ottawa 20-30 sand received two applications of the same EICP enzyme solution used in the acrylic columns at approximately 250-ml per application. The triaxial columns were allowed to stand for at least a week after the second EICP application and then drained. Draining was accomplished by piercing the temporary silicone seal in the pedestal port with a needle. The port was resealed with a dab of silicone before the second EICP application. Upon termination of the EICP portion of the experiment, the triaxial columns were drained and then triple-washed with DI water. The DI water was allowed to drain from the columns and then the columns were moved to a triaxial testing device. The Ottawa 20-30 triaxial column specimens were washed and acid digested upon completion of mechanical testing.

The triaxial column using Ottawa F-60 sand received two applications of EICP solution, the first one with enzyme and the second one without enzyme, at approximately 250-ml per application. The EICP solution for the first of the two applications contained approximately 2.0 g/L enzyme (low-grade), 400 mM urea (reagent grade, Sigma-Aldrich), 300 mM $\text{CaCl}_2 \cdot 2\text{H}_2\text{O}$ (laboratory grade, BDH) at pH=7.7. The EICP solution for the second application contained 1 M urea- $\text{CaCl}_2 \cdot 2\text{H}_2\text{O}$ solution at pH=7.8 without any enzyme. After the test, the Ottawa F-60 triaxial specimen was washed and acid digested in the same manner as the Ottawa 20-30 triaxial specimens.

In each application of the EICP solution (with and without enzyme) for all acrylic and triaxial columns, the solution was added until it rose to

approximately 12 mm (½-inch) above the soil line. After two applications, Acrylic Columns #2 and #3 were triple washed and drained as described above, and then allowed to air dry for several days before being analyzed. Treatment of Acrylic Column #1 was continued for several more days as three more batches of EICP solution were applied. The last two applications of EICP solution to Acrylic Column #1 were allowed to slowly drain through a needle in the base of the column immediately after application rather than sit for 24 hours (drainage rate \approx 10-25ml/hour)--needles were replaced as needed due to clogging. After initial draining, the columns were drained and rinsed as previously described. A summary of the set-up and composition of the percolation type columns is shown in Table 17.

Table 17 Summary of the **percolation type** columns. Asterisk indicates that dry enzyme powder was mixed with the sand rather than the urea-CaCl₂ solution.

Name	Column Type	Soil Type	Total volume of EICP Solution	Vol. that Contained Enzyme
Column #1	Acrylic	20-30 sand	350-ml	100-ml
Column #2	Acrylic	20-30 sand	150-ml	100-ml
Column #3	Acrylic	20-30 sand	150-ml	0*
Triaxial #1	Triaxial	20-30 sand	500-ml	500-ml
Triaxial #2	Triaxial	20-30 sand	500-ml	500-ml
Triaxial #3	Triaxial	F-60 sand	500-ml	250-ml

Mix-and-Compact Type

The three PP-lined mix-and-compact sand columns (Acrylic Columns #4-6) were assembled and treated as follows: Acrylic Columns #4 and #5 each received a single application of approximately 100-ml of a pH=8.7 EICP

solution containing 1.3 M CaCl₂·2H₂O and 1.6 M urea (Sigma Aldrich, reagent grade), stabilizer (4.0 g/L), and 0.85 g/L low-grade urease enzyme (previously described). Acrylic Column #6 was a control that received the same EICP solution as the other 3 mix-and-compact columns but without enzyme. The columns were compacted by applying light to moderate pressure to the mixed soil surface using a metal compaction rod. The sand columns were prepared one at a time and were loosely covered with plastic wrap and lab tape after compaction was complete. The columns were allowed to cure for approximately 30 days, after which time they were drained, rinsed, and acid digested as previously described. A summary of the set-up and composition of the mix-and-compact type columns is shown in Table 18.

Table 18 Summary of the **mix-and-compact type** columns.

Name	Column Type	Soil Type	Total volume of EICP Solution	Vol. that Contained Enzyme
Column #4	Acrylic	20-30 sand	100-ml	100-ml
Column #5	Acrylic	F-60 sand	100-ml	100-ml
Column #6	Acrylic	20-30 sand	100-ml, no enzyme	0

5.3.1 Mechanical Testing, Chemical Analysis and Physical Characterization

Unconfined compressive strength testing was conducted in a GCTS brand load frame on cemented sand samples extracted from the mix-and-compact Acrylic Columns (#4-5). Drained triaxial testing was performed on the triaxial columns using the GCTS load frame. Wet laboratory techniques were used to confirm the presence of precipitated carbonate minerals after

mechanical testing. Quantification of CaCO₃ was performed by the method of mass loss after acid digestion described in the methods section of Chapter 4.

The three non PP-lined percolated Acrylic Columns #1-3 were not strength tested but were tested for CaCO₃ content as follows: Acrylic Columns #2 and #3 were separated into three layers for CaCO₃ quantification, while Acrylic Column #1 was separated into six layers for better resolution. Each layer from the specimens in the percolated acrylic columns and the entire mass of each of the triaxial specimens were quantified. The CaCO₃ content of each of the mix-and-compact columns was quantified as one entire mass rather than in separate layers.

Scanning electron microscopy and X-ray diffraction were used for analysis and characterization of cemented chunks of soil as previously described in Section 3.2.2. Some specimens were analyzed using a different type of SEM called a Low-Voltage SEM. These analyses were performed using an Agilent 8500 Low-Voltage SEM (LV-SEM). An LV-SEM is a field emission scanning electron microscope capable of imaging insulating materials, such as organic and biological substances without the need for a metal coating and without causing radiation damage to samples.

5.4 Results and Discussion

5.4.1 Percolation Type

Acrylic Columns

The results of subjective, qualitative measures of NH₃ gas and color changes in the sand columns (presumably due to mineral precipitation) are

presented in Table 19 along with the quantitative tests for the presence of carbonate minerals and other general observations. None of the columns leaked and fluid evaporation was not observed during treatment of these columns since these columns received multiple applications of EICP solution over short intervals during the course of the experiment.

Table 19 Qualitative-general observations for **percolation** Acrylic Columns #1-3 and Triaxial Columns #1-3. ++ = strong odor of NH₃ detected. Color changes in the triaxial columns were observed from the top as this was the only place soil was visible.

Name	Soil Type	NH ₃ Odor	Color Change	Carbonate Present
Column #1	20-30 sand	++	Yes	Yes
Column #2	20-30 sand	++	Yes	Yes
Column #3	20-30 sand	++	Yes	Yes
Triaxial #1	20-30 sand	++	Yes-top view	Yes
Triaxial #2	20-30 sand	++	Yes-top view	Yes
Triaxial #3	F-60 sand	++	Yes-top view	Yes

At the conclusion of the experiment, white mineral precipitation was visible along the entire length of unlined Acrylic Columns #1 and #2. Figure 16 shows the columns with the white internal precipitate that was later determined to be a carbonate mineral (presumably CaCO₃) via acid testing. The bottom third of Acrylic Column #3 (dry enzyme added to soil) was mostly cemented with some areas more cemented than others.



Figure 16 Percolation Acrylic Columns #1, #2, #3 (left to right). Acrylic Columns #1 and #2 showing carbonate mineral precipitate along the inside walls.

Percolation Acrylic Column #1 yielded mostly small, loose chunks of sand with strong effervescence upon digestion. Most of this column appeared un-cemented and exhibited unusually viscous behavior when wet. A fairly large piece (in comparison to the column diameter) of strongly cemented sand formed in the deepest layer of Acrylic Column #1. This strongly cemented piece was difficult to break without the use of hand tools. Acrylic Column #2 had many small chunks of weakly cemented sand with strong effervescence upon digestion. Acrylic Column #3 had little to no precipitation in the top layer based upon acid digestion results. The deepest layer of Acrylic Column #3 contained many pieces of weakly cemented sand that effervesced strongly upon digestion. The middle layer of Acrylic Column #3 contained a few pieces of cemented sand that effervesced moderately upon digestion. The results from the acid digestion tests for Acrylic Columns #1-3 are presented in Table 20.

Table 20 Summary of results from the acid digestion tests for **percolation** Acrylic Columns #1-3.

Test		% Change	Amount of CaCO ₃ (g)		
Column #	Layer	Wt. Change via Digestion	via Acid Digestion	Total via Digestion	Stoich. Max
1	1	11%	3.57	11.8	≈14.5
	2	3.80%	1.67		
	3	2.70%	1.73		
	4	2.10%	1.4		
	5	2.30%	1.74		
	6	2.00%	1.64		
2	1	0.76%	0.63	2.07	≈ 4.35
	2	0.65%	0.69		
	3	0.49%	0.75		
3	1	0.23%	0.31	3.57	≈ 4.35
	2	0.58%	0.63		
	3	1.70%	2.63		

The theoretical maximum CaCO₃ content is the stoichiometric maximum based upon the concentrations and volumes of solution applied to the columns. The primary experimental differences between the tests are (1) the number of applications of cementation fluid and (2) the manner in which the urease was delivered. The results indicate that there is greater carbonate precipitation with increasing number of applications, as expected. The data show more precipitation in (or on) the top layer of Acrylic Columns #1 and 2 but not in Acrylic Column #3 (not unexpected, as the enzyme was physically confined to the lower-third layer in Acrylic Column #3 during sample preparation). In the top layer of Acrylic Column #3, where no urease enzyme was mixed with the sand, carbonate precipitation was nearly undetectable (as expected). There was no visual evidence of precipitation and practically no

measurable change in weight of this layer after acid digestion (weight change = 0.23%). In the bottom layer of Acrylic Column #3, where approximately 3 grams of dry enzyme was mixed with the soil, there was a weight change of approximately 1.7% following acid digestion. The middle layer of this specimen had a minor change in weight ($\approx 0.58\%$), possibly due to uneven distribution of the layers during preparation or splitting of the specimen. It is also possible that there was some upward migration of urease that was in solution from the bottom layer.

XRD analysis, presented in Figure 17, confirms that calcite is the mineral phase present in the cemented soil chunks. LV-SEM images, presented in Figure 18, show silica (quartz) sand particles cemented with CaCO_3 and various morphological features associated with the cementation process on the silica surface.

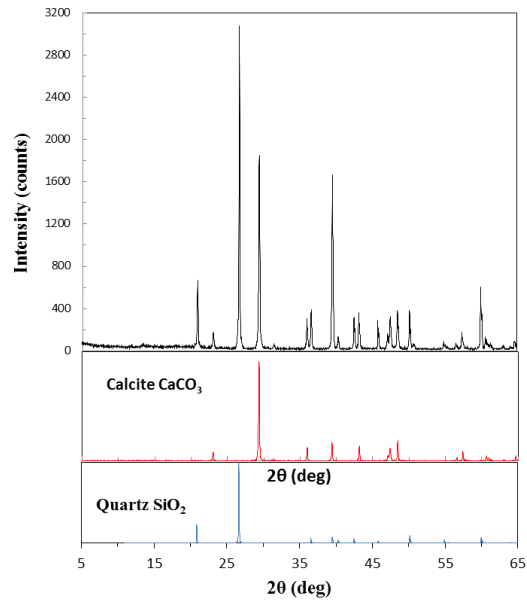


Figure 17 XRD results from a cemented sand sample (top plot). Calcite and quartz & calcite standards are shown in the middle & bottom plots, respectively.

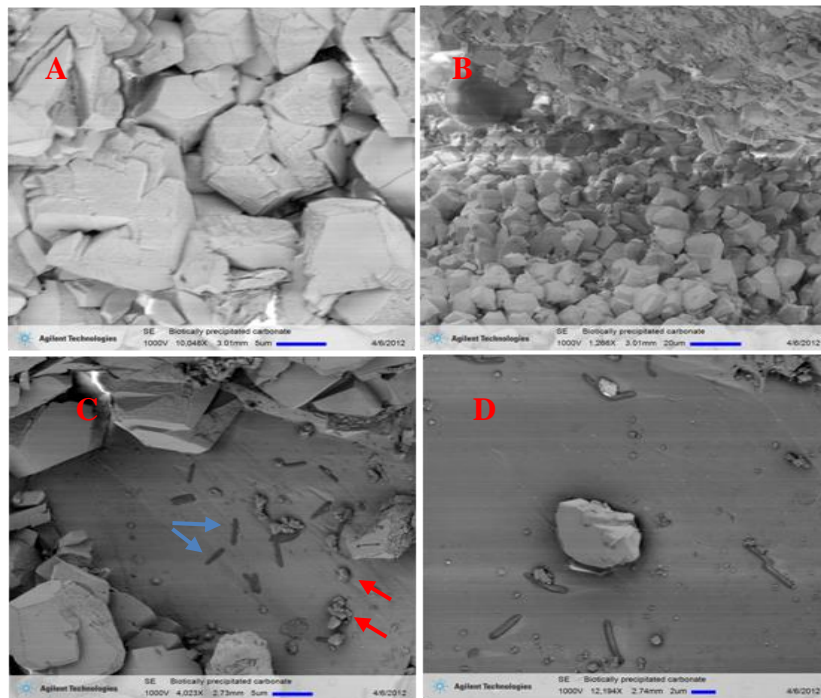


Figure 18 LV-SEM images: a.) Well-grown and cementing calcite crystals; b.) Cementing calcite crystals at inter-particle contact; c.) Indentation of quartz surface (blue arrows) and nucleation of calcite crystals (red arrows); d.) Calcite crystal growing on quartz surface.

Triaxial Columns

The three triaxial sand columns (2 Ottawa 20-30 sand columns and 1 Ottawa F-60 sand column) were tested in drained triaxial compression subject to a confining pressure of 60 kPa and then acid digested. All three columns were able to stand upright after removal of the split mold. The results of the triaxial compression tests performed on the 20-30 Ottawa sand are presented in Figure 19 and the results for the F-60 Ottawa sand are presented in Figure 20. The carbonate cement content for one of the 20-30 silica sand columns was 2.0% CaCO_3 (w/w). The carbonate content of the other 20-30 Ottawa sand column could not be quantified due to unintended sample loss. The carbonate cement content for the finer grained F-60 Ottawa sand was 1.6% CaCO_3 (w/w). The results show substantial strength increase for all three sand columns tested.

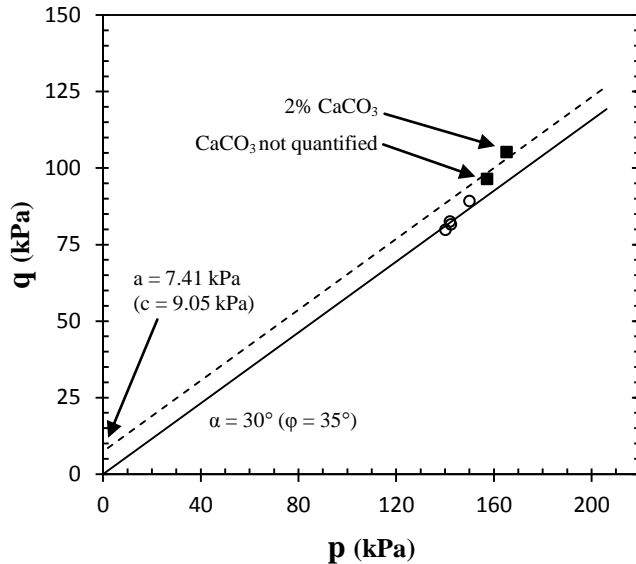


Figure 19 p-q plot failure envelopes for 20-30 silica sand: ■Cemented ($D_r = 60\%$); ○ Uncemented ($D_r = 60\%$) specimens used for strength comparison to the cemented specimens.

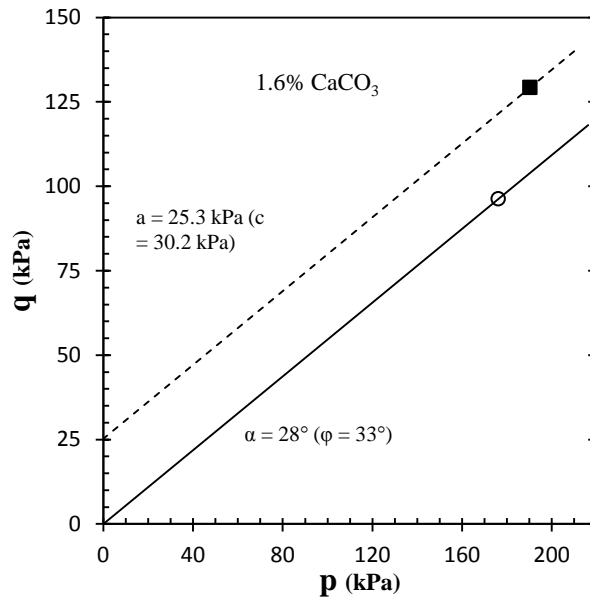


Figure 20 p-q plot failure envelopes for F-60 silica sand: ■Cemented ($D_r = 35\%$); ○ Uncemented ($D_r = 37\%$).

A few small fragments of Triaxial Column #1 were saved for further analysis after mechanical testing. Triaxial Column #1 is shown before and after triaxial testing in Figure 21. Triaxial Column #1 showed a large and strongly cemented center and several broken chunks and many loose pieces of 20-30 sand after triaxial testing. Figure 22 shows SEM images from Triaxial Column #1 show the surfaces of rounded sand particles covered in rough, cauliflower-like layers of CaCO₃.



Figure 21 Triaxial sand Column #1 standing without support with a weighted stainless steel top-cap (left image). A large strongly cemented center and several broken pieces found after triaxial testing (right).

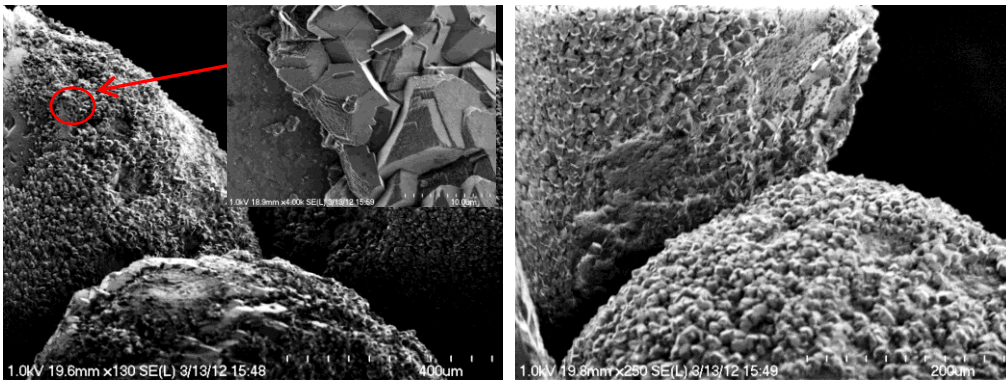


Figure 22 SEM images from triaxial sand Column #1 of sand particles (round) covered in cauliflower-like patches of CaCO_3 .

5.4.2 Mix-and-compact Type

The results of subjective, qualitative measures of NH_3 gas and color changes (presumably due to mineral precipitation) for the mix-and-compact columns #4-6 are presented in Table 21 along with the quantitative tests for the presence of carbonate minerals and other general observations. None of the columns leaked during the experiment, but some small but unquantified amount of fluid was lost due to evaporation.

Table 21 Qualitative-general observations for mix-and-compact Acrylic Columns #4-6 (#6 is the control).

Name	Soil Type	NH₃ Odor	Color Change	Carbonate Present
Column #4	20-30 sand	++	Yes	Yes
Column #5	F-60 sand	++	Yes	Yes
Column #6	20-30 sand	--	No	No

The drained and rinsed soil masses for Acrylic Columns #4-6 were extracted from the acrylic tubes by carefully pulling on the PP liner after removal of the rubber bottom caps. The sand columns were solid and difficult to pull out of the acrylic tubes especially during the first few inches of extraction. Acrylic Column #4 was cemented and remained intact after extraction and removal of the PP liner. Acrylic Column #5 was cemented but broke into two pieces of roughly equal size during extraction. The soil in Acrylic Column #6 (control) was loose and did not appear to be cemented. The three columns were allowed to stand for approximately 7 days and then tested for the presence of CaCO₃. Acrylic Columns #4-5 tested positive for CaCO₃ and control Acrylic Column #6 tested negative. Acrylic Columns #4-5 appeared to be strongly cemented and were trimmed and then moved to a triaxial device for unconfined compressive strength (UCS) testing. Figure 23 shows Acrylic Columns #4 and #5 prior to and during UCS testing.



Figure 23 Acrylic Columns #4-5 prior to and during UCS testing. The 2 left images are 20-30 sand and the 2 right images are F-60 sand.

The results of the UCS tests performed on the 20-30 Ottawa sand (Col. #4) and the F-60 Ottawa sand (Col. #5) are presented in Table 22. The carbonate cement content for the 20-30 silica sand column was 2.82% CaCO_3 (w/w). The carbonate cement content for the finer grained F-60 Ottawa sand was 4.30% CaCO_3 (w/w). The results show substantial strength increase for both sand columns tested. The carbonate content of the control Acrylic Column #6 was estimated to be approximately zero since multiple acid spot tests were negative for the presence of carbonate.

Table 22 Results of UCS testing and acid digestion for Acrylic Columns #4 and 5.

Column #	Peak strength (kPa)	% CaCO_3	Axial Strain (%)
4	529	2.82	0.70
5	392	4.30	1.60

A few small fragments from Acrylic Column #4 were saved for SEM analysis after mechanical testing. Two SEM images from Acrylic Column #4

that illustrate the inter-particle cementation are shown in Figure 24. The images are taken at different magnifications and show (1) CaCO_3 at inter-particle contacts and (2) a detachment point on a concave CaCO_3 surface that is still attached to another sand particle.

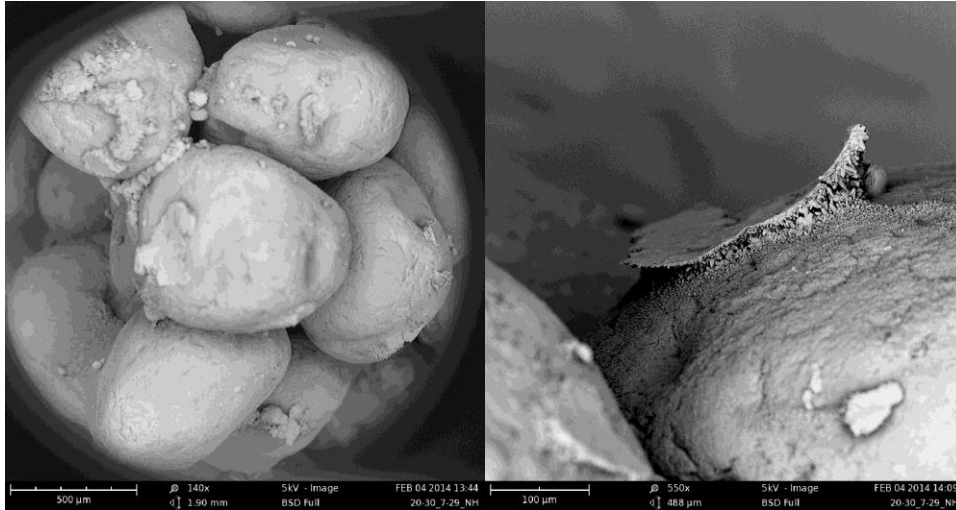


Figure 24 SEM images from mix & compact Acrylic Column #4 (20-30 sand). Note detachment point on concave CaCO_3 surface (right).

5.5 Conclusion

EICP was applied to soil through two different methods: percolation and mix-and-compact, using both medium-coarse and medium sands. The percolation method was applied in two different manners: dry pluviation followed by percolation of a calcium-urease-urea cementation solution and mixing the sand with dry urease powder prior to pluviation with a calcium-urea only solution (no enzyme). The mix-and-compact method was applied by pouring soil into a column containing the EICP solution followed by thorough mixing and light to moderate compaction effort.

Cementation of soil particles was observed in all test columns except the control column prepared without urease. XRD testing performed on selected columns from each method type confirmed that calcite phase CaCO_3 was the cementing agent. SEM imaging indicates that the morphological features of EICP in silica sand through mix-and-compact and percolation methods appeared to be similar in both cases. This preliminary finding is generally consistent with previous results that show morphological features are mostly likely related to concentrations and environmental conditions of precipitation, both of which were in a similar range across these experiments.

Acid digestion showed that the multiple applications used in the percolation method yielded correspondingly greater carbonate precipitation. The quality of cementation, as determined by the effort needed to break apart cemented chunks of sand, varied depending on the sampling location within the column. Triaxial test results on cemented columns showed substantial strength increase over non-cemented columns at the same relative density. The results of unconfined compressive testing show substantial strength increase for both mix-and-compact test columns: the mix-and-compact column prepared with Ottawa 20-30 sand and the mix-and-compact column prepared with F-60 sand.

It is worth noting that the initial urea to CaCl_2 ratios used in these experiments ranged from approximately 1.2:1 to 1.5:1. But, the low-grade Fischer enzyme used here has a specific activity (200 units/gram) that is approximately 150 to 250 times *lower* than the Sigma Aldrich enzyme used in experiments presented in Chapters 3 and 4. Although unconfirmed, it is

reasonable to expect that an overall slower EICP process and that a slower CaCO_3 growth mechanism will prevail under these conditions. In addition, the highest initial concentration used in these experiments was approximately 1.3 M CaCl_2 ($I = 3.25 \text{ M}$) for mix-and-compact Acrylic Columns #4-6, which resulted in inhibited ureolysis and enzyme salting-out in previous tests using a highly active (purified) urease. This did not appear to be the case using low-grade enzyme.

CHAPTER 6

COLUMNAR STABILIZATION USING EICP

6.1 Introduction

This chapter illustrates the applicability of EICP as a method of improving soil by creating columns of cemented sand. The columns were made by infusing an EICP cementation solution through a perforated injection tube embedded within the soil. In Chapters 4 and 5, cemented specimens were created in cylindrical molds through (1) wet pluviation of soil into the EICP solution, (2) mixing and compacting the soil and EICP soil, (3) percolation of the EICP solution into soil, and (4) percolation of a CaCl_2 and urea solution into a dry mixed soil containing enzyme powder. One reason the cemented soil specimens were formed in cylindrical molds was to provide a uniform shape amenable to mechanical testing.

The experiments described in this chapter were performed in progressively larger soil containers. Columnar cementation was induced through EICP using Ottawa 20-30 and F-60 silica sand in 102-mm (4") diameter PVC columns and 19-L (5-gallon) buckets, and using native (Arizona) sand in an approximately 1-m^3 soil box. Three tests were conducted in the 102-mm diameter columns using Ottawa 20-30 and F-60 sand, six tests were conducted in the 19-L buckets using the 20-30 silica sand, and one test was conducted in the $\approx 1\text{-m}^3$ soil box using the native sand. Chemical analyses presented in Chapter 3 indicated that the EICP process performs best at initial urea to CaCl_2 ratios between approximately 1.50:1 and 2.0:1. Except for a smaller follow-up

injection at approximately 1.1:1 for the experiments using 102-mm diameter PVC columns, the experiments performed here received an initial ratio of urea to CaCl_2 of approximately 1.5:1 to 1.7:1 (+/-0.05).

6.2 Set-up and Methods

6.2.1 Four-inch Diameter PVC Tubes

Experiments were conducted in three clear PVC columns (Schedule 40) that were approximately 305-mm (12") long by 102-mm (4") in inner diameter (I.D.). The columns were labeled "PVC Column #1," "PVC Column #2," and "PVC Column #3." One end of each PVC column was closed-off with a flexible black rubber cap (Qwik Cap) and fastened with a hose clamp. The three PVC columns were filled with sand to a depth of approximately 102-mm (4") and then densified via firm tapping along the column circumference using a blunt object. Sand was added as necessary during densification to maintain the 102-mm depth. Next, a 305-mm (12") long, 3.2-mm (1/8") I.D. x 6.4-mm (1/4") outer diameter (O.D.) injection tube was made using Tygon laboratory tubing (R-3603 PVC). The injection tube had 6-8 holes in a radial pattern, made using an 18 gauge needle, along the last 38-mm (1.5") of the tubing. The end of the tube near the perforations was plugged and the tube was suspended lengthwise along the center axis of the column with the perforated end approximately 6.4-mm above the 102-mm densified soil layer.

The PVC columns were then filled with soil to a height of 254-mm (10") from their bottom. Ottawa 20-30 silica sand was used in PVC Columns #1-2, and finer-grained Ottawa F-60 silica sand was used in Column #3 (both soil

types were described in Chapter 4). The respective dry soil weights for Column #1, Column #2, and Column #3 were 3408 g, 3324 g, and 3235 g. These weights correspond to dry unit weights of 16.3 kN/m^3 (103.5 lb/ft^3), 15.9 kN/m^3 (100.9 lb/ft^3), and 15.4 kN/m^3 (98.2 lb/ft^3), respectively. Each column was then filled with 700-ml of tap water through the injection tube so that the water level was just above the soil line at a height of 254-mm from the bottom of the column. The columns were then densified as described above, but without the addition of soil, which reduced the final soil depths from 254-mm to approximately 239-mm (9.4") in each column. This increased the dry unit weight in the columns to 17.2 kN/m^3 (109.8 lb/ft^3), 16.8 kN/m^3 (107.1 lb/ft^3), and 16.4 kN/m^3 (104.2 lb/ft^3) for PVC Columns #1-3, respectively. Based upon a maximum dry unit weight of 17.7 kN/m^3 (112.6 lb/ft^3) and a minimum dry unit weight of 15.2 kN/m^3 (97.1 lb/ft^3) for Ottawa 20-30 silica sand (Katapa 2011), the unit weights for Columns #1 and #2 correspond to relative densities of 97.5% and 95.1%, respectively ($G_s = 2.71$). Based upon a maximum dry unit weight of 16.6 kN/m^3 (105.6 lb/ft^3) and a minimum dry unit weight of 14.5 kN/m^3 (92.3 lb/ft^3) for Ottawa F-60 silica sand (Gutierrez 2013), the unit weight for Column #3 corresponds to a relative density of 98.6% ($G_s=2.71$).

Column #2 was first injected with approximately 40-ml of dilute sodium bentonite slurry with unit weight of 10.5 kN/m^3 (67 lb/ft^3) pushed through the injection tubing using a syringe. Each of the three columns then received approximately 155-ml of a pH=7.3 EICP solution at 35° C consisting of Sigma Aldrich ACS Grade 1.36 M urea and 0.77 M CaCl_2 -dihydrate in tap water

(initial urea to CaCl_2 ratio $\approx 1.7:1$). The injection tubes were then flushed with 2.0-ml water followed by 15-20 ml of enzyme solution consisting of 0.44g/L urease enzyme (Sigma Aldrich Type-III, Jack Bean Urease, 26,100 U/g activity) and 4.0 g/L stabilizer. Finally, another 3-4 ml of EICP reaction medium was injected followed by 2-ml of water to flush the line. All fluids were delivered to the soil by a syringe through the injection tube. A pH measurement of the “head fluid” at the top of the column (above the soil line) was taken and then the injection tubes were closed with PP pinch clamps and the columns were capped with clear plastic wrap and placed in dark, warm (30°C) environment.

On day 7, pH measurements were taken from the (a) “head fluid” and (b) pore space fluid drawn from the injection tube that presumably represents the conditions near the perforated zone within the soil mass. After the pH measurements, a smaller follow-up EICP solution of 115-ml (pH=7.3) consisting of 3.7 M urea, 3.5 M CaCl_2 -dihydrate and 10-ml of enzyme solution was delivered to each column in the manner previously described, i.e. by syringe (final urea to CaCl_2 ratio of the follow-up solution was $\approx 1.1:1$). Two more sets of pH measurements of the head fluid and the pore fluid were taken on days 14 and 21 of the experiment (a total of four sets of pH measurements). The columns were also qualitatively assessed for the odor of NH_3 and color change. The three PVC sand columns were allowed to run for a total of 28 days. On day 26, 1-ml ($\approx 0.1\%$ pore volume) of 1.0 M NaOH was injected into each column followed by 2-ml of water. The purpose of the NaOH was to shift the NH_3 - NH_4^+ balance towards NH_3 by neutralizing NH_4^+ and thereby maintain

(or promote) the conditions favorable to CaCO_3 precipitation (high pH and alkalinity).

Upon termination of the experiments, it was found that the cemented soil masses in each of the three PVC columns were not amenable to in-place draining and rinsing as previously described for the acrylic columns in Chapters 4 and 5. The PVC columns were disassembled by removing the flexible bottom rubber cap, pouring out the loose sand, and dislodging the cemented portion using hand tools. After removal, the entire soil mass (both intact and loose) from each column was rinsed using 18.2 M Ω DI water (>5 pore volumes) in large PP beakers and sieved (250- μm PP) to capture any loosely cemented pieces. The cemented soil masses were allowed to air dry for 7 days before any further analyses were performed.

Due to its highly irregular shape and strong attachment to the PVC column, the intact portion of Column #2 was partially destroyed during extraction and was not amenable to unconfined compressive testing. Therefore, the entire soil mass from Column #2 was used to quantify carbonate mineral content via acid digestion. The loose portions of Columns #1 and #3 (20-30 and F-60 sand, respectively) were also tested for carbonate mineral content. The cemented portions of Columns #1 and #3 were easier to remove from the PVC columns, but were also irregularly shaped and therefore were not tested for mechanical strength. However, the intact soil masses Columns #1 and #3 were saved for long-term physical observation such as soil friability. A small chunk of cemented sand was chipped off each column and characterized using via

SEM/EDX as described in Section 3.2.2 (FEI/Philips XL-30 Field Emission ESEM).

6.2.2 Five-gallon Bucket Tests

Columnar cementation experiments in dry and flooded Ottawa 20-30 silica sand were conducted in six standard U.S. 5-gallon buckets (\approx 19-liters) labeled Buckets #1-6. The six experiments consisted of three initially dry soil buckets and three soil buckets that were flooded with tap water. The 5-gallon buckets have a standard tapered design with average dimensions of approximately 350-mm (13.8") tall, 290-mm (11.4") I.D. at the top of the bucket, and 260-mm (10.2") I.D. at the bottom.

Perforated injection tubes were made for the buckets using 51-mm (2") I.D. x 610-mm (24") long PVC tubes (schedule 40). Each injection tube had 16 holes made in a radial pattern using a 2-mm ($5/64$ ") drill bit along the last 76-mm (3") of the PVC tube. The end of the tube below the perforations was plugged with a flush-fitting glued-in PVC cap. The 2-mm diameter holes were drilled pointing downward at an orientation of approximately 45° from horizontal. Next, a circular approximately 203-mm (8") diameter "apron" made of 10-mil (0.02 mm) HDPE plastic was placed around the tube approximately 203-mm (8") from the capped end of the tube to serve as a barrier to reduce vertical fluid flow along the outside of the injection tube (i.e. along the soil and injection tube interface) during fluid delivery, as shown in Figure 25. The apron was taped to the injection tube. The capped ends of the PVC tubes were then placed lengthwise along the center axis of the buckets with the perforated end

resting against the bottom of the buckets. A tight fitting PVC ballast ≈ 48 -mm (1.9") O.D was also fabricated for insertion into the injection tube (51-mm, 2" I.D.) to displace the EICP solution ("dead volume") after each episode of fluid injection.

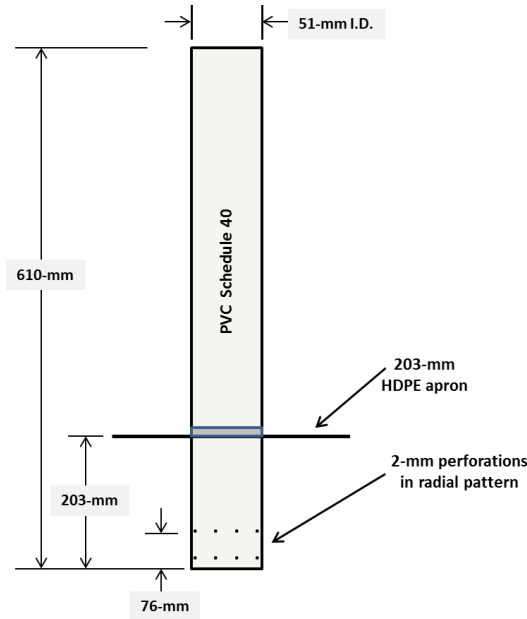


Figure 25 PVC injection tube used in the 19-L bucket experiments.

Each 19-L bucket was placed in a 28-L secondary containment tray and then filled with soil by dry pluviation from a fall height of approximately 254-mm (10") as follows: (a) Buckets #1-3 for dry soil testing were filled to an average depth of 159-mm (6.25"), and (b) Buckets #3-6 for wet testing were filled to an average depth of 322-mm (12.7").

The respective dry soil weights for Bucket #1, Bucket #2, and Bucket #3 were 17.0 kg, 15.6 kg, and 17.4 kg; these weights correspond to dry unit weights of 17.1 kN/m^3 (108.3 lb/ft^3), 16.7 kN/m^3 (106.1 lb/ft^3), and 17.2 kN/m^3

(109.3 lb/ft³), respectively. The respective dry soil weights for Bucket #4, Bucket #5, and Bucket #6 were 31.1 kg, 32.2 kg, and 31.4 kg; these weights correspond to dry unit weights of 14.7 kN/m³ (93.3 lb/ft³), 15.6 kN/m³ (99.1 lb/ft³), and 15.1 kN/m³ (96.0 lb/ft³), respectively. Buckets #4-6 were then filled with approximately 7.5 to 8.0-L of pH≈7.8 reverse osmosis (R.O.) filtered water through the injection tube so that the water level was approximately 12.5-mm (0.5”) below the soil line. The water depth in the soil was measured by forming a temporary observation well in the soil that was 25-mm deep x 12.5-mm wide (1” x 0.5”). Note that after filling the buckets with water, there was approximately 43-mm (1.7”) of space remaining between the phreatic surface and the top of the bucket to allow for the addition of approximately 2.0-L of EICP solution before overtopping the buckets.

All buckets then received approximately 1.7-L of pH=9.0 EICP solution consisting of 3.0 M Sigma Aldrich laboratory grade urea and 2.0 M CaCl₂-dihydrate in DI water, and 100-ml of a urease enzyme solution consisting of 0.44g/L urease enzyme (Sigma Aldrich Type-III, Jack Bean Urease, 26,100 U/g activity) and 4.0 g/L stabilizer (initial urea to CaCl₂ ratio ≈1.5:1). The urea-CaCl₂ and enzyme solutions were mixed in a 2.0-L glass bottle immediately prior to delivery and then quickly added to the injection tubes. The effective concentration of the EICP solution after the addition of the urease solution to the urea-CaCl₂ mix was reduced to approximately 2.8 M urea and 1.9 M CaCl₂ (note that the urea to CaCl₂ ratio is still ≈1.5:1). The EICP solution was poured into the injection tube at a rate such that fluid head in the injection tubes did not

exceed approximately 457-mm (18”) in order to limit soil piping. EICP solution was delivered to only one bucket at a time. After the fluid level in the tube reached equilibrium with the fluid level in the soil the ballast was inserted into the injection tube to force the remaining EICP solution into the soil. After delivery of the EICP solution and insertion of the ballast, the buckets were covered in clear plastic wrap and loosely taped. The experiments were allowed run for 26 days at room temperature.

On day 21, pH measurements of the fluid at the bottom of the injection tubes, presumably representing the pore fluid near the perforated zone, were made by removing the ballast and lowering the pH probe into the tubes. The buckets were also qualitatively assessed for the odor of NH_3 in the injection tube and over the head fluid. After pH measurements were made, 20-ml (0.1% v/v) of 1.0 M NaOH was added to each tube followed by 200 to 800-ml of R.O. water (dry buckets required more water, wet buckets less) to clear the tube of NaOH. Some of the water added was to raise the fluid levels in the buckets to their original values at the start of the experiment that was lost due to evaporation.

Upon termination of the experiments, the fluid was pumped out of the buckets using a hand operated pump that was inserted into the injection tubes. This process took approximately 5 minutes per bucket, but had to be repeated several times for each bucket as pore fluid slowly drained into the injection tubes. After pumping was complete, approximately 20 to 25-L of tap water (approximately 3 times the pore volume) was slowly added to the injection

tubes to rinse the soil of excess salts. Fluid was allowed to overtop and spill out of the buckets into the secondary containment during this process. The remaining fluid was pumped out and the buckets were allowed to stand for approximately 5 days before disassembly.

Large cemented soil masses were found upon disassembly in each of the six buckets. Removal of these cemented masses depended upon how they were attached to the bucket and the injection tubes. Some of the cemented masses were extracted through excavation. Some of the cemented masses were attached to the injection tubes. Some cemented masses required hand tools to break them free from the bucket. There was no apparent pattern to these circumstances. After removal, only the cemented soil masses that were either still attached to the tubes or fragments larger than approximately 25-mm (1") in diameter were collected and saved. The cemented masses (both intact and loose) were rinsed by soaking them in either a 19-L bucket or 5-L PP beaker (depending on size of the cemented fragment) that was filled with 18.2 M Ω DI water. The cemented masses were collected by hand after rinsing. The cemented soil masses were then allowed to air dry for 7 days until further testing was conducted.

Most of the collected specimens were not amenable to mechanical testing due to damage during extraction and irregular shapes. But, the cemented mass in Bucket #8 appeared to be largely intact and symmetric and was therefore amenable to coring to recover specimens for unconfined compressive strength (UCS) testing. Several specimens from each bucket were acid tested

for the presence of a carbonate mineral. Only the soil masses that were used for UCS testing were used to quantify carbonate mineral content via acid digestion. The remaining intact soil masses from all buckets were saved for long-term physical observation such as soil friability.

6.2.3 Large Soil Box Test (1 m³)

A columnar cementation experiment was conducted in an approximately 1-m³ wooden box using a native sand common to the lower elevation deserts of the state of Arizona (AZ). The grain size distribution for the soil used in this experiment is shown in Figure 26.

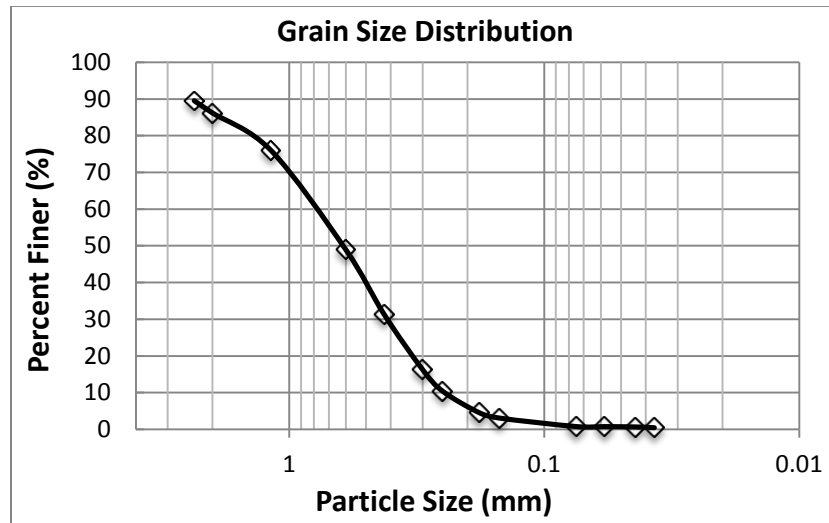


Figure 26 Grain size distribution of native AZ soil.

The base of the wooden box was approximately 1.1-m square (3' x 3') and the walls were 1.1-m wide x 0.9-m tall (3' x 2.8'). The walls and base were made of 19-mm (¾") thick plywood and were connected using metal L-brackets at the internal joints and as needed to temporarily provide lateral support to the box.

The walls were laterally reinforced using 1.25-m (4') long U.S. standard 2' x 4" wood studs (actual dimensions 1.5" x 3.5", 38-mm x 89-mm) along each wall that were connected by 12.5-mm (0.5") thick threaded steel rods. Two 12.5-mm (0.5") I.D. drain holes were installed along two opposite facing walls of the box approximately 127-mm (5") below the top of the box and connected to PP tubing to catch fluid overflow. A U.S. standard 2' x 4" wood stud was used for bracing along top of the box and also served as the attachment point to brace the PVC (schedule 40) injection tube. The injection tube was approximately 1.5-m (5') long with a 76-mm (3") I.D. and with 2.4-mm (3/32") diameter radial perforations along the last 305-mm (1') of the tube. The perforated end of the tube was wrapped in PP mesh with 0.400-mm openings to prevent soil intrusion into the tube. The metal brackets inside of the box were sprayed with a plastic coating to soften their hard edges and the box was then lined with a double layer of 10-mil HDPE. The box was placed in a lined secondary containment and then filled with approximately 230-L of tap water that was allowed to stand overnight to test for leaks.

The box was filled with approximately 1027-kg (2260 lbs.) of the native sand by pluviation into approximately 254-mm (10") of water from an approximate drop height of 610-mm (2') above the water surface. After pluviation, the soil line was approximately 152-mm (6") below the top of the box and the water level was approximately 152-mm below the top of the box. The perforated end of the injection tube was then embedded approximately 610-

mm (2') into the soil (approximately 610-mm below the top of the soil and 152-mm (6") above the bottom of the box).

The soil-filled box was allowed to sit overnight after filling with soil (to test for leaks once again). During the initial injection of EICP solution, the hydraulic head reached nearly 1.5-m (5') in the injection tube and there were signs of fluid leakage around the tube leading to concerns that hydraulic fracturing had occurred in the soil mass. To limit fluid leakage, the sand along the top 51-mm (2") of the interface between the soil and the tube was replaced with a hydrated sodium bentonite seal approximately 254-mm (10") in diameter. To help in reducing further the potential for hydraulic fracturing, a two-piece 610-mm square wooden plate was placed on top of the soil mass and approximately 45-kgs (100 lbs.) of weight was placed on the plate to provide additional overburden. The soil-filled box with the sodium bentonite seal is shown in Figure 27 sitting in the lined secondary containment system.



Figure 27 Soil-filled box with Na-bentonite seal around injection tube.

The initial cementation fluid injection for this test was approximately 33-L of pH \approx 8.1 EICP solution at 45°C using tap water that consisted of approximately 1.5 M CaCl₂-dihydrate, 2.2 M urea, and a 1.0-L urease enzyme solution (initial urea to CaCl₂ ratio \approx 1.5:1). The enzyme solution contained 4.0 g/L stabilizer and enough enzyme (11.2 grams) to reach a target concentration of 0.34g/L of urease in the 28-L EICP solution (Sigma Aldrich Type-III, Jack Bean Urease, 26,100 U/g activity). The enzyme solution reduced the effective concentrations of CaCl₂ and urea to 1.4 M and 2.1 M. The second injection of EICP solution was delivered 14 days after the first injection. The EICP solution consisted of 40-L of CaCl₂ and urea at the same effective concentrations and temperature as the first injection, and the urease solution was formulated to reach same target concentration of 0.35 g/L (12.2 grams) as used in the first injection. The injection tube was flushed with approximately 2-L of tap water after each injection and then a tight fitting ballast (70-mm diameter, 2.75") was

slowly inserted into the injection tube to displace the residual EICP solution into the soil. The EICP fluid head was maintained at 1.2 to 1.4-m (4' to 4.5') in the injection tube and drained slowly. The experiment was allowed to run for approximately 46 days and was monitored for leaks. Approximately 60-L of tap water was added to maintain the water depth in the soil over the duration of the experiment. Several pH and temperature measurements were made over the 46 days by inserting pH and temperature probes into the injection tube. The presence of NH_3 in the injection tube and over the soil was qualitatively assessed by detection of NH_3 odor. On day 42, 200-ml ($\approx 0.1\%$ pore volume) of 1.0 M NaOH was added to the soil box and then the injection tube was flushed with 2.0-L of tap water before replacing the ballast.

Upon termination of the experiment, several intact chunks of soil were tested for the presence of a carbonate mineral and other intact chunks were saved for long-term physical observation such as soil friability. A few intact chunks of soil were also collected for characterization using via SEM (FEI/Philips XL-30 Field Emission ESEM).

6.3 Results and Discussion

6.3.1 Four-inch Diameter PVC Tubes

Each one of the three PVC columns contained a cemented soil mass. The soil masses in Columns #1 and #2 are shown in their PVC columns before extraction and Column #3 is shown after extraction in Figure 28.

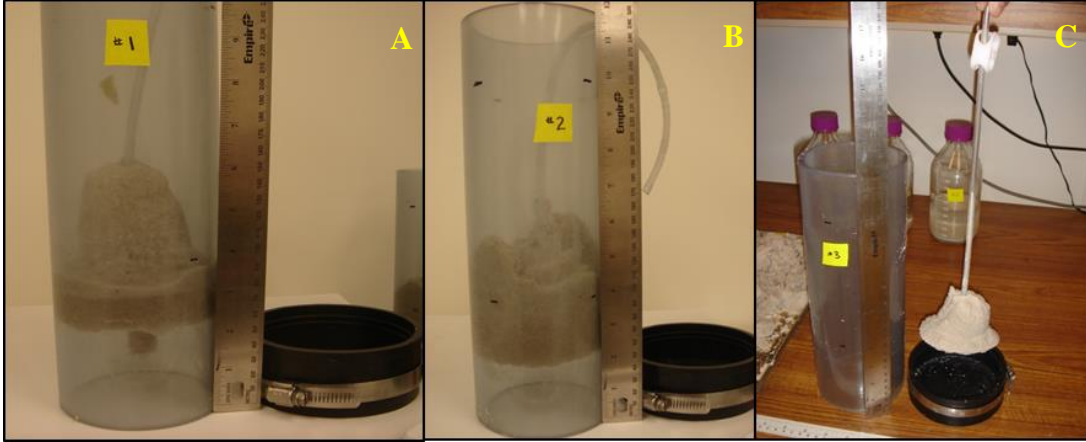


Figure 28 (A) Column #1 (20-30 silica sand); (B) Column #2 (20-30 silica sand w/40 ml Na-bentonite slurry) was strongly cemented to the PVC column and heavily damaged during extraction; (C) Column #3 (F-60 silica sand).

The soil in the area closest to the end of the perforated injection tube was strongly cemented in all three PVC columns. In Column #1 (20-30 silica sand), a region of strongly cemented soil began ≈ 64 -mm (2.5”) from the column bottom, was ≈ 114 -mm (4.5”) in length and displayed a prominent rounding at the top and a squarely flat surface at the bottom as shown in Figure 28A. Overall, the cemented region appeared to have a cylindrical bottom and bulb-shaped upper portion. Several chunks of cemented soil were dislodged to access the strongly cemented region in which the injection tube was firmly embedded.

In Column #2 (20-30 silica sand w/40 ml sodium bentonite slurry), a region of strongly cemented soil began ≈ 76 -mm (3”) from the column bottom, was 102-mm in length and displayed small rounding near the top and a squarely flat surface at the bottom, as shown in Figure 28B. Overall, the cemented region appeared mostly cylindrical and appeared to have distinctive soil “fingering” along the top portion of the cemented mass. Several chunks of

loosely cemented soil were dislodged to isolate the strongly cemented region (shown in Figure 28B) that was cemented to the inside wall of the PVC column.

In Column #3 (F-60 silica sand), a region of strongly cemented soil began ≈ 76 -mm from the column bottom, was ≈ 64 -mm in length and displayed a clear bell-shaped top and a squarely flat surface at the bottom, as shown in Figure 28C. Overall, the cemented region appeared bell-shaped. The entire soil column was dislodged upon disassembly and many chunks of cemented soil were dislodged to access the strongly cemented region in which the injection tube was firmly embedded. The soil mass in Column #3 contained many small (1-3 mm) pieces of cemented sand.

As previously noted, the intact portion of Column #2 was not amenable to unconfined compressive testing and was instead used for carbonate mineral quantification. The cemented portions of Columns #1 and #3 were also irregularly shaped, but were retained for long-term observations to assess the potential of time-related degradation. The injected column (#1) that received Na-bentonite slurry was acid digested and had a CaCO_3 content of approximately 1.8%. Specimens from Columns #1 and #3 were acid digested after long term physical observation (approximately 1 year) and had CaCO_3 contents of 4.17% and 4.67% (respectively). Acid digestion of the sand in PVC Column #2 indicates that the CaCO_3 content was 1.8% (w/w) for the intact section while none was detected in the loose portion. Acid digestion of the loose sand fraction in Column #3 indicates that the CaCO_3 content was

approximately 0.26%, while no carbonate minerals were detected in loose sand in Column #3.

SEM analyses were conducted on cemented specimens taken from the PVC columns. The SEM images show that CaCO_3 formed on and in between sand particles as illustrated in Figure 29. This material was verified to be $\text{CaCO}_{(s)}$ via EDX analysis (not shown).

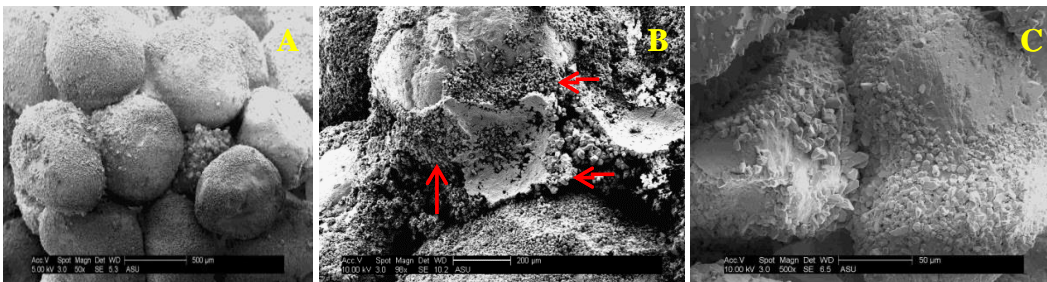


Figure 29 CaCO_3 coating on and in-between sand grains. (A) Column #1 (20-30 silica sand); (B) Column #2 (20-30 sand w/Na-bentonite slurry), arrows indicate points of particle detachment, note extensive CaCO_3 -clay bridging between sand particles; (C) Column #3 (F-60 silica sand).

The results of pH measurements of the head fluid and pore fluid taken at approximately regular intervals are shown in Table 23. Overall, the pH of the pore fluid near injection tube increased from 7.3 to approximately 8.4 to 8.8 depending on the specific column and sampling date. The pH change for the head fluid was slower and increased to approximately 7.2 to 8.4 depending on the specific column and sampling date.

Table 23 pH measurements of pore and head fluid from the PVC Columns

Column #	Initial		Day 7		Day 14		Day 21	
	Head Fluid	Pore Fluid						
1	7.3	7.3	7.2	8.4	8.2	8.6	8.2	8.8
2	7.3	7.5	7.5	8.7	8.2	8.2	8.3	8.5
3	7.3	7.3	7.4	8.6	7.8	8.5	8.4	8.5

A faint odor of NH_3 was detected over the head fluid of all three PVC columns on pH measurement days 14 and 21, and a strong to very strong odor of NH_3 was detected in the pore fluid at every sampling event (days 7, 14, 21). The odor of NH_3 was very strong in all three columns upon disassembly on day 28. By day 14, Columns #1 and #2 developed a whitish haze around the middle of the PVC column and a well-defined white ring that approximately coincided with the flat bottoms cemented masses discussed above. No definitive color observations were observed in Column #3 during the course of the experiment, but this column used F-60 sand which is generally much lighter in color than 20-30 sand used in the columns.

6.3.2 Five-gallon Bucket Tests

Each one of the six bucket experiments contained cemented soil masses located in the area below the plastic apron, none were found above this area in any of the buckets. The cemented soil masses in the dry buckets (#1-3) were as follows: Bucket #1 contained many small cemented masses that varied in size between approximately 19 to 25-mm ($\frac{3}{4}$ " to 1") in diameter and were found in a radial pattern around the injection tube, but did not appear to be attached to the tube; Bucket #2 contained larger cemented masses that varied in size between

approximately 38 to 89-mm (1.5” to 3.5”) in diameter, some were broken away from the tube and others were found in a radial pattern around the tube; Bucket #3 contained a large donut-shaped cemented soil mass that was approximately 76-mm thick x 260-mm in diameter (3” x 10.25”) that broke away from the injection tube in one intact piece and required hand tools to dislodge from the 5-gallon bucket. The cemented soil mass from dry Bucket #2 is shown in Figure 30.



Figure 30 Donut-shaped cemented soil mass from dry Bucket #2.

The largest cemented soil masses (i.e. >25-mm in diameter) in the wet Buckets #4-6 were found attached to their injection tubes in bulb-shaped forms with the following physical characteristics: Bucket #4 several large cemented

chunks (≈ 51 to 302 -mm, $2''$ - $6''$) broken away during extraction; the resulting intact portion was a slightly irregular bulb-shape approximately 203 -mm ($8''$) in diameter by 127 -mm ($5''$) deep. In Bucket #5 several large cemented chunks (≈ 25 to 76 -mm, $1''$ - $3''$) were broken away during extraction: the resulting intact portion was a mostly uniform bulb-shape approximately 152 -mm ($6''$) in diameter by 127 -mm ($5''$) deep. In Bucket #6 additional effort was required to dislodge the cemented mass during extraction, which resulted in additional breakage, but the cemented mass was otherwise very similar in size and shape to Bucket #5. Representative cemented soil masses from Buckets #4 through #6 are shown in Figure 31.



Figure 31 Bulb-shaped cemented soil masses from wet Buckets #4-6. Note that the apron in Bucket #6 moved down the injection tube during pullout.

The results of pH measurements of the head fluid and the pore fluid in the injection tubes on day 21 are shown in Table 24. The pore fluid pH in Bucket #1 increased from 9.0 to approximately 9.1, while Buckets #2 and #3 decreased slightly to 8.7 and 8.9, respectively. Note that these are pH values are occurring in actively precipitating CaCO₃ systems. The pH of the head fluid could not be determined in Buckets #1-3 because the fluid level fell below the soil line due to evaporation (the glass pH probe was not designed for solid media). The pore fluid pH in Buckets #4, #5, and #6 decreased from 9.0 to approximately 8.8, 8.5, and 8.3 (respectively), while the pH of the head fluid increased from 7.8 to 8.1, 8.4, and 8.0 (respectively). A strong odor of NH₃ was detected over the head fluid of Buckets #1-3, while no NH₃ odor was detected in Buckets #4-6. A very strong odor of NH₃ was detected in the injection tubes of all six buckets.

Table 24 Summary of pH measurements from head fluid and the pore fluid.

Bucket		Initial		Day 21	
Type	#	Head Fluid	Pore Fluid	Head Fluid	Pore Fluid
Dry	1	n/a	9.0	n/a	9.1
	2	n/a	9.0	n/a	8.7
	3	n/a	9.0	n/a	8.9
Wet	4	7.8	9.0	8.1	8.8
	5	7.8	9.0	8.4	8.5
	6	7.8	9.0	8.0	8.3

Acid tests on small cemented chunks obtained from each of the buckets indicate that the cemented soil masses contained a carbonate mineral.

Specimens from Bucket #2 were cored for mechanical testing and then acid digested. Five cored specimens from Bucket #2 were used for UCS testing. The results of the UCS tests on the 5 specimens from Bucket#2 are shown in Table 25. The CaCO₃ content of the cored samples from Bucket #2 was not possible due to sample loss (a lab accident) during quantification. The remaining intact soil masses from the other buckets (#1, #3, and #4-6) were acid digested after long term physical observation (approximately 8 months). The CaCO₃ contents of Buckets #1, #3, #4, #5, and #6 were 2.9%, 1.0%, 3.4%, 2.3%, and 2.2% (respectively).

Table 25 Unconfined compressive strength test results of five cores from Bucket #2.

Core #	Peak strength (kPa)	Axial Strain (%)
1	64	2.96
2	35	3.42
3	68	2.82
4	35	0.95
5	125	6.27

6.3.3 Large Soil Box Test (1 m³)

The large soil box experiment was terminated by draining the soil box from the bottom edge the box through a 12.5-mm (0.5”) hole. Fluid drained quickly during the first 10-12 minutes, but then slowed to a slow stream followed by no flow after approximately 10 minutes. The fluid that drained in the first few minutes (\approx 3-4 minutes) had a faint to moderate odor of NH₃. Next, a garden hose was placed in the injection tube and allowed to run at a slow rate (unquantified) for approximately 1 hour to rinse the soil of salts. The injection

tube was overtopped during most of this time which caused water to spill directly onto the soil surface. Draining occurred predominately from the lower drain hole but some water also drained through the top drain ports. Approximately 51-mm (2") of fluid collected in the secondary catchment over the course of experiment, which equates to approximately 15 to 20-L of fluid based on the dimensions of the catchment.

On day 7 of the experiment (before the 2nd injection), the pH in the injection tube had increased from the initial value of 8.1 to approximately 8.9 and the fluid temperature dropped from approximately 45°C (the initial temperature of the EICP solution) to 14°C. The fluid temperature in the top 25-mm (1") of soil was approximately 9°C. A strong odor of NH₃ was detected in the tube and a faint odor was detected over the top of the soil. Several whitish colored spots developed near the injection tube (presumably CaCO₃) that ranged in size from 51-mm to 76-mm (2" to 3") in diameter. This is a strong indication that the EICP solution from the 1st injection reached the soil surface.

On day 14 of the experiment, immediately before the 2nd injection, the pH in the injection tube was approximately 8.9. The fluid temperature in the tube dropped from the 7-day measurement of 14°C to 11°C, while the surface fluid temperature remained at 9°C. A very strong odor of NH₃ was detected in the tube, but no NH₃ odor was detected over the top of the soil. The temperature in the injection tube increased once again to approximately 45°C immediately after the 2nd injection.

On day 21 of the experiment, the pH in the injection tube was approximately 8.1. A strong odor of NH_3 was detected in the tube, but no NH_3 odor was detected over the top of the soil. The decline in temperature over the next 14 days of the experiment (days 28 and 35) followed approximately the same pattern that was observed over the first 14 days. By day 35, the temperature in the injection tube was approximately 11°C where it remained until the termination of the experiment on day 46.

On days 28, 35, and 42 of the experiment, the pH in the injection tube was approximately 8.8, 8.3, and 7.9, respectively. The odor of NH_3 was detected in the tube on each of the three pH measurement days (28, 35, and 42) and ranged from very strong on days 28 and 35 to strong by day 42. No NH_3 odor was detected over the top of the soil at any of these three test days.

After rinsing and draining with tap water was complete, two opposite walls of the soil box were removed to access the soil mass. Large amounts of soil on both sides fell away from a central soil mass upon removing the walls. A vertical soil block stood nearly 1.1-m (2') high on one side of the box after the loose soil fell away. A strong odor of NH_3 was detected near the area that had intact soil. Excavation of the loose soil around the central mass was performed by hand six days later (to allow for additional drying), revealing a roughly saddle-shaped columnar soil mass that appeared to be weakly cemented and is shown in Figure 32. It was found that approximately the top 203-mm (8") of the 1.1-m vertical soil block was loose uncemented soil that was resting on the cemented soil mass beneath it. A slightly stronger cemented and better

defined columnar region of soil that was approximately 203 to 229-mm (8" to 9") in diameter occurred along the injection tube as shown in Figure 32. After moving all the loose soil from box area, the injection tube was excavated using hand tools that required only light to moderate effort to break the saddle-shaped region of cemented soil. A roughly bulb-shaped region of strongly cemented soil was discovered near the perforated end of the injection tube that extended radial approximately 178-mm (7") from the edge of the 89-mm (3.5") O.D. tube.

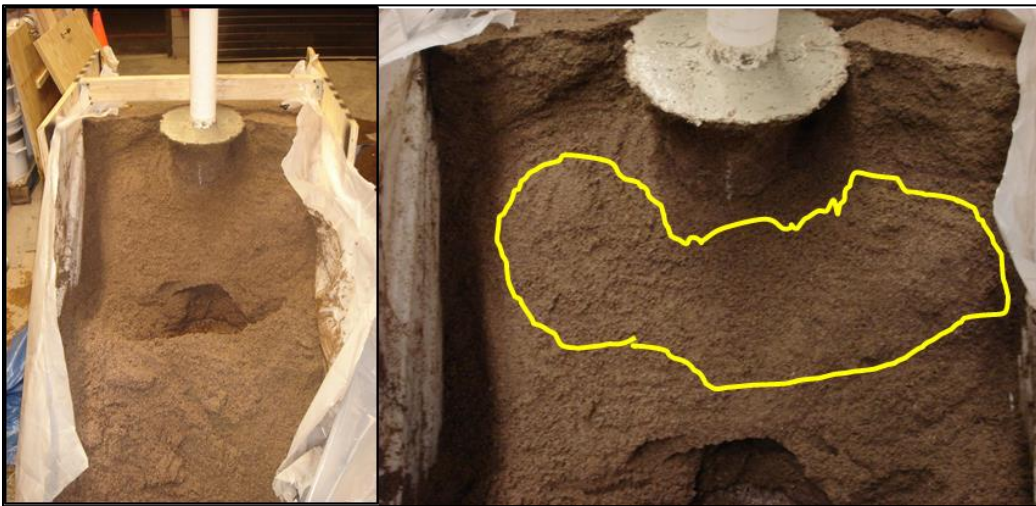


Figure 32 Soil box after disassembly. The yellow outline delineates a roughly saddle-shaped columnar soil mass that was weakly cemented.

Several intact chunks of soil were collected from the saddle area and the strongly cemented area near the perforated end of the injection tube that ranged in size from 25.4 to 101-mm (1" to 4"). The presence of a carbonate mineral was detected in specimens from both areas. Quantification of CaCO_3 showed that the specimens from the saddle area contained approximately 0.23 % to

1.6% (w/w) CaCO_3 (average $\approx 1.1\%$), while the cemented soil recovered from the injection tube area contained approximately 2.4% to 3.3% CaCO_3 (average $\approx 2.9\%$). The soil in the saddle area was too weakly cemented for coring and the injection area was too irregular to obtain a symmetric core.

SEM analysis showed that CaCO_3 formed on and between soil particles in both the saddle and tube regions, as shown in Figure 33. The samples obtained from the injection tube area are shown in the left pane of Figure 33 (A-C) and the saddle area samples are shown in the right pane. The calcite crystals are seen growing on and between soil particles in all specimens and soil particle detachment points are seen in images B and C.

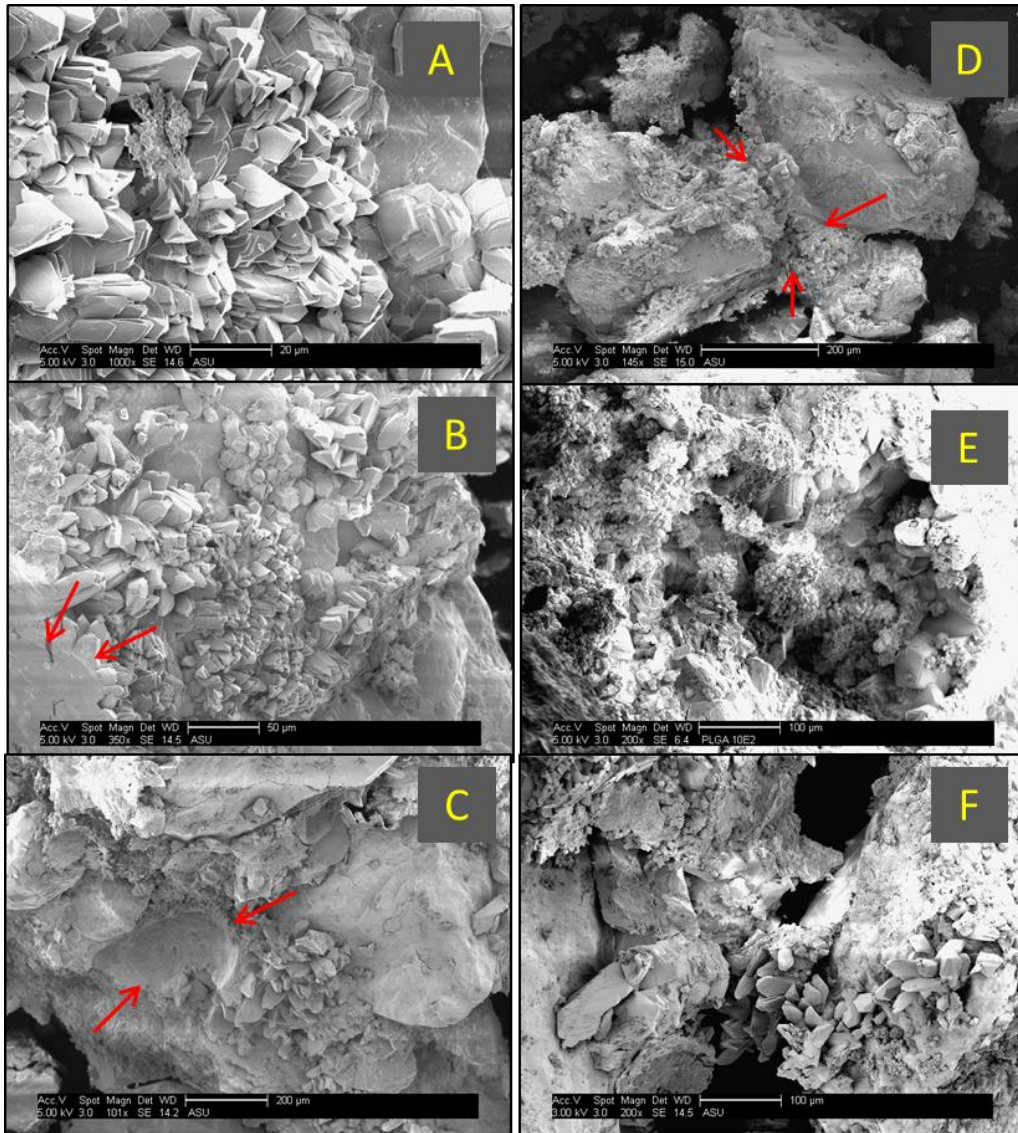


Figure 33 The left pane is for samples obtained from the injection tube area (A-C) and the right pane is for saddle area samples. The red arrows in image B show a planer detachment of CaCO_3 , image C shows a cavity where particle detachment occurred, and image D shows inter-particle soil cementation surrounded by finer grained soil.

6.4 Conclusion

The experiments performed in this chapter demonstrate that an EICP solution delivered through a perforated injection tube can be used to induce columnar soil cementation. These experiments were performed in increasingly larger soil

containers. The odor of NH_3 was detected in every test conducted here and ranged from strong to very strong in the pore fluid or the injection tube. Faint odors of NH_3 were detected in the fluid on or very near the top soil layers of every test, at least temporarily. The addition of 0.1% 1.0 M NaOH near end of each experiment helped increase pH (at least locally) and shift the nitrogen balance towards NH_3 (rather than NH_4^+) to further favor the conditions conducive to CaCO_3 precipitation. This may have facilitated the strong to very strong odor of NH_3 detected in every experiment upon disassembly.

The smallest columnar experiment was developed using three PVC sand columns filled with either Ottawa 20-30 or F-60 sand and were injected with EICP cementation solution through a 3.2-mm (1/8") I.D. tube under saturated soil conditions. One of these columns was injected with sodium bentonite slurry prior to delivery of the cementation solution. Cementation was observed in all of the columns treated with the EICP solution. The injected PVC column that received Na-bentonite slurry displayed a cylindrically-shaped zone of strongly cemented soil, while the columns that did not receive Na-bentonite displayed bulb-shaped cemented zones. The injected column (#2) that received Na-bentonite slurry was acid digested and had a CaCO_3 content of approximately 1.8%. Specimens from Columns #1 and #3 were acid digested after long term physical observation (approximately 1 year) and had CaCO_3 contents of 4.17% and 4.67% (respectively). None of these columns were amenable to coring for mechanical testing. SEM and XRD analysis of cemented sand specimens from all three PVC columns show that a precipitated

mineral coating is visible on and in between sand particles and that it is calcite phase CaCO_3 .

The next larger-sized experiment used six 5-gallon buckets filled with 20-30 silica sand that were injected with EICP cementation solution through a 51-mm (2") I.D. tube under (a) dry and (b) fully wet soil conditions. Cementation was observed in all six buckets treated with the EICP solution. The wet soil buckets formed bulb-shaped cementation zones that were firmly attached to the injection tubes upon removal. The dry soil buckets produced either a donut-shaped cemented soil mass (Bucket #2) or cemented chunks that formed radially around the perforated tube. Only one of the six buckets, Bucket #2, contained a symmetric and accessible cemented soil mass that could be used to extract a cored specimen. UCS testing results of five specimens from Bucket #2 show that the shear strength of cemented specimens ranged from approximately 35 kPa to 125 kPa (CaCO_3 content was not available due to a lab accident). The remaining intact soil masses from the other buckets (#1, #3, and #4-6) were acid digested after long term physical observation (approximately 8 months). The CaCO_3 contents of Buckets #1, #3, #4, #5, and #6 were 2.9%, 1.0%, 3.4%, 2.3%, and 2.2% (respectively).

The largest experiment used a wooden box that was approximately 1-m^3 in volume filled with approximately 1027-kg of native AZ well-graded sand. The soil-filled box was injected with EICP cementation solution through a 76-mm (3") I.D. tube under flooded soil conditions. Cementation was observed in a saddle-shaped column that was subjectively stronger near the perforated tube.

Acid digestion showed that the cemented areas near the perforated tube contained approximately three times more CaCO_3 on a dry weight percentage basis (1.1% vs. 2.9% on average) than the cemented areas farther away (i.e. in the saddle area). These experiments demonstrate that EICP may potentially be used to form cemented columns of sand for ground improvement purposes.

CHAPTER 7

SURFICIAL SOIL STABILIZATION USING EICP

7.1 Introduction

This chapter presents the results of experiments to assess the potential applicability of enzyme induced carbonate precipitation (EICP) for surficial stabilization of soils against wind erosion in semi-arid to arid environments. Stabilization of erodible surficial soils, typically fine to medium grain soils, mitigates several important environmental and geotechnical problems associated with soil erosion. Both EICP and microbially induced carbonate precipitation (MICP) can potentially be employed to stabilize erodible surficial soils. However, the rapid carbonate precipitation induced by the EICP process, in contrast to slower microbial methods, makes it well-suited for surface treatments that have a relatively short temporal frame within which they need to become effective. Furthermore, since EICP does not consume or compete for the organic substrate (urea), EICP in itself is more efficient with respect to utilization of the substrate than processes that rely on microbial urease.

This chapter provides insight on the use of EICP process for stabilization of erodible surficial soils. The use of EICP for surficial stabilization of soils against wind driven erosion is investigated by wind tunnel testing of soil filled cake pans topically treated with an EICP solution. The testing program focuses on the following key areas: (1) developing an application method to induce surficial calcium carbonate (CaCO_3) precipitation via EICP, (2) quantifying the resistance of typical erosion-susceptible soils to wind erosion after topical

application of an EICP solution, and (3) assessing the primary factors affecting the formation of a wind erosion resistant CaCO_3 crust on typical wind erosion susceptible soils.

None of the application methods discussed in the previous chapters (mix-and-compact, percolation, and injection) is applicable to topically applied solutions for an erosion-resistant CaCO_3 crust. In developing a method for topical application of an EICP solution, a fundamental question that must be answered is should the method simply involve spraying a complete pre-mixed precipitation solution of urea, CaCl_2 , and urease or should the reagents that constitute the precipitation solution be applied separately. If the constituents are to be applied separately, another question is whether the sequence of reagent application matters. Additional questions are whether the rate of reagent application and the number of applications of the various solutions affect the formation of CaCO_3 crust on the soil. For example, what is the impact of applying an EICP solution in a continuous manner vs. applying a similar volume in several smaller portions?

In attempting to address the above questions, it is reasonable to take the lessons learned from the previous chapters and apply them here. But, it is important to recognize that these lessons serve as a preliminary starting point and that there may be limitations to their applicability for the surficial stabilization of soils. The initial ratio of urea to CaCl_2 used in these experiments is 1.5:1 and the initial CaCl_2 concentrations of the solutions used in 8 of the 56 pans were at either 1.0 M or 2.0 M (initial tests), consistent with the

tests in previous chapters. However, the solution applied to the other 48 pans contained concentrations of CaCl_2 varying from 0.05 M to 0.40 M. Treated specimens were tested in the ASU-NASA Wind Tunnel to quantify the resistance to wind driven erosion.

7.2 Methods

7.2.1 Soil Pan Set-up and Wind Tunnel Testing

Preparation of Soil-filled Pans

Wind tunnel tests were performed to evaluate the applicability of EICP for stabilization of surficial soils against wind erosion. The tests were conducted in commercially available metal 229-mm (9") diameter cake pans that were approximately 38-mm (1.5") deep. Three different types of soils were used to make 56 soil pans: (1) uniform medium-grained, clean Ottawa F-60 silica sand, (2) a well-graded native Arizona (AZ) silty fine sand, and (3) mine tailings obtained from a site in southern AZ. The grain size distributions for the native sand and mine tailings are shown in Figures 34 and 35 (respectively), and a manufacturer's data sheet for the F-60 soil, a uniform medium sand with a mean grain size 0.275 mm and coefficient of uniformity 1.74, can be found in Appendix B.

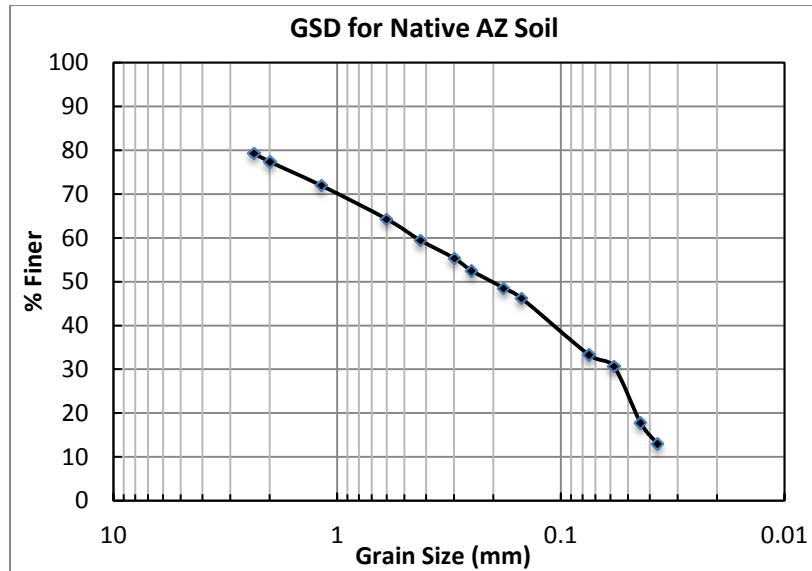


Figure 34 Grain size distribution for native sand.

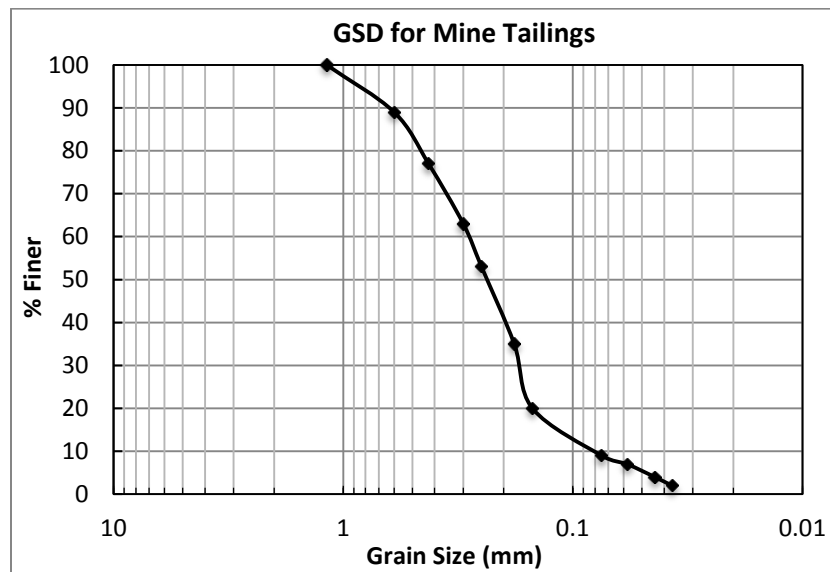


Figure 35 Grain size distribution for mine tailings obtained from southern AZ.

The size of a soil particle plays a significant role in the wind driven erosion. Wind typically detaches and moves smaller cohesionless soil particles at lower velocities than larger particles. However, very fine-grained soil particles tend to be cohesive and can resist detachment. The soil particle diameter in the

grain size distribution curve corresponding to 10% finer is defined as the D_{10} particle size and describes the smallest sized soil fraction. The D_{10} particle diameters for F-60 sand, native sand, and mine tailings are approximately 0.18-mm, 0.05-mm, and 0.08-mm (respectively).

The following general procedure was repeated as needed to make level, densified soil-filled pans that resisted settlement during handling that could lead to soil crust cracking: (a) the pans were filled with soil to a level slightly below the top of the pan, (b) the pans were tapped along outside edge 10-15 times with a blunt object while rotating the pans, (c) soil was added to a level slightly above the top of the pan, (d) the pans were tapped 10-15 times while rotating, (e) the soil was leveled with the top of the pan using a metal straight edge, (f) and chunks of soil that protruded from the surface (if present) were removed, broken up, and placed back in the area from which the chunk was removed, and then the soil surface was leveled again until smooth. Soil pans filled native AZ and F-60 silica sand are shown in Figure 36 immediately prior to treatment.



Figure 36 Two soil pans native sand (left) and F-60 sand (right) prior to treatment. Black PVC shield was used to reduce overspray.

Wind Tunnel Testing

The NASA/ASU Planetary Wind Tunnel (ASUWIT) was used to measure the soil particle detachment velocities of the soil in the pans. This wind tunnel was designed for the specific purpose of creating laminar airflow for soil wind erosion experiments and other geomorphological studies. The wind tunnel is part of the Planetary Aeolian Laboratory (PAL) at ASU. PAL is associated with NASA's Planetary Geology and Geophysics program. It is a unique facility used for conducting experiments and simulations of Aeolian processes (windblown particles) under different planetary atmospheric environments.

The ASUWIT is a 13.7-m long, 0.7 m high, 1.2 m wide open circuit boundary-layer wind tunnel that operates under ambient temperature and pressure conditions and is capable of wind speeds of up to 30 m/s (Williams, 2013). Air is pulled through the tunnel by a large fan mounted in the downwind section of the tunnel. A honeycomb structure at the entrance to the wind tunnel is designed to smooth out eddies. Roughness elements (machine nuts) are placed just past the honeycomb structure to "trip" the air flow and create a boundary layer. Soil detachment velocity (DV), i.e. the wind velocity at which soil particles begin to detach from the soil surface, is visually monitored through a viewing area in the test stage encased by plexiglass. Doors are provided to access the test section for the setup of experiment (Williams, 2013). A well in the test stage was fitted with plastic adapter ring that allowed the pans to sit flush with the wind tunnel stage, as shown in the inset of Figure 37.



Figure 37 Wind tunnel stage area. The inset photograph shows the arrangement of the adapter ring (white) and cake pan in the wind tunnel.

Particle detachment is induced by slowly increasing the wind speed in small increments while visually monitoring the soil surface for particle detachment. The observation process is aided by lighting effects that include the reduction of ambient light while simultaneously projecting a bright, focused light on the soil surface. While the wind tunnel is capable of wind speeds of up to 30 m/s, the experiments conducted here were limited to a wind speed of 25 m/s for a maximum of 30 seconds due to safety concerns resulting from pan instability (i.e. lift-off). Modifications to the pans and/or wind tunnel stage to increase pan stability were deemed unnecessary for the test program goals.

7.2.2 Treatment Type, Application Method and EICP Solution Formulation

Treatment Types

For different treatments were employed for the 56 pans of soil tested in these experiments: (1) Bare, dry soil (control), (2) bare soil wetted immediately before testing (water control), (3) soil treated with CaCl_2 and urea only (salt control), and (4) EICP treated soil. The pans with bare, dry soil were tested “as is” without any treatment and represent the baseline dry soil condition. The water control pans were treated with water sprayed onto the soil surface immediately prior to testing to represent the current standard of practice for control of wind erosion of soil (also referred to as fugitive dust mitigation). Pans with soil treated with a CaCl_2 and urea solution (without enzyme) were assumed to model the effectiveness of treating soil with a salt solution to mitigate fugitive dust (a common practice in the mining industry). Pans with EICP treated soil received a CaCl_2 -urea solution with enzyme to model the effectiveness of a topically applied EICP solution in mitigating fugitive dust. After treatment, the soils were loosely covered in plastic wrap and allowed to stand approximately four days. After four days, the pans were allowed to stand uncovered for 3-4 days to air dry (if wet) and equilibrate at room temperature before wind tunnel testing. A treated soil pan is shown in Figure 38.



Figure 38 Treated soil pan containing F-60 silica sand loosely covered in plastic wrap.

Application Method

Topical treatment of water or the salt or EICP solution was accomplished using a handheld bottle sprayer. The EICP solution was delivered via one of two possible *application methods*: Type 1 application for soil pans #1-29, and Type 2 application for soil pans #30-56. In Type 1 application, the pans of soil received their EICP solution application by spraying 150-ml of urea-CaCl₂ solution that was immediately followed by spraying of 25-ml of enzyme solution from a separate sprayer so that the entire treatment (175-ml) was applied in a continuous manner. In Type 2 application, the pans of soil received 200-ml of pre-mixed EICP solution (urea-CaCl₂ w/enzyme) in four separate spray passes of 50-ml each, with approximately 1 minute between passes.

During the initial work with pans #1-29, it was observed that a significant but unknown quantity of solution collected on the countertops and secondary catchment trays during spraying due to overspray. Efforts were made to reduce overspray, including the use of a plastic shield around the pans, but

solution continued to be lost. It was also noted that solution tended to temporarily pool on some areas of the soil surface, leading to the possibility of penetration of the treatment solution deeper into the soil in those areas. Therefore, additional solution (200-ml instead of 175-ml) was used in treating pans #30-56 to compensate for overspray losses. Furthermore, the treatment for pans #30-56 was applied over four passes to prevent pooling. The flow chart shown in Figure 39 summarizes the soils used, the application method, and the corresponding pan numbers for the 56 pans of soil that were tested.

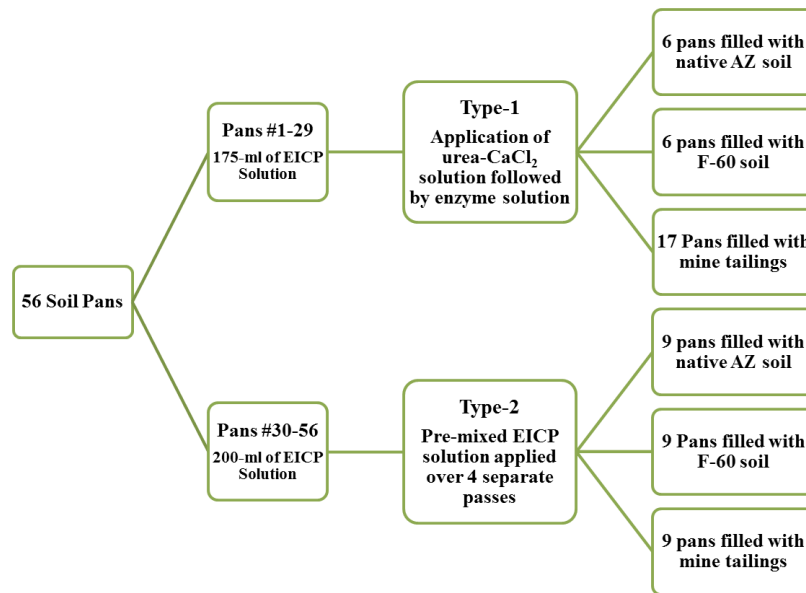


Figure 39 Flowchart summarizing the soils used and application type for the 56 soil pans. The two application types were (1) separate solutions continuously sprayed or (2) pre-mixed solutions sprayed over 4 passes. Note the additional 25-ml of solution for the Type-2 application.

EICP Solution Formulation

All of the EICP solutions used in these experiments were formulated to obtain a target initial ratio of urea to CaCl_2 of approximately 1.5:1. The initial

concentrations used in these experiments varied from 0.05 M to 2.0 M CaCl₂ for initial tests conducted in pans #1-29, and from 0.05 M to 0.40 M CaCl₂ for later tests conducted in pans #30-56. The enzyme solution was formulated to obtain a final target concentration of 0.45g/L urease enzyme (Sigma Aldrich Type-III, Jack Bean Urease, 26,100 U/g activity) and 4.0 g/L stabilizer. The CaCl₂ and urea used in these experiments were obtained from Sigma Aldrich (laboratory grade urea and calcium chloride dihydrate) and Alfa Aesar (laboratory grade calcium chloride dihydrate). The initial pH values of the EICP solutions used in these experiments ranged between 7.8 and 9.2 depending on date of preparation without any specific reason for the variation. Summaries of the chemical formulations used in the treatment Type 1 and treatment Type 2 are shown in Tables 26 and 27 (respectively).

Table 26 Chemical formulations for Type-1 application (Pans #1-29)

Type-1 Application									
Native AZ Soil					F-60 Sand				
	<u>Pan #</u>	<u>[CaCl₂]</u>	<u>Enzyme</u>	<u>pH</u>	<u>Pan #</u>	<u>[CaCl₂]</u>	<u>Enzyme</u>	<u>pH</u>	
Controls	1	Bare soil	No	--	6	Bare soil	No	--	
	2	Water only	No	7.8	7	Water only	No	7.8	
	3	1.0 M	No	7.8	8	1.0 M	No	7.8	
EICP Tests	4	1.0 M	Yes	7.8	9	1.0 M	Yes	7.8	
	5	2.0 M	Yes	8.3	10	2.0 M	Yes	8.3	
	11	2.0 M	Yes	8.3	12	2.0 M	Yes	8.3	
Mine Tailings									
	<u>Pan #</u>	<u>[CaCl₂]</u>	<u>Enzyme</u>	<u>pH</u>	<u>Pan #</u>	<u>[CaCl₂]</u>	<u>Enzyme</u>	<u>pH</u>	
Controls	13	Bare soil	No	--	27	0.20 M	No	9.1	
	14	Water only	No	7.8	16	0.37 M	No	8.4	
	21	0.05 M	No	9.2	15	0.75 M	No	8.6	
	24	0.10 M	No	9.2	--	--	--	--	
EICP Tests	22	0.05 M	Yes	9.2	29	0.20 M	Yes	9.1	
	23	0.05 M	Yes	9.2	19	0.37 M	Yes	8.4	
	25	0.10 M	Yes	9.2	20	0.37 M	Yes	8.4	
	26	0.10 M	Yes	9.2	17	0.75 M	Yes	8.6	
	28	0.20 M	Yes	9.1	18	0.75 M	Yes	8.6	

Table 27 Chemical formulations for Type-2 application (Pans #30-56)

Type-2 Application												
	Native AZ Soil				F-60 Sand				Mine Tailings			
	<u>Pan #</u>	<u>[CaCl₂]</u>	<u>Enzyme</u>	<u>pH</u>	<u>Pan #</u>	<u>[CaCl₂]</u>	<u>Enzyme</u>	<u>pH</u>	<u>Pan #</u>	<u>[CaCl₂]</u>	<u>Enzyme</u>	<u>pH</u>
Controls	39	0.05 M	No	9.1	30	0.05 M	No	9.2	54	0.40 M	No	8.1
	42	0.10 M	No	9.1	33	0.10 M	No	9.1	55	0.40 M	No	8.3
	45	0.20 M	No	9.0	36	0.20 M	No	9.0	--	--	--	--
EICP Tests	40	0.05 M	Yes	9.1	31	0.05 M	Yes	9.2	48	0.15 M	Yes	9.3
	41	0.05 M	Yes	9.1	32	0.05 M	Yes	9.2	49	0.15 M	Yes	9.3
	43	0.10 M	Yes	9.1	34	0.10 M	Yes	9.1	50	0.15 M	Yes	9.3
	44	0.10 M	Yes	9.1	35	0.10 M	Yes	9.1	51	0.30 M	Yes	9.0
	46	0.20 M	Yes	9.0	37	0.20 M	Yes	9.0	52	0.30 M	Yes	9.0
	47	0.20 M	Yes	9.0	38	0.20 M	Yes	9.0	53	0.30 M	Yes	9.0
	--	--	--	--	--	--	--	--	--	56	0.40 M	Yes

7.2.3 Chemical Analysis and Physical Characterization

Only limited chemical and physical analyses were performed on soil crusts sampled after wind tunnel testing. The analyses that were performed were chosen such that the presence of CaCO_3 could be chemically and visually confirmed and that evidence of the mode of soil improvement (e.g. inter-particle cementation) could be observed. The following tests were performed on randomly selected soil crusts: acidification using 1.0 M HCl acid for carbonate mineral detection and SEM imaging to visually confirm the presence of CaCO_3 and provide evidence of the mode of soil improvement. The presence of NH_3 was qualitatively monitored by the odor of NH_3 over the soil pans. Color changes on the soil surface were also monitored.

7.3 Results and Discussion

Qualitative Observations

The odor of NH_3 was detected over every EICP treated soil pan within the first 5-10 minutes after solution application. Depending on the test type, this odor ranged from faint to strong. In general, the soils that received the pre-mixed one-part precipitation solution used in the Type-2 tests generated a stronger NH_3 odor than the Type-1 tests, wherein the precipitation solution was applied in two separate parts. This odor persisted for a longer time in the Type-2 tests. The odor NH_3 was usually (but not always) undetectable by 2nd or 3rd day after treatment. The odor of NH_3 was not detected in any of the soils that received a salt solution only.

No changes in soil color were observed for any of the F-60 or mine tailings soil pans, but these soils are white to grayish-white in appearance which makes it difficult to observe color changes due to salt accumulation or CaCO_3 precipitation. All of the pans with native soil that were treated with either the EICP solution or salt solution developed a whitish colored precipitate. But, it was observed that the Type-2 EICP treated test pans developed a white precipitate within minutes after spray. The white color change did not appear as quickly in any of the Type-1 EICP or salt only tests.

Acid tests were performed on small sections of soil crust for pans randomly selected after wind tunnel testing. Many of the specimens from the Type-1 EICP-treated pans tested negative for the presence of a carbonate mineral, while most the specimens from the Type-2 EICP-treated pans tested positive for carbonate. It was observed that the higher concentration EICP treated soils, regardless of application type (1 or 2), almost always tested positive for the presence of a carbonate mineral. There are at least a couple of possible explanations for these observations including: (1) the small randomly selected test specimens from the Type 1 EICP-treated soil prepared using low concentration solutions did not contain CaCO_3 ; (2) the amount of CaCO_3 in the test specimens from the Type 1 EICP-treated soil prepared using low concentration solutions was too small to produce sufficiently strong effervescence; and (3) the recovered test specimens from the Type 1 EICP-treated soil prepared using low concentration solutions were not representative of the overall soil surface. Uniform topical application was difficult to achieve

and maintain across test pans; this remained a concern throughout testing and may explain the inconsistency in the acid test results.

Wind Tunnel Results

The wind tunnel testing results for the Type-1 tests of the soil in pans #1 to 29 are shown in Figure 40. Figure 40 includes six plots organized as follows: the left panel (A'-C') shows the test results using the same vertical scale (0-25 m/s) for detachment velocity (DV), and the right panel (AA'-CC') shows the test results using relative DV scales that are adjusted (or "zeroed") to the DV of the respective bare soil (the baseline condition). For example, plot B' for the F-60 sand has a DV scale of 0-25 m/s, while the adjacent plot BB' shows the same test results offset to the DV of bare F-60 sand (9 m/s). The DV of bare soil represents the soil's inherent/natural resistance to wind erosion as prepared in these experiments. The DVs of the specimens that were treated with water only are 22m/s for native sand, 23 m/s for F-60 sand, and 23 m/s for mine tailings and are shown as dashed horizontal lines on the plots.

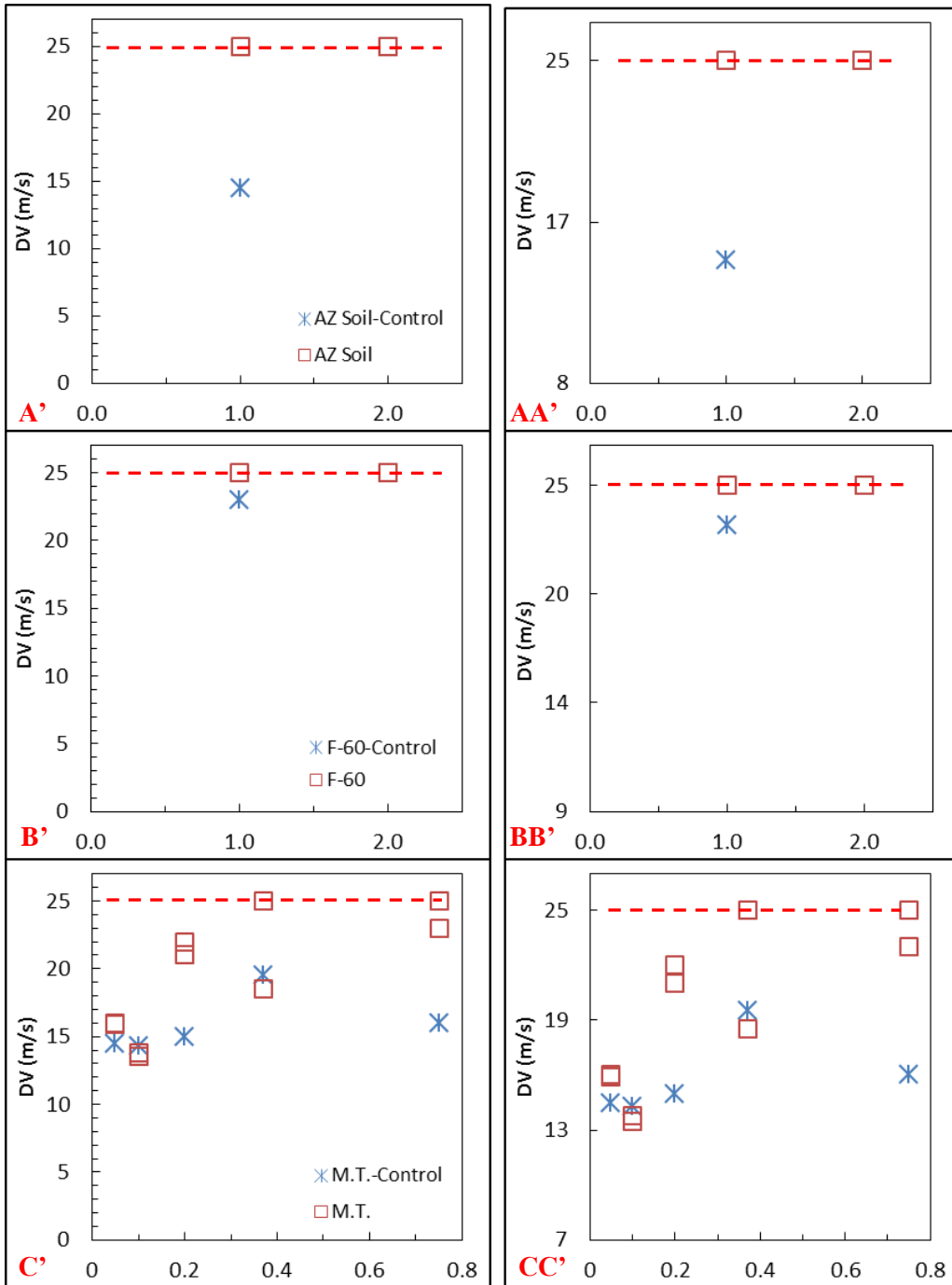


Figure 40 Type-1 wind tunnel test results of native sand, F-60 soil, and mine tailings (M.T.)—29 data points, overlapping points not visible. Red dashed line is maximum wind speed of the wind tunnel. Horizontal axis represents the initial CaCl₂ concentration. Trends in the EICP treated specimens are highlight by the solid line and dashed lines for the controls.

In general, the initial CaCl_2 concentrations used for the F-60 sand and native sand Type 1 tests are too high for the maximum wind speed employed in the test program (i.e. 25 m/s). The reported DVs are the lower bound value of 25 m/s for all of the EICP treated native sand tests plotted in Figs. 40A' and 40AA' and F-60 sand tests plotted in Figs. 40B' and 40BB' (the 4th data points in each plot are not visible due to overlap). The DVs of the three EICP treated pans with native sand were >25 m/s vs. approximately 14.5 m/s for the one salt-only treated specimen. The DVs of the three EICP treated F-60 specimens was >25 m/s vs. approximately 23 m/s for the one salt-only treated specimen. All of the native sand and F-60 soils that were EICP treated had greater DVs than the salt-only soils.

The mine tailings test results shown in plots C' and CC' of Figure 40 are for specimens treated at lower solution concentrations than the native sand and F-60 test specimens (i.e. CaCl_2 concentrations of 0.05 M to 0.75 M for the mine tailings tests). Only two of the 15 mine tailings tests have DVs greater than 25 m/s (1 each from duplicates at 0.37 M and 0.75 M CaCl_2). The overall trend is that EICP treated mine tailings had greater DVs than the salt-only treated specimens, but this trend appears to be less obvious than for the Type-2 tests on the mine tailings (Figure 40).

The wind tunnel testing results for the pans #30 to 56 treated using the Type-2 application method are shown in Figure 41 (note that overlapping data points are not visible). The results in Figure 41 are shown as six plots with the same vertical axis adjustments that were applied to the Type-1 results in Figure

40. The DVs of the specimens that were treated with water only are the same as the Type-1 tests.

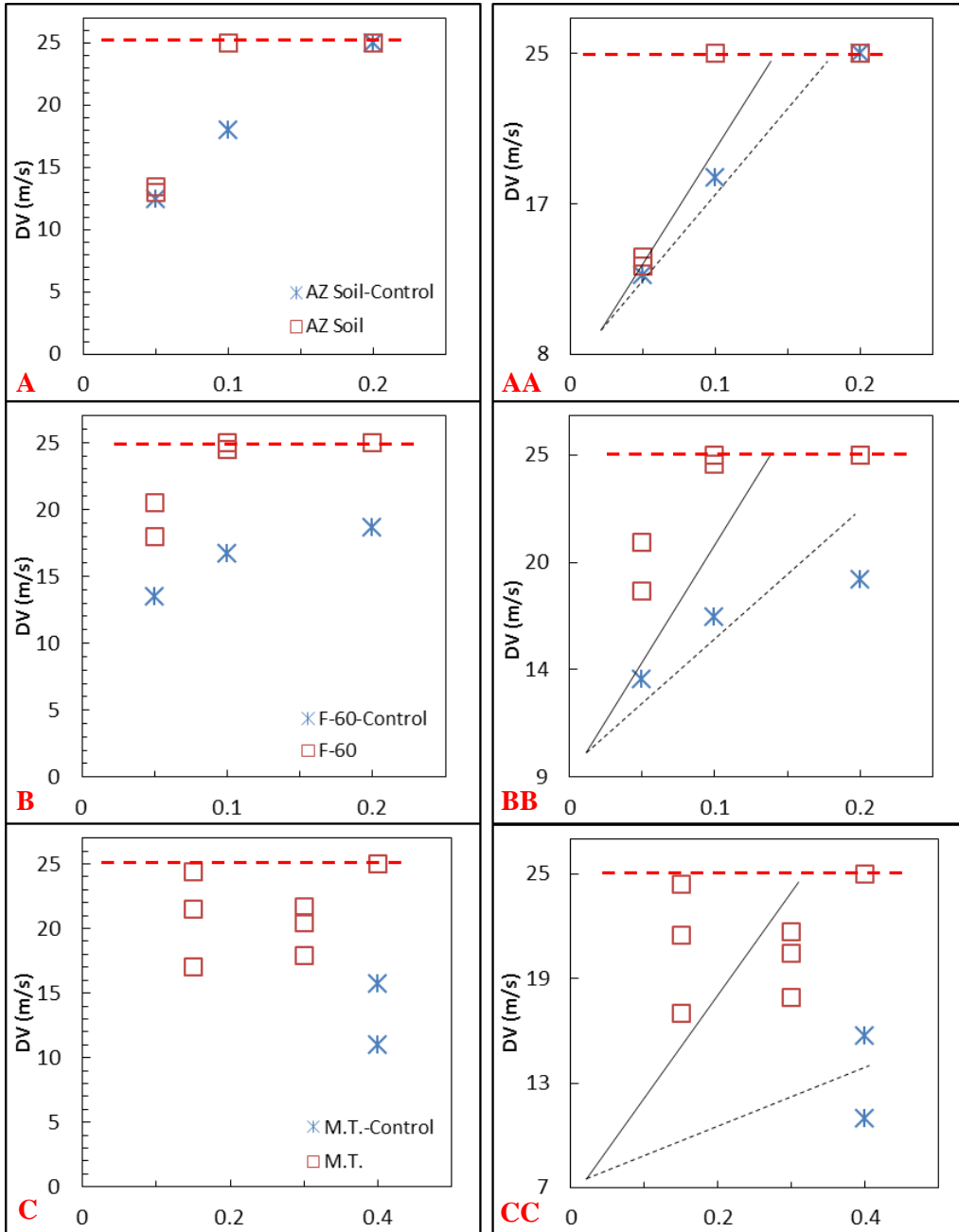


Figure 41 Type-2 wind tunnel test results of native sand, F-60 soil, and mine tailings (M.T.)—27 data points, overlapping points not visible. Plots shown in the right panel (AA-CC) are adjusted for the DV of bare soil (untreated). Max DV=25 m/s. Panels have the same meaning as in Figure 40.

The maximum wind speed for these tests was 25 m/s, therefore the data points at 25 m/s do not represent the actual DVs at the associated solution concentration. Rather, the data points at 25 m/s should be considered minimum DVs at the associated solution concentration. The plots AA to CC in the right panel contain two types of trend lines: (1) a solid line for the EICP treated soils, and (2) a dashed line for the salt treated soils (controls). The results indicate that the EICP treated soils are more resistant to wind erosion than soils treated with salt-only solution of the same concentration. More importantly, the soil treated with the EICP solution may be expected to be much more durable than soil treated with salt only, as the EICP-treated soils will be more resistant to degradation due to moisture effects (precipitation and possibly even condensation, e.g. morning dew and fog). Furthermore, the EICP treated F-60 sand and mine tailings soils at their lowest EICP treatment concentrations (0.05 M and 0.15 M, respectively) yielded greater improvements than the same soils treated with salt only at highest concentrations (0.2 M and 0.4 M, respectively).

The native sand appears to show little difference between the EICP and salt-only treated soils. However, this observation may be explained by the test limitation on assessment of the erosion resistance of these soils imposed by the 25 m/s maximum wind speed. At the lower concentrations of 0.05 M and 0.10 M, the associated DVs are approximately 13 m/s and 18 m/s for the salt-only treatment and 14 m/s and 25 m/s for EICP treatment.

In general, the EICP treated soils in the Type-1 tests had smaller margins of improvement over the salt-treated soils than the Type-2 tests. Part of this difference may be due to the extra 25-ml of solution used in the Type-2 tests. Another possible explanation for the smaller margins of improvement in the Type-1 tests may be due to poor mixing of the urea-CaCl₂ and enzyme solutions. The more even distribution of the EICP solution in the Type-2 tests (4 passes) may have also contributed to the differences between the tests. Type-2 tests used well-mixed solutions applied in four passes whereas Type-1 tests relied on mixing of the two solutions at the soil surface as they were being sprayed separately. The use of four separate application passes of smaller volume individually (50-ml) but greater total volume (200-ml) and the resulting more even distribution of the EICP solution in the Type-2 tests may have also contributed to the differences between the tests.

SEM Analysis

SEM analysis of these topically treated soils was challenging. One of the major difficulties in analyzing any natural soil is trying to locate the particle of interest (i.e. a soil particle with precipitated carbonate around it) against a background of heterogeneous features. This was the case for the native sand and mine tailings. The most difficult background features to work around in these experiments were the residual salts (NH₄⁺ and CaCl₂) and organic (urea) materials that coated the soils (in earlier experiments, soils were washed with deionized water before imaging). Residual CaCl₂, urea, and crystalized NH₄⁺

leave an amorphous coating that covers and conceals underlying features such as carbonate minerals.

Images “A” and “B” in Figure 42 show clean silica sand particles (F-60 sand) from the Type 1 experiments covered in an amorphous film and with evaporites filling in the inter-particle void spaces in some cases. Another effect of evaporites and/or salt-hydrates (for example $\text{CaCl}_2 \cdot n\text{H}_2\text{O}$) coating soil particles is seen in Figure 42B as a bright glow on and around soil particles known as “charging.” Charging results from poor conductivity between the specimen and the stage that is due to poorly conductive substances such as some salts and organics. Charging can be seen at higher magnifications as well as on poorly conductive substances. A relatively low voltage of 7.0 kV resulted in charging of the unrinsed specimen at low magnification (150x) as seen in Figure 42B. At a much higher voltages (7.0-15.0 kV) and magnifications (350x – 650x), the rinsed specimens did not charge. Rinsing with deionized water was not done in any of the Type 1 tests due to fear that the rinsing would also wash away the (presumably) very thin and most likely discontinuous CaCO_3 precipitation in the soil crust(s). This may be a reason why the presence of CaCO_3 could not be visually confirmed by SEM in any of the Type 1 samples, including those that tested positive for carbonate during acid testing.

Despite concerns about washing away the carbonate, two different Type-2 EICP treated F-60 soils were rinsed (DI water) and then analyzed (after drying). The results are shown in images “B” through “D” of Figure 42. Figures 42 E through F show the presence of CaCO_3 in both F-60 soil

specimens. Broken inter-particle contacts are seen in Figures 42 C and D and appear as flat CaCO_3 detachment points that highlight the mode of attachment between the soil particles. However, the light rinsing did not remove the residuals entirely, as illustrated by image “C” in Figure 42, where a thin connective film is seen holding two sand particles together.

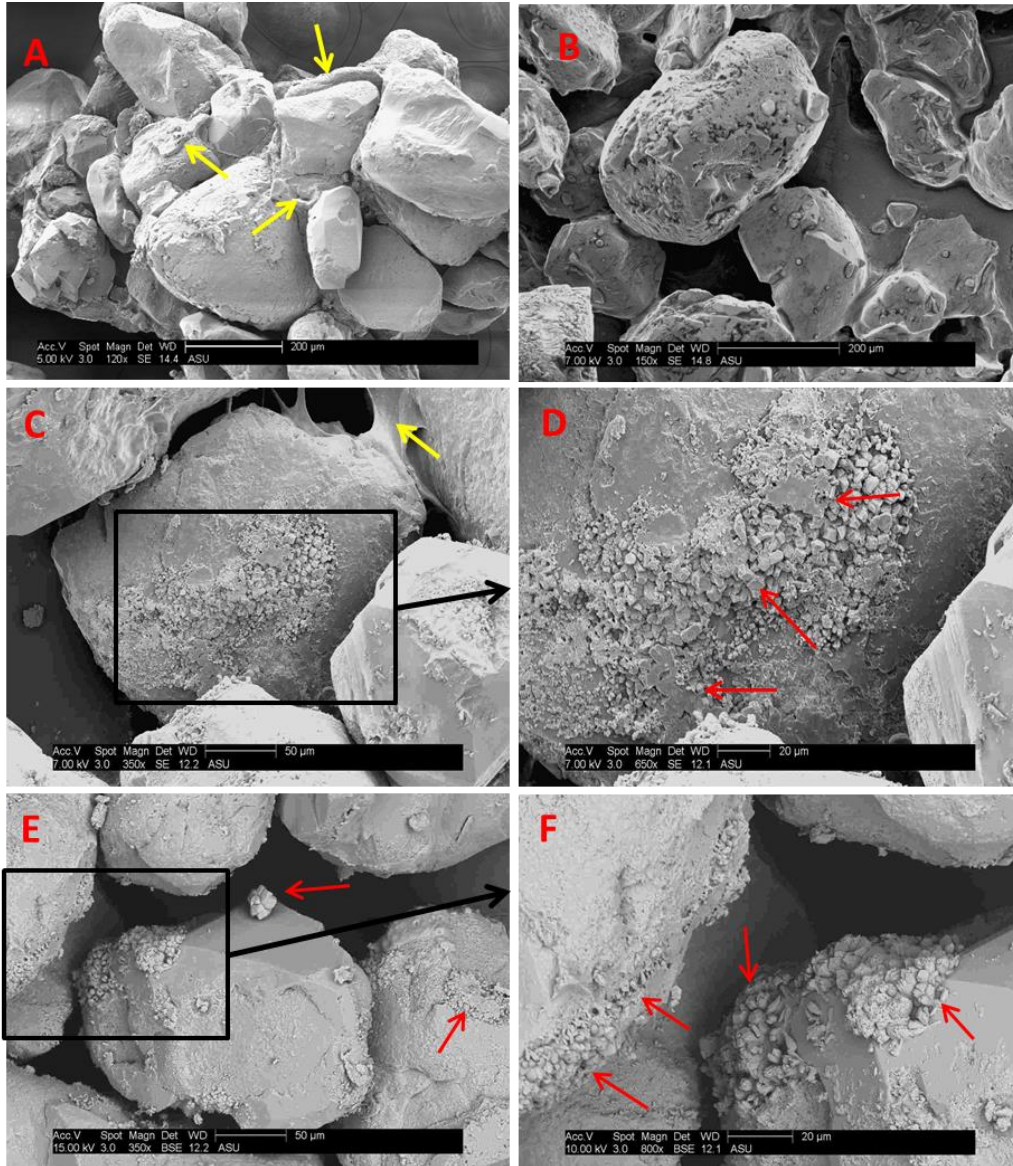


Figure 42 SEM analysis of Type-2 EICP treated F-60 soils from Pan #32 (images C and D) and Pan #35 (images E and F) after rinsing with DI water. “A” and “B” are unrinsed specimens from Pans #9 and #10, respectively. Red arrows indicate CaCO_3 , yellow arrows indicate residual salts and/or evaporites/organics. Note the much higher voltage applied in E and F (15.0 and 10.0 kV) compared to A and B (5.0 and 7.0 kV) without evidence of charging (the bright glow on and around soil particles due to poor conductivity).

7.4 Conclusion

Experiments described in this chapter indicate that a topically applied EICP solution can be used to increase the resistance to wind driven erosion of soils. Resistance to wind erosion after topical application of an EICP solution increased with increasing solution strength for both Type-1 and Type-2 application methods. The primary factor affecting the formation of a wind erosion-resistant crust as determined by detachment velocity on the fine grained sand used were solution concentration and application method. Increasing concentration of the salt, urea, and enzyme solution increased wind erosion resistance. The Type-2 application method of using a pre-mixed EICP solution was more effective than the Type-1 method of separate applications of the enzyme and salt solutions.

Evidence for ureolysis was observed in all EICP tests through the detection of an odor of NH_3 immediately following application of the precipitation solutions. Additional evidence for the formation of a carbonate mineral was observed via acid testing of randomly chosen specimens. Acid testing indicated that a carbonate mineral was present in all specimens tested using high concentration EICP solutions and in all EICP specimens treated using the Type-2 application method. Direct evidence of the presence of CaCO_3 was also found through SEM analyses on F-60 sand treated in Pans #32 and #35 using the Type-2 method. Based on the SEM images, it appears that the mode of soil improvement in these specimens was through inter-particle cementation.

CHAPTER 8

EICP WITH BIOMATERIALS

8.1 Introduction

This chapter presents the results of experiments to assess the potential applicability of EICP in a biodegradable hydrogel for surficial stabilization of soils in semi-arid to arid environments. The research presented in Chapter 7 on surficial stabilization using EICP informed some the work presented in this chapter. For example, it was noticed that the native soils and mine tailings tended to exhibit hygroscopic behavior that accelerated the desiccation of the EICP solution at the soil surface. Water is a necessary component of ureolysis and it was postulated that enhanced moisture retention may improve the EICP process by extending the reaction time. The clean, medium grained silica sand (F-60) tended to allow rapid penetration of the applied EICP solutions into deeper soil layers reducing the amount of EICP mixture available at the soil surface. The rapid penetration of the EICP mixture into deeper soil could be reduced by the increased viscosity of a hydrogel-assisted EICP solution.

Hydrogels are three-dimensional polymer networks that are primarily composed of water (typically >90% w/w) and capable of drastic volume changes. The biodegradable hydrogels used here are xanthan gum, guar gum, and KY-Jelly. Both xanthan and guar gum are polysaccharide biopolymers commonly used as thickening agents and stabilizers in food, cosmetic, and industrial applications. KY-Jelly is a synthetic polysaccharide polymer

composed primarily of methyl cellulose and typically used as a lubricant or carrier fluid in certain applications.

The Type-2 application method presented in Chapter 7 employed multiple passes (effectively increasing the “dwell time” for the EICP solution at the surface) that resulted in higher detachment velocities (DV) than the single pass, Type-1 method. A consequence of longer dwell time was longer periods of EICP activity at the soil surface. Application of a hydrogel laden with the EICP solution was postulated to provide a viscous, water-laden reaction matrix that would also extend the reaction time for EICP at the soil surface. This should lead to greater substrate utilization and CaCO_3 precipitation and, thereby, improve EICP efficiency. Hydrogel-assisted EICP may also focus CaCO_3 precipitation on the soil surface via temporary reduction in soil permeability. Furthermore, the increased viscosity of a hydrogel-assisted EICP solution may temporarily slow the off gassing of CO_2 and NH_3 which may lead to greater CaCO_3 precipitation, further enhancing the EICP process.

Experiments were set-up to evaluate hydrogel-assisted EICP. The primary objectives of these experiments were to determine the following: (1) can EICP occur in a hydrogel, i.e., will the hydrogel interfere with enzyme-mediated CaCO_3 precipitation; (2) can a hydrogel temporarily retain the EICP solution at the surface of a permeable granular soil; and (3) does the EICP-hydrogel matrix retain moisture for an extended period of time and thereby enhance EICP? The initial ratio of urea to CaCl_2 used in these experiments was

1.5:1 and the initial CaCl_2 concentrations were 2.0 M and 0.40 M for high and low concentration tests, respectively.

8.2 Methods

8.2.1 Set-up

An experiment was set-up using 15 unwaxed paper cups (89-ml, 3-oz) filled with F-60 sand to assess the potential applicability of EICP in biodegradable hydrogels for surficial stabilization of soils. The paper cups were tapered and approximately 55-mm high with an opening of approximately 50-mm in diameter. The cups were filled with sand by pouring approximately 100 grams of F-60 sand into the empty cups using a funnel at a drop height of approximately 25-mm (1"). This filled the cups with sand to a height of approximately 15-mm below their rim. The cups were then gently shaken in order to level the sand in the cups. Sand was then added or removed as necessary to achieve a uniform depth of 15-mm below the rim of the cup. Seven 50-ml glass beakers were also used in these experiments to evaluate hydrogel-assisted EICP without the complication of soil.

Three biodegradable hydrogels were employed to evaluate hydrogel-assisted EICP: xanthan gum, guar gum, and KY-Jelly. Xanthan gum and guar gum were obtained in the powder form and K-Y Jelly was procured in liquid form. High and low concentration urea and CaCl_2 solutions were prepared as follows: (1) a 200-ml high concentration solution consisting of 3.0 M urea and 2.0 M CaCl_2 -dihydrate (Sigma Aldrich laboratory grade) in reverse osmosis-purified (RO) water at pH=9.40; and (2) a 200-ml low concentration solution

consisting of 0.6 M urea and 0.4 M CaCl₂-dihydrate (Sigma Aldrich laboratory grade) in RO water at pH=9.40. Two grades of urease enzyme were used in these experiments, each prepared in RO water containing 4.0 g/L stabilizer: high-activity Type III Jack Bean, 26,100 units/gram (avg. activity) and low-activity Fisher Jack Bean 200 units/gram. The enzyme solutions were prepared to reach target concentrations of 0.44 g/L for the high-activity urease enzyme and a 0.85 g/L for the low-activity urease enzyme when added to the urea-CaCl₂ solutions.

A test that employed either xanthan gum or guar gum was started by adding approximately 15-ml of urea-CaCl₂ solution into a 50-ml glass beaker and then very slowly adding the hydrogel powder under high-speed stir at approximately 60°C. Tests that used xanthan and guar gums received approximately 0.2 g and 0.3 g of powder (respectively) per 15-ml of *high concentration* urea-CaCl₂ solution, and 0.05 g and 0.1 g of powder (respectively) per 15-ml of *low concentration* urea-CaCl₂ solution. After the hydrogel powder appeared sufficiently dissolved (i.e. little to no solids visible), 3-ml of urease enzyme solution was added to the beaker while stirring. The percent by weight of the hydrogel solids used after adding 3-ml of urease solution to the high concentration urea-CaCl₂ solutions were approximately 1.1% w/w (0.2 g) for xanthan and 1.6% w/w (0.3 g) for guar (assuming a CaCl₂-urea solution density of ≈1 g/ml). The percent by weight for the low concentration urea-CaCl₂ solutions were approximately 0.2% w/w (0.05 g) for xanthan and 0.5% (0.1 g) for guar.

The xanthan gum and guar gum hydrogel-urea-CaCl₂-enzyme solutions were stirred for approximately 30-seconds and then poured onto the soil in one of the paper cups. Since the hydrogel-EICP solution was viscous and tended to stick to the beaker, less than the entire 18-ml was added to the paper cups containing soil. It was estimated that approximately 10 to 12-ml was poured from the glass beakers rather than entire 18-ml. This process was repeated for each cup using the designated urea-CaCl₂ and enzyme solutions. Note that the initial urea-CaCl₂ concentrations of 2.0 M CaCl₂ and 0.40 M CaCl₂ were reduced to 1.66 M and 0.33 M (respectively) by the addition of 3-ml of urease solution.

The KY-Jelly experiments were started by adding approximately 15-ml of urea-CaCl₂ solution into a 50-ml glass beaker and then adding 3-ml of liquid KY-Jelly diluted by 50% with RO water prior to the urea-CaCl₂ solutions. Next, 3-ml of urease enzyme solution was added to the beaker while stirring and the mixture was then poured onto the soil in the one of the sand-filled paper cups. The seven glass beaker experiments without soil were started in the manner as described for the paper cup experiments using the high activity enzyme and the same initial total volume of approximately 18-ml. The hydrogel-EICP mixtures for the glass beaker experiments were left in the glass beakers in which they were made, rather than being transferred to new glass beakers (all 18-ml were used in these tests). Beakers #1 to #6 contained the following EICP-hydrogels mixtures: Beaker #1-2 used xanthan gum with high and low concentration EICP solutions, respectively; #3-4 used guar gum with

high and low concentration EICP solutions, respectively; #5-6 used KY-Jelly with high and low concentration EICP solutions, respectively. A control beaker #7 contained high concentration EICP solution without hydrogel (control).

Three high concentration urea-CaCl₂ controls were set-up using xanthan, guar, and KY-jelly in paper cups with soil, but without enzyme solution (3-ml of RO water was used). One high concentration urea-CaCl₂ control was set-up using guar in glass beaker without soil. The 15 paper cups containing soil and the 7 soil-less glass beakers were loosely covered and allowed to stand for 7 days. Summaries of the chemical formulations, enzyme activity (high/low), and type of hydrogel used in the soil filled paper cups and soil-less glass beakers are shown in Tables 28 and 29 (respectively).

Table 28 Summary of the chemical formulations, enzyme activity (high/low), and type of hydrogel used in the soil filled paper cups. Dashed lines indicate control specimen.

Paper Cups with F-60 Sand			
<u>Test</u>	<u>Cup #</u>	<u>[CaCl₂]</u>	<u>Enzyme Activity</u>
KY	7	2.0 M	Low
	8	2.0 M	High
	9	2.0 M	---
	10	0.4 M	Low
	11	0.4 M	High
Guar Gum	1	2.0 M	Low
	2	2.0 M	High
	3	2.0 M	---
	12	0.4 M	Low
	13	0.4 M	High
Xanthan Gum	4	2.0 M	Low
	5	2.0 M	High
	6	2.0 M	---
	14	0.4 M	Low
	15	0.4 M	High

Table 29 Summary of the chemical formulations, enzyme activity (high/low), and type of hydrogel used in the soilless filled glass beakers.

Glass Beakers without Soil			
<u>Test</u>	<u>Beaker #</u>	<u>[CaCl₂]</u>	<u>Enzyme Activity</u>
KY	20	2.0 M	Low
	21	2.0 M	High
Guar Gum	17	2.0 M	Low
	19	2.0 M	High
	22	2.0 M	---
Xanthan Gum	16	2.0 M	Low
	18	2.0 M	High

8.2.2 Sampling

Seven days after introducing the hydrogel solutions to the paper cups, a vertical “window” was cut out of the paper cups using a razorblade. The window was approximately 20-mm wide and 55-mm high (the vertical height of the cup). After peeling open the viewing window in the paper cups, the cups were tilted and tapped to allow loose soil to pour out and leaving behind a hard soil crust in some cups. The soil crust (if present) was measured and then observations were made regarding its durability by using metal tweezers to score the soil exposed by the vertical window. The soils that remained in the cups were either (a) bound to well-defined surficial crusts, (b) weakly cemented in thicker layers (compared to a crust) penetrated by the EICP solution, or (c) held together due to residual unreacted CaCl₂ salt (controls). A soil crust was considered well-

defined if the soil unit could remain intact after being lightly scored 3-4 times using a metal tweezer.

After the physical observations were completed, the soils were triple rinsed in 18.2 MΩ DI water and allowed to dry for approximately 18 days before further testing. The soil-less glass beakers that initially contained an 18-ml hydrogel-EICP mixture (or EICP solution for the control) appeared to still be wet after the 7 day experiment period. The glass beakers were allowed to stand uncovered for an additional 18 days to dry before further testing, but still appeared to be hydrated after this time.



Figure 43 Paper cups were cut open longitudinally to provide a “window” view of the soil profile. The cups were tilted and tapped to allow loose soil to pour out.

8.2.3 Chemical Analysis and Physical Characterization

Limited chemical and physical analyses were performed on soil-filled cups and glass beakers. The analyses that were performed were chosen such that the presence of CaCO_3 could be chemically and visually confirmed and that evidence of the mode of soil improvement (e.g. inter-particle cementation) could be observed. Acidification using 1.0 M HCl acid for carbonate mineral detection was performed on all hydrogel-assisted EICP soil crusts and soilless beakers. The presence of NH_3 was qualitatively monitored based upon the odor of NH_3 over individual paper cups and soil-less glass beakers. Color changes and the appearance of moisture on the soil surface (and color changes in the beakers) were also monitored. Observations were made every 30 minutes during the first 3 hours of the experiment, and then daily thereafter. SEM imaging was used to visually confirm the presence of CaCO_3 on a few selected specimens of the soil crusts to provide evidence of the mode of soil improvement.

8.3 Results and Discussion

During the first three hours of the experiment, a visible but unmeasured amount of guar-EICP and xanthan-EICP solutions remained on the soil surface of all of the paper cups treated with these hydrogel-assisted solutions. Guar and xanthan solutions that did not receive enzyme were also visible on the soil surface of the control cups. The KY-Jelly solutions (both enzyme and control) infiltrated the soil within approximately 1-minute after application. Tiny bubbles (presumably the off gassing of NH_3 and CO_2) began to develop in the cups and glass beakers

that received guar- and xanthan-assisted EICP solutions. There was no visible difference in the number of bubbles that formed based on enzyme activity. No bubbles were seen in any of the soil filled cups that received KY-Jelly based EICP solution, nor were any bubbles seen in any of the control specimens. The odor of NH_3 was detected in all cups and beakers that received a solution containing urease enzyme, but NH_3 odor was not detected in any of the controls that did not receive enzyme.

By the second day of the experiments, the tiny gas bubbles that developed during the first three hours became smaller and appeared to increase slightly in number in the xanthan-EICP solutions. The amount of gas bubbles in the guar-EICP solutions decreased by the second day of the experiment and was completely gone by the third day as the guar-EICP solutions advanced into the soil. The odor of NH_3 was strong on day two of the experiment in all of the guar- and xanthan-EICP specimens, but was only faintly detectable by the 3rd to 4th days of the experiment and without any specific pattern between the specimens. The odor of NH_3 was faintly detectable on day two of the experiment with the KY-Jelly EICP specimens and was undetectable by day three. All of the xanthan mixtures applied to sand appeared glossy until the 3rd day of the experiment and the guar mixtures applied to sand were glossy until the 2nd day of the experiment. The lack of a glossy or wet appearance in the xanthan gum and guar gum soil-filled cups was taken to mean the soil surface was essentially dry (or dehydrated). The 18-ml guar and xanthan solutions in the glass beakers remained hydrated for approximately 25 days, far longer than

EICP solution in Beaker #7 that was dry within 7 days. This required placing the glass beakers containing guar and xanthan mixtures in a drying oven for 24 hours at approximately 90°C before further testing. All KY-Jelly mixtures were dry in all of the soil cups by the 2nd day and were dry by the 7th day in the glass beakers. Color changes were not seen in the cups containing soil, possibly because the soil had a natural white to grayish appearance. All of the glass beakers that contained hydrogel-EICP solutions contained a white precipitate. Some of the white precipitate was partially suspended within the hydrogel for the guar and xanthan specimens, while the rest of the precipitate fell to (or formed at) the bottom of the hydrogel. The white precipitate appeared to be entirely at the bottom of the beakers in both KY-EICP specimens.

The following principal observations were made regarding the soil crusts: (1) soil crusts of varying thicknesses (2 to 12-mm) were formed in all cups where enzyme solution was added (later confirmed to contain CaCO₃); (2) the soil crusts formed with xanthan and guar were generally thinner and well-defined, while the KY soil crusts were highly variable; (3) the soil crusts were thicker and harder than crusts that formed in previous surficial soil stabilization tests conducted without hydrogel, presented in Chapter 7.

The depth of EICP solution penetration was determined by the fraction of loose sand that fell out of the viewing window after shaking and tapping. Sand that was penetrated with EICP solution or the salt only solution did not fall out of the cup. For example, the sand in the “Xanthan Control” cup shown in Figure 43 did not fall out of the cup even after being scored with a metal

tweezer, while the soil below the soil crust in the “Xanthan” cup (EICP-hydrogel) fell out as loose sand. The following principal observations were made regarding the effectiveness of the hydrogels at the limiting penetration of the EICP solution into cups filled with 40-mm of soil: (1) xanthan gum limited solution penetration to approximately 18–mm on average; (2) guar gum limited solution penetration to approximately 15–mm on average; and (3) KY-Jelly limited solution penetration to approximately 33–mm on average. A summary of the EICP solution penetration depth, crust thickness, and the perceived hardness of the crusts formed are shown in Table 30 along with a summary of the initial conditions. It should be noted that crusts with a perceived hardness of “soft” were flexible, indicating that the hydrogel may be the primary agent holding sand particles together. The “hard” crusts were brittle and the “medium” crusts had some initial flexibility before a brittle break.

Table 30 Summary of the EICP solution penetration depth, crust thickness, and the perceived hardness of the crusts. Asterisk indicates that several spots were tested before carbonate was detected.

Dixie Cups with F-60 Sand						
Test	Cup #	Carbonate Present	Solution Penetration Depth (mm)	Approximate Crust Thickness & Relative Hardness	[CaCl ₂]	Enzyme Activity
KY	7	Yes*	40	2-mm, soft	2.0 M	Low
	8	Yes*	40	2-mm, soft	2.0 M	High
	9	No	40	None	2.0 M	---
	10	Yes*	25	2-mm, medium	0.4 M	Low
	11	Yes	25	2-mm, medium	0.4 M	High
Guar Gum	1	Yes*	25	2-mm, soft	2.0 M	Low
	2	Yes*	13	10-mm, hard	2.0 M	High
	3	No	17	2-mm, soft	2.0 M	---
	12	Yes	10	10-mm, hard	0.4 M	Low
	13	Yes	10	10-mm, hard	0.4 M	High
Xanthan Gum	4	Yes	15	10-mm, hard	2.0 M	Low
	5	Yes	15	10-mm, hard	2.0 M	High
	6	No	40	2-mm, soft	2.0 M	---
	14	Yes	25	5-mm, hard	0.4 M	Low
	15	Yes	15	12-mm, hard	0.4 M	High

The presence of carbonate was detected in the soil crusts of all specimens that received enzyme solution indicating that hydrogel-assisted EICP does not prevent carbonate precipitation. However, Cups #1 and #2 that used guar gum and Cups #7, #8, and #10 that used KY-Jelly had to be tested in several locations before carbonate was detected (this is indicated by an asterisk in Table 30). Carbonate was detected in all of the glass beakers that received enzyme solution. Carbonate was not detected in any of the control specimens.

The results of SEM imaging of the soil crust obtain from Dixie cup #4 (xanthan-assisted EICP at high CaCl₂ concentration) are shown in Figure 44. Unfortunately, the images in Figure 44 were unintentionally saved in a low

resolution format which makes them appear pixilated. The soil crust shown in Figure 44 was aggressively rinsed, in addition to the initial rinsing previously described, in preparation for SEM analysis. Note that the images in Figure 44 do not show signs of charging (poor conductivity between the specimen and the stage that is due to poorly conductive substances such as some salts and organics) despite the relatively high voltage used (15.0 kV) and a higher magnification than used on the soil crusts in Chapter 7 that showed signs of charging (350x to 1500x vs. 120x to 650x). However, rinsing did not remove the residual materials entirely, as seen in the image in Figure 42D that shows a thin connective film (hydrogel polymer) detached from one sand particle while still attached to another. Figures 44 A through C show the presence of CaCO_3 on F-60 soil specimens. A broken inter-particle soil contact is seen in Figures 44A and 44D and appears as concave a CaCO_3 detachment point, highlighting the mode of attachment between the soil particles.

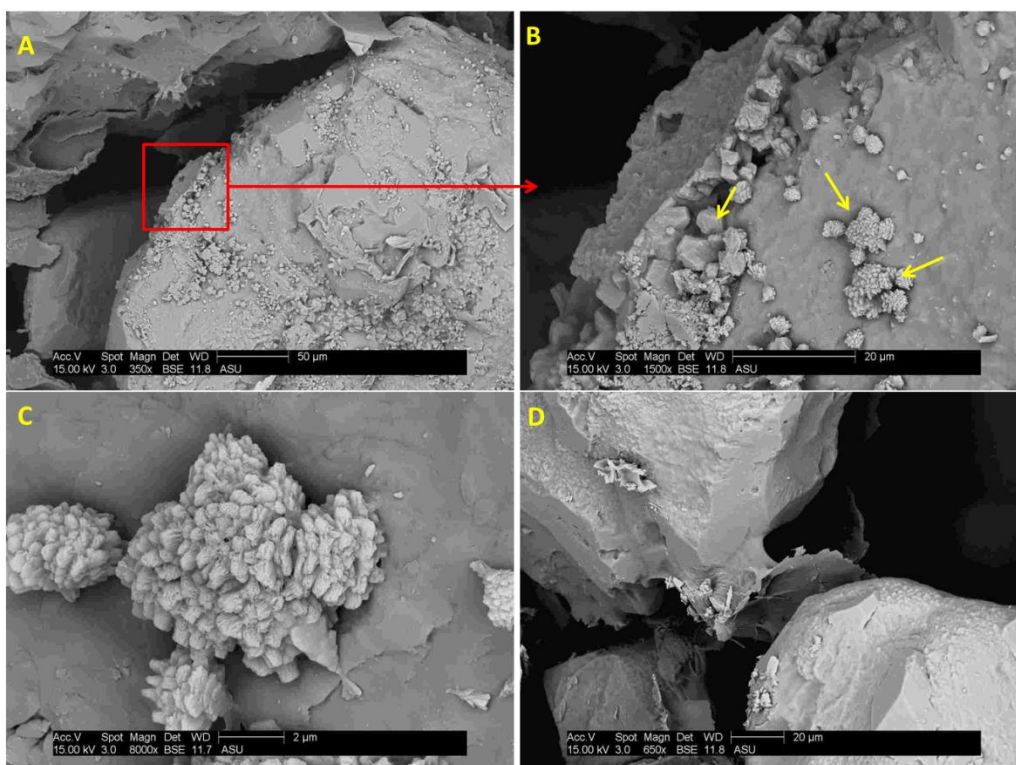


Figure 44 SEM imaging of the soil crust obtain from Cup #4 using xanthan-assisted EICP at high CaCl_2 concentration. Yellow arrows indicate CaCO_3 . Figures A-C show inter-particle CaCO_3 detachment, C shows a CaCO_3 mass growing sand particle, and D shows hydrogel detachment from a sand particle.

8.4 Conclusion

Experiments described in this chapter indicate that a topically applied hydrogel-EICP solution can be used to mediate the formation of a CaCO_3 soil crust. Hydrogel-assisted EICP occurred in sand-filled paper cups and in soil-less beakers at high (2.0 M, effective ≈ 1.66 M) and low (0.4 M, effective ≈ 0.33 M) initial CaCl_2 concentrations and with high activity and low activity enzymes. Evidence for ureolysis was observed in all hydrogel-assisted EICP tests through the detection of an odor of NH_3 immediately following application of the precipitation solutions. Acid testing provided additional evidence for the

formation of a carbonate mineral in all specimens that received hydrogel-EICP solution. Direct evidence of the presence of CaCO_3 was also found through SEM analyses of the soil crust obtained from soil-filled Cup #4 using xanthan gum. Based on the SEM images, it appears that the mode of soil improvement in these specimens was through inter-particle cementation.

Hydrogel-assisted EICP appears to retain complete the reaction matrix for extended periods of time, extending the EICP reaction time and potentially increasing precipitation efficiency. Furthermore, observations of gas bubble formation in xanthan and guar hydrogels imply that off gassing of NH_3 and/or CO_2 may be temporarily reduced, which may also increase precipitation efficiency. Hydrogel-assisted EICP also appear to have “localized” the EICP reaction matrix by reducing solution penetration into the soil.

CHAPTER 9

SUMMARY AND CONCLUSIONS

9. Summary and Conclusions

9.1 Overview

The original work described in this dissertation addresses the use of agriculturally-derived urease enzyme to induce calcium carbonate precipitation in granular soils, a process referred to herein as enzyme induced carbonate precipitation (EICP), in order to improve the mechanical properties of the soil. After a review of relevant work by others in Chapter 2, Chapter 3 addresses the optimal concentrations of constituents in the solution (or solutions) employed to induce carbonate precipitation. Chapter 4 evaluates the application of EICP in acrylic columns filled with soil. The intact, cemented columns produced from these experiments are tested for unconfined compressive strength (UCS). Chapter 5 examines the impacts of different methods of preparation (e.g., percolation and mix-and-compact) in acrylic columns and triaxial columns which are then tested for UCS and confined strength in a triaxial device. Two different soil types are used these experiments and the EICP solutions that are employed are at or near the optimal concentrations estimated in Chapter 2.

Chapter 6 illustrates the applicability of EICP as a method of improving soil by creating columns of cemented sand. The columns are made by infusing an EICP cementation solution through a perforated injection tube embedded within the soil. Mechanical strength tests on cemented specimens from these experiments are conducted when a cemented mass is symmetric and accessible

for coring. Chapter 7 describes work conducted to assess the potential applicability of enzyme induced carbonate precipitation (EICP) for surficial stabilization of soils against wind erosion. Three different soil types are used (native Arizona soil, F-60 silica sand, and mine tailings) and two different topical application methods are examined. Soil-filled pans are tested in a wind tunnel to determine soil particle detachment velocities. Chapter 8, the last research chapter in this dissertation, assesses the potential applicability of EICP in a biodegradable hydrogel for surficial stabilization of soils. Hydrogel-assisted EICP is performed in sand-filled paper cups and in soil-less beakers to determine if hydrogels can mediate the formation of a calcium carbonate (CaCO_3) soil crust. Observations pertaining to the “localization” of CaCO_3 to the soil surface and increased retention of the EICP reaction matrix in a water-laden hydrogel are monitored in this experiment.

9.2 Summary

9.2.1 Chemical Ratios and Concentration Effects in Soil-less Test Tubes

Experiments were performed in closed 15-ml and 50-ml test tubes without soil to assess the impacts on the EICP process of (1) the initial ratios of urea to calcium chloride (CaCl_2) and (2) the initial concentrations of urea and CaCl_2 . The knowledge gained from these experiments was used to estimate a “benchmark range” for the urea to CaCl_2 ratio for use in EICP. The experiments helped to understand the geochemical changes pertaining to carbonate mineral precipitation that are induced by the EICP process for potential uses in geotechnical applications.

It was determined that the geochemical changes induced by EICP depended on the initial chemical formulation of the EICP solution. The results of these experiments established the “benchmark range” of the initial urea to CaCl_2 ratio that induces a substantial rise in pH, sufficiently buffers the EICP system against rapid declines in pH during calcium carbonate (CaCO_3) precipitation, and minimizes residual nitrogen production. It was found that the benchmark range of this initial ratio is between 1.75 and 2.0 (urea to CaCl_2). The primary benefits of inducing and maintaining a sufficiently high pH environment (e.g., $\text{pH} > 9$) during CaCO_3 precipitation include: (1) increased CaCO_3 saturation that drives the EICP reaction further towards completion; (2) ammonia-ammonium ($\text{NH}_3\text{-NH}_4^+$) speciation that shift towards NH_3 which limits the acidic form (NH_4^+) and reduces the potential for reaction reversal; (3) suppression of typical nitrifying organisms that produce acidic conditions via ammonium to nitrate ($\text{NH}_4^+ \rightarrow \text{NO}_3^-$) oxidation since these organisms are typically inhibited at high pH (e.g. $\text{pH} > 9$) and/or NH_3 concentrations.

The benchmark range was shown to be valid at low concentration with an initial CaCl_2 ionic strength of 0.50 M and urea concentrations less 0.60 M. The tests performed at low ionic strength show that pH and alkalinity both increase with an increasing initial ratio of urea to CaCl_2 , and that nearly all available Ca^{2+} and urea was consumed. The benchmark range did not appear to apply to EICP at very high (i.e. $I=6.0\text{M}$) initial concentrations of CaCl_2 . Tests performed at this very high ionic strength with urea concentrations up to 6.0 M resulted in enzyme precipitation (“salting-out”), stalling the EICP process. The

enzyme precipitation appeared to be mostly reversible upon water dilution of the EICP solution, which allowed for a “restart” of EICP process. However, enzyme precipitation appeared to be less reversible at higher initial concentrations of urea, a phenomenon that is not unexpected as enzyme solubility is strongly affected by the presence of NH_4^+ . Ammonium is highly capable (more so than CaCl_2) of driving enzyme precipitation, which further illustrates the need for high pH and alkalinity in the EICP process to keep NH_4^+ levels low in order to limit enzyme precipitation.

9.2.2 Chemical Concentration Effects in Small Soil Filled Columns

Experiments were performed to assess EICP in soil-filled acrylic columns (51-mm x 102-mm) rather than soil-less test tubes. The type of soil used was Ottawa 20-30 silica sand and the EICP solution was percolated from the top of the columns. The columns were then loosely covered and allowed to stand undisturbed at room temperature for 15 days. Soil was included in this experiment to (1) determine the impact of a static and partially open soil environment on the chemical changes in the EICP process and (2) to assess the impact of CaCO_3 precipitation on the soil properties. The column tests were performed using equimolar ratios of urea and CaCl_2 at increasing initial concentrations ranging from 0.20 M to 2.20 M. While the molar ratio (1:1) that was used here deviated from the benchmark range, an equimolar ratio was considered to be a good starting point for these experiments.

In tests with initial urea- CaCl_2 concentrations of up to 0.50 M, the results of these soil-filled column experiments show a logical and recognizable

pattern of geochemical changes that are generally typical of what was anticipated for the EICP process. This pattern was not the case for the tests with initial urea-CaCl₂ concentrations of from 0.80 M to 2.20 M (the maximum tested concentration). The tests with the higher urea-CaCl₂ concentrations exhibited large variability and unexpected increases in Ca²⁺ and urea in the sampled pore fluid from the initial values, as well as discontinuous carbonate precipitation. Although it is uncertain what the actual reasons were for the large discrepancies (i.e. Ca²⁺ and urea concentrations higher than initial concentrations) in the chemical analysis data, poorly mixed environments may have played a role in this phenomenon. Dehydration and leakage of the pore fluid were also implicated as potential causes for the large discrepancies in the chemical analysis data and discontinuous carbonate precipitation. For example, the effective concentration of the bulk solution in the loosely covered columns may be greater than the initial value due to dehydration, but this could be even greater along the dehydration fronts. The results of these soil filled column tests were also affected by the limitations involved with obtaining representative pore fluid samples.

Unconfined compression tests on the soil properties of columns treated with initial concentrations of up to 0.50 M indicate that the shear strength of EICP treated soils increases with increasing CaCO₃ content. The unconfined compressive strength (UCS) testing results showed that the shear strength of cemented specimens ranged from approximately 38 kPa (0.20 M initial concentration, 0.82% CaCO₃) to 220 kPa (0.50 M, CaCO₃ not determined due

to a lab accident). Although the CaCO_3 content for the strongest specimen was not quantified, strength likely increased due to increasing CaCO_3 content. Columns treated with a 0.80 M EICP solution were partially cemented and broke into large fragments upon extraction and were therefore not amendable to UCS testing. The columns with initial concentrations from 1.10 M to 2.20 M were discontinuously cemented and composed of mostly small chunks of weakly cemented soil and thus also could not be tested in unconfined compression.

9.2.3 Influence of Soil Type and Preparation Method on Cemented Sand Columns

Triaxial compression tests and additional unconfined compression tests were conducted on columns of two different sands improved using EICP in two different ways. The sand column tests used a medium-coarse Ottawa 20-30 silica sand and a medium grain F-60 silica sand improved by percolation of the EICP solution through the sand specimens and by mixing the sand with the EICP solution and then compacting it by gentle tamping. Experiments were performed in six soil-filled acrylic columns (51-mm diameter x 152-mm tall) to evaluate the effect of the sample preparation method on EICP soil improvement as follows: three columns were prepared using the percolation method (Columns #1-3), and three columns were prepared using the mix-and-compact method (Columns #4-6). The Ottawa 20-30 sand split mold columns were prepared in two different manners: dry pluviation followed by percolation of a calcium-urease-urea cementation solution (Columns #1-2) and mixing the sand

with dry urease powder prior to percolation (Column #3) with a calcium-urea only solution (no enzyme). Two control columns in which the urease was omitted were prepared, one for each preparation method.

Experiments were also conducted in three columns prepared in membrane-lined split molds approximately 71mm-diameter x 152 mm-tall for subsequent triaxial compression testing. Two of the columns prepared in the split molds were prepared using Ottawa 20-30 sand and the third split-mold column was prepared using Ottawa F-60 sand. The percolation of a calcium-urea-urease cementation solution was used to treat all three triaxial columns prepared in the split-molds. The objective of these tests was to evaluate (1) the influence of application of a confining pressure on EICP improved soil; (2) the effectiveness of the EICP process on the mechanical strength properties of two different soil types (medium and fine sand); and (3) the influence of the method of percolation on the properties of the cemented soil.

The results of these tests demonstrate the effect of the method of sample preparation on the unconfined strength of EICP-improved sand, the effects of EICP on the mechanical strength properties of two different soil types (medium-coarse and medium sands), the influence of a confining pressure on the behavior of EICP-treated sand, and highlight the morphological features of EICP in sand via SEM analysis. Cementation of soil particles was observed in all test columns except for the control acrylic columns. XRD testing performed on selected columns from each method of preparation confirmed that calcite phase CaCO_3 was the cementing agent. SEM imaging indicates that the

morphological features of EICP in silica sand through the mix-and-compact and percolation methods appeared to be similar in both cases. This preliminary finding is generally consistent with previous results that show morphological features are most likely related to concentrations and environmental conditions of precipitation, both of which were similar across these experiments.

The multiple applications (between 2 and 5 depending on the column type) used in the percolation method applied to the acrylic columns yielded correspondingly greater CaCO_3 precipitation. However, the effort needed to break apart cemented chunks of sand (i.e., the quality of cementation) varied depending on the sampling location within the column in all cemented columns. Triaxial test results on cemented columns showed substantial strength increases over non-cemented columns at the same relative density. The results of UCS testing show substantial strength increase for both percolation and mix-and-compact test columns prepared with Ottawa 20-30 sand and F-60 sand.

The initial urea to CaCl_2 ratios used in these experiments ranged from approximately 1.2:1 to 1.5:1, which is lower than the benchmark range between 1.5:1 and 2.0:1. But, the low-grade (or low-activity) Fischer enzyme used here has a specific activity (200 unit/gram) that is approximately 150 to 250 times *lower* than the Sigma Aldrich enzyme used in experiments presented in the others chapters. In addition, the highest initial concentration used in these experiments was approximately 1.3 M CaCl_2 ($I = 3.9$ M) for mix-and-compact Acrylic Columns #4-6, a concentration which resulted in inhibited ureolysis and

enzyme salting-out in previous tests using a highly active (purified) urease. This did not appear to be the case using low-grade enzyme.

9.2.4 Columnar Stabilization using EICP

Experiments were performed to demonstrate that an EICP solution delivered through a perforated injection tube can be used to induce columnar soil cementation. The experiments described in this chapter were performed in progressively larger soil containers. Columnar cementation was induced through the injection of an EICP solution into Ottawa 20-30 and F-60 silica sand in three 102 mm-diameter PVC columns, Ottawa 20-30 in six 19 L (5 gallon) buckets, and native (Arizona) sand in an approximately 1 m³ wooden box. Except for a smaller follow-up injection at an initial ratio of urea to CaCl₂ of approximately 1.1:1 for the experiments using 102-mm (4") diameter PVC columns, the experiments performed here received an initial ratio of urea to CaCl₂ of approximately 1.5:1 to 1.7:1 (+/-0.05).

The odor of NH₃ was detected in every test conducted here and ranged from strong to very strong in the pore fluid or the injection tube. Faint odors of NH₃ were detected in the fluid on or very near the top soil layers of every test, at least temporarily. The addition of 0.1% 1.0 M NaOH near end of each experiment helped increase pH (at least locally) and shift the nitrogen balance towards NH₃ (rather than NH₄⁺) to further favor the conditions conducive to CaCO₃ precipitation.

The three PVC sand columns were filled with either Ottawa 20-30 or F-60 sand and were injected with EICP cementation solution under inundated (or

flooded) soil conditions. One of these columns was injected with a dilute sodium bentonite slurry (unit weight = 10.5 kN/m^3) prior to delivery of the cementation solution. Cementation was observed in all of the PVC columns treated with the EICP solution. The PVC column that received sodium bentonite slurry displayed a cylindrically-shaped zone of strongly cemented soil, while the columns that did not receive sodium bentonite displayed bulb-shaped cemented zones. The column that received sodium bentonite slurry was acid digested and had a CaCO_3 content of approximately 1.8%. Specimens from the columns that did not receive sodium bentonite were acid digested after long term physical observation (approximately 1 year) and had CaCO_3 contents of 4.17% (Ottawa 20-30 sand) and 4.67% (Ottawa F-60 sand). None of these columns were amenable to coring for mechanical testing. SEM and XRD analysis of cemented sand specimens from all three PVC columns show a visible precipitated mineral coating on and in between sand particles and that the precipitated mineral is calcite phase CaCO_3 .

The six 19 L buckets filled with Ottawa 20-30 silica sand were injected with EICP cementation solution under (a) dry and (b) inundated soil conditions. Cementation was observed in all six buckets treated with the EICP solution. In the inundated soil buckets, bulb-shaped cementation zones that were firmly attached to the injection tubes upon removal formed. In the dry soil buckets either a donut-shaped cemented soil mass or cemented chunks formed radially around the perforated tube. One of the dry soil buckets contained a symmetric and accessible cemented soil mass that could be cored to extract specimens for

strength testing. Unconfined compressive strength testing results on five cemented specimens from this bucket yielded shear strengths from approximately 35 kPa to 125 kPa (CaCO₃ content of these specimens was not available due to a lab accident). The remaining intact soil masses from the other buckets (#1, #3, and #4-6) were acid digested after long term physical observation (approximately 8 months). The CaCO₃ contents of Buckets #1, #3, #4, #5, and #6 were 2.9%, 1.0%, 3.4%, 2.3%, and 2.2% (respectively).

The approximately 1 m³ box filled with approximately 1027-kg of native (Arizona) well-graded sand was injected with EICP cementation solution through a perforated vertical tube in the center of the box under inundated soil conditions. Cementation was observed in a saddle-shaped column that was subjectively stronger near the perforated tube. Acid digestion showed that the cemented areas near the perforated tube contained approximately three times more CaCO₃ on a dry weight percentage basis than the cemented areas farther away (2.9% vs. 1.1% on average).

9.2.5 Surficial Soil Stabilization

Experiments were performed to assess the potential applicability of enzyme induced carbonate precipitation (EICP) for surficial stabilization of soils against wind erosion. Both microbially induced carbonate precipitation (MICP) and EICP can potentially be employed to stabilize erodible surficial soils. However, the advantages to the EICP method are that it induces rapid carbonate precipitation and is more efficient than MICP since EICP does not consume or compete for the organic substrate (urea). These two advantages make EICP

well-suited for surface treatments that have a relatively short temporal frame within which they need to become effective and increases the overall efficiency of carbonate precipitation.

The use of EICP for surficial stabilization of soils against wind driven erosion was investigated by wind tunnel testing of soil filled pans that were topically treated with an EICP solution. The testing program focused on the following key areas: (1) developing an application method to induce surficial calcium carbonate (CaCO_3) precipitation via EICP; (2) quantifying the resistance of typical erosion-susceptible soils to wind erosion after topical application of an EICP solution; and (3) assessing the primary factors affecting the formation of a wind erosion resistant CaCO_3 crust on typical wind erosion susceptible soils.

In developing a method for the topical application of the EICP solution, the following fundamental questions regarding how the EICP solution should be applied were investigated: (1) what is the effect of spraying an EICP solution as a complete pre-mixed solution of urea, CaCl_2 , and urease vs. application as separate solutions; (2) if the constituents are to be applied separately, does the sequence of reagent application matter. Additional questions that were addressed in the testing program include whether the rate of reagent application and the number of applications of the various solutions affect the formation of CaCO_3 crust on the soil.

The initial ratio of urea to CaCl_2 used in these experiments was 1.5:1 and the initial CaCl_2 concentration of the solutions used in the first 8 of the

initial 56 pans tested was either 1.0 M or 2.0 M, consistent with the tests in previous chapters. However, the solution applied subsequently to another 48 pans contained concentrations of CaCl_2 varying from 0.05 M to 0.40 M. Treated specimens were tested in the ASU-NASA Wind Tunnel to quantify the soil particle detachment velocity (DV), a key parameter describing resistance to wind driven erosion. The following three soil types were used in these experiments: (1) native Arizona soil, (2) clean, medium grained silica sand (F-60), and (3) mine tailings. Two topical application treatment methods were used in these experiments: (a) Type-1 treatment employed separate applications of the enzyme and salt solutions and (b) Type-2 treatment employed a pre-mixed EICP solution.

For the Type-1 tests, the DVs for the EICP treated native AZ and F-60 soils exceeded the wind tunnel maximum velocity of 25 m/s at both CaCl_2 concentrations tested (1.0 M and 2.0 M). The DVs for control specimens treated using the same CaCl_2 concentrations (1.0 M and 2.0 M) but without enzyme were 14.5 m/s and 23 m/s (respectively). The CaCl_2 concentrations used for the mine tailings ranged from 0.05 M to 0.75 M. The average DVs for the EICP treated mine tailings ranged from 14.0 m/s to >25 m/s. The DVs for the treated mine tailings were greater than the control specimens in every case except at a CaCl_2 concentration of 0.10 M, where the DV for the control specimen was 14.5 m/s and the DV for the EICP treated specimen was 14.0 m/s. The DVs for native AZ soil, F-60, and mine tailings that were wetted with water only were 22 m/s, 23 m/s, and 23 m/s, respectively. A CaCl_2 concentration of

0.4 M for the EICP treated mine tailings was required to achieve a DV equal to wetted mine tailings. For the Type-2 tests, CaCl_2 concentrations of 0.10 M, 0.10 M, and 0.15 M were required for the EICP treated soils to achieve DVs equal to wetted native AZ soil, F-60 soil, and mine tailings (respectively). The average DVs for all three soil types ranged from 14.5 m/s to >25 m/s and were greater than the control specimens at every CaCl_2 concentration.

Resistance to wind erosion after topical application of an EICP solution increased with increasing solution strength for both Type-1 and Type-2 application methods. The primary factors affecting the formation of a wind erosion-resistant crust as determined by detachment velocity on the medium grained sand used were solution concentration and application method. Increasing concentration of the salt, urea, and enzyme solution increased wind erosion resistance.

Evidence for ureolysis was observed in all EICP tests through the detection of an odor of NH_3 immediately following application of the precipitation solutions. Additional evidence for the formation of a carbonate mineral was observed via acid testing of randomly chosen specimens. The acid testing indicated that a carbonate mineral was present in all specimens tested using high concentration EICP solutions and in all EICP specimens treated using the Type-2 application method. Direct evidence of the presence of CaCO_3 was also found through SEM analyses on F-60 sand treated in Pans #32 and #35 using the Type-2 method. Based on the SEM images, it appears that the mode of soil improvement in these specimens was through inter-particle cementation.

9.2.6 EICP in Biomaterials

Experiments were performed to assess the potential applicability of EICP in a biodegradable hydrogel for surficial stabilization of soils. The research on surficial stabilization using EICP (Chapter 7) informed some the work presented in this chapter. The primary objectives of these experiments were to determine the following: (1) can EICP occur in a hydrogel, i.e., will the hydrogel interfere with enzyme-mediated CaCO_3 precipitation; (2) can a hydrogel temporarily retain the EICP solution at the surface of a permeable granular soil; and (3) does the EICP-hydrogel matrix retain moisture for an extended period of time and thereby enhance EICP? The initial ratio of urea to CaCl_2 used in these experiments was 1.5:1 and the initial CaCl_2 concentrations were 2.0 M (effective ≈ 1.66 M) and 0.40 M (effective ≈ 0.33 M) for high and low concentration tests, respectively.

Hydrogel-assisted EICP occurred in sand-filled paper cups and in soil-less beakers at high (2.0 M) and low (0.4 M) initial CaCl_2 concentrations and with high activity and low activity enzymes. Evidence for ureolysis was observed in all hydrogel-assisted EICP tests through the detection of an odor of NH_3 immediately following application of the precipitation solutions. Acid testing provided additional evidence for the formation of a carbonate mineral in all specimens that received hydrogel-EICP solution. Direct evidence of the presence of CaCO_3 was also found through SEM analyses of the soil crust obtained from soil-filled Cup #4 using xanthan gum. Based on the SEM

images, it appears that the mode of soil improvement in these specimens was through inter-particle cementation.

9.3 Conclusions

Isolated urease enzyme can be employed to induce carbonate mineral precipitation for soil improvement processes. A benchmark range of the optimal initial ratio of urea to CaCl_2 was estimated to be between approximately 1.75:1 and 2.0:1. This optimal initial ratio range was found to substantially increase pH after the removal of Ca^{2+} , sufficiently buffer the EICP system against a rapid decline in pH due to CaCO_3 precipitation, and release the least amount of residual nitrogen. Elevated pH (e.g. >9) and increased buffering capacity can mitigate the formation of ammonium and suppress nitrification, both of which may have detrimental impacts on calcium carbonate. The results from the high concentration tests imply that the EICP process may be very limited at high initial concentrations of urea and/or CaCl_2 unless enzyme precipitation can be addressed. On the other hand, controlled enzyme precipitation may open the possibility to a controlled EICP process that can be initiated upon water dilution of an enzyme- CaCl_2 -urea matrix.

Experiments performed in soil-filled acrylic columns that were prepared by percolation with an EICP solution show that CaCO_3 contents between 0.82% and 1.44% achieved unconfined compressive strengths between 38 kPa and 210 kPa. Triaxial columns that were treated by percolation with EICP solution in the same manner as the acrylic columns produced CaCO_3 contents between 1.6% and 2.0% and the shear strengths were between 9.0 kPa to 30 kPa greater

than the untreated specimens at a confining pressure of 60 kPa. Soil-filled acrylic columns that were prepared through a mix-and-compact method yielded CaCO_3 contents between 2.82% and 4.30% and had associated unconfined compressive strengths between 529 kPa and 392 kPa (respectively). Both the carbonate content and unconfined strength of the specimens prepared by the mix-and-compact method were higher than those of the specimens prepared by percolation.

Experiments were performed to demonstrate that an EICP solution delivered through a perforated injection tube can be used to induce columnar soil cementation. Tests were carried out in 102-mm diameter clear PVC columns, 19-L buckets, and in a soil-filled box that was approximately 1-m^3 in dimension. Cementation was observed in all three test arrangements.

One of the PVC columns was injected with sodium bentonite slurry prior to delivery of the cementation solution. The injected PVC column that received sodium bentonite slurry displayed a cylindrically-shaped zone of strongly cemented soil, while the columns that did not receive Na-bentonite displayed bulb-shaped cemented zones. EICP applied with a Na-bentonite slurry may be useful for creating low-permeability barriers in addition to the soil strength improvement from CaCO_3 precipitation.

The cementation in the inundated 19 L buckets treated with the EICP solution was bulb-shaped and firmly attached to the injection tubes upon removal from the buckets. The dry soil buckets produced either a donut-shaped cemented soil mass or cemented chunks that formed radially around the

perforated tube. Only one of the six buckets contained a symmetric and accessible cemented soil mass that could be used to extract a cored specimen. Unconfined compressive testing results of five specimens from this bucket show that the shear strength of cemented specimens ranged from approximately 35 kPa to 125 kPa (CaCO_3 content was not available due to a lab accident). The remaining intact soil masses from the other buckets (#1, #3, and #4-6) were acid digested after long term physical observation (approximately 8 months). The CaCO_3 contents of Buckets #1, #3, #4, #5, and #6 were 2.9%, 1.0%, 3.4%, 2.3%, and 2.2% (respectively).

The largest experiment used a wooden box that was approximately 1 m^3 in volume filled with approximately 1027-kg of native AZ well-graded sand. Cementation was observed in a saddle-shaped column that was subjectively assessed to be stronger near the perforated tube. Acid digestion showed that the cemented areas near the perforated tube contained approximately three times more CaCO_3 on a dry weight percentage basis (1.1% vs. 2.9% on average) than the cemented areas farther away (i.e. in the saddle area). These experiments demonstrate that EICP may potentially be used to form cemented columns of sand for ground improvement purposes.

The results of the wind erosion experiments indicate that a topically applied EICP solution can be used to increase the resistance to wind driven erosion of soils. Resistance to wind erosion after topical application of an EICP solution increased with increasing solution strength for both Type-1 and Type-2 application methods. The primary factors affecting the formation of a wind

erosion-resistant crust as determined by detachment velocity on the medium grained sand used were solution concentration and application method. Increasing concentration of the salt, urea, and enzyme solution increased wind erosion resistance. The Type-2 application method of using a pre-mixed EICP solution was more effective than the Type-1 method of separate applications of the enzyme and salt solutions.

Hydrogel-assisted EICP appears to retain the complete reaction matrix for extended periods of time, extending the EICP reaction time and potentially increasing precipitation efficiency. Furthermore, observations of gas bubble formation in xanthan and guar hydrogels imply that off gassing of NH_3 and/or CO_2 may be temporarily reduced, which may also increase precipitation efficiency. Hydrogel-assisted EICP also appears to have “localized” the EICP reaction matrix by reducing solution penetration into the soil.

9.4 Recommendations for Future Work

The work presented herein has provided insight to the influence of initial chemical concentrations on enzyme induced carbonate precipitation (EICP). However, additional experiments focusing on important parameters of interest would be useful in further understanding and successfully developing EICP. One important parameter is the maximum initial concentration of reagents that yield inter-particle cementation. The rate of carbonate mineral precipitation is affected by the geochemical conditions induced by the EICP process, and the initial chemical concentrations directly affect the temporal extent of these changes. In pursuing the maximum concentration parameter, questions relating

to the solubility of the urease enzyme must also be addressed in future work. One important aspect of urease enzyme solubility is the impact of a changing chemical environment. During EICP, one ion type (Ca^{2+} e.g.) that is capable of precipitating the enzyme is removed while another more detrimental one is produced in its place (NH_4^+). An important question that needs to be answered is at what point does this evolving chemical environment hinder EICP and is it different than the initial chemical concentration?

EICP appears to be exceptionally promising for columnar stabilization of soil. Additional work is needed to identify the optimal delivery method for the cementation solution(s), e.g. the impact of solution injection rate into the soil. EICP relies on producing the conditions conducive to CaCO_3 precipitation and high injection rates may result in the dispersal of the EICP solution over a broader area than intended resulting in dilution. This may effectively dilute the chemical matrix that would ordinarily lead to saturation with CaCO_3 and result in CaCO_3 precipitation. Other aspects of columnar stabilization that should be investigated include the range of soil types (or grain sizes) over which the method is applicable and the impact of using a two-part injection scheme (e.g. a CaCl_2 solution followed by a urease solution, or vice-versa).

Pre-injection of a bentonite slurry is particularly intriguing variation on EICP for both columnar and mass stabilization, considering the uniform improvement observed in the laboratory column test using sodium bentonite. More laboratory work is needed to understand the interaction between the bentonite particles, the soil particles, and the cementation solution. The use of

calcium bentonite should also be explored due to the possibility of some sort of beneficial interaction between the calcium ions in the bentonite, the cementation solution, and the alkaline pH conditions induced via ureolysis.

An additional area that should be pursued in future work is related to the use of biodegradable hydrogels for both surficial and subsurface stabilization. Hydrogel-assisted EICP for surficial stabilization via application of a topical solution appears promising for applications where a simple EICP solution cannot be applied (e.g. on vertical surfaces) and in environments where rapid desiccation of the EICP solution is anticipated (e.g. dry and/or porous soils and/or warm climates). Hydrogel-assisted EICP may also facilitate improvement of granular fill soil using conventional admixture compaction and creation of bio-bricks using EICP by minimizing segregation of the soil and cementation medium. Additional work on these applications seems warranted, as they can help address important problems in sustainable infrastructure development and environmental protection.

REFERENCES

- Al Qabany, Ahmed, Kenichi Soga, and Carlos Santamarina. "Factors affecting efficiency of microbially induced calcite precipitation." *Journal of Geotechnical and Geoenvironmental Engineering* 138.8 (2012): 992-1001.
- Al-Thawadi, Salwa Mutlaq. "Ureolytic bacteria and calcium carbonate formation as a mechanism of strength enhancement of sand." *J Adv Sci Eng Res* 1 (2011): 98-114.
- Alberts, B. (2002). *Molecular Biology of the Cell*. 4th Ed. New York, Garland Science.
- Anthonisen, A. C., R. C. Loehr, T. B. S. Prakasam, and E. G. Srinath. "Inhibition of nitrification by ammonia and nitrous acid." *Journal (Water Pollution Control Federation)* (1976): 835-852.
- Antoniou, P., J. Hamilton, B. Koopman, R. Jain, B. Holloway, G. Lyberatos, and S. A. Svoronos. "Effect of temperature and pH on the effective maximum specific growth rate of nitrifying bacteria." *Water Research* 24, no. 1 (1990):97-101.
- Bang, Sookie S., Sangchul Bang, Sabine Frutiger, Leah M. Nehl, and Beth L. Comes. "Application of novel biological technique in dust suppression." In *Transportation Research Board 88th Annual Meeting*, no. 09-0831. 2009.
- Baumert, K.A., Herzog, T., and Pershing, J. (2005). *Navigating the Numbers, Greenhouse Gas Data and International Climate Policy*. World Resources Institute.
- Benini, Stefano, Wojciech R. Rypniewski, Keith S. Wilson, Silvia Miletti, Stefano Ciurli, and Stefano Mangani. "A new proposal for urease mechanism based on the crystal structures of the native and inhibited enzyme from *Bacillus pasteurii*: why urea hydrolysis costs two nickels." *Structure* 7, no. 2 (1999): 205-216.
- Bernardi, D., J. T. DeJong, B. M. Montoya, and B. C. Martinez. "Bio-bricks: Biologically cemented sandstone bricks." *Construction and Building Materials* 55 (2014): 462-469.
- Blakely, R.L. and Zerner, B. (1984). "Jack Bean Urease: The First Nickel Enzyme." *Journal of Molecular Catalysis*, Vol. 23, pp. 263 – 292.

- Burbank, Malcolm, Thomas Weaver, Ryan Lewis, Thomas Williams, Barbara Williams, and Ronald Crawford. "Geotechnical tests of sands following bioinduced calcite precipitation catalyzed by indigenous bacteria." *Journal of Geotechnical and Geoenvironmental Engineering* 139, no. 6 (2012): 928-936.
- Chou, Chiung-Wen, Eric A. Seagren, Ahmet H. Aydilek, and Michael Lai. "Biocalcification of sand through ureolysis." *Journal of Geotechnical and Geoenvironmental Engineering* 137, no. 12 (2011): 1179-1189.
- Ciurli S., Marzadori C., Benini S., Deiana S. and Gessa C. (1996). "Urease from the soil bacterium *Bacillus pasteurii*: Immobilization on Ca-polygalacturonate." *Soil Biol. & Biochem.* Vol. 28, pp 811-817.
- Das, N., Kayastha, A.M. and Srivastava, P.K (2002). "Purification and characterization of urease from dehusked pigeonpea (*Cajanus cajan L.*) seeds." *Phytochemistry*, Vol. 61:5, pp. 513-521.
- De Muynck, Willem, Dieter Debrouwer, Nele De Belie, and Willy Verstraete. "Bacterial carbonate precipitation improves the durability of cementitious materials." *Cement and concrete Research* 38, no. 7 (2008): 1005-1014.
- De Muynck, Willem, Nele De Belie, and Willy Verstraete. "Microbial carbonate precipitation in construction materials: a review." *Ecological Engineering* 36, no. 2 (2010): 118-136.
- DeJong, J.T., Fritzes, M.B., Nusslein, K. (2006). "Microbially Induced Cementation to Control Sand Response to Undrained Shear." *J. Geotech. and Geoenv Eng.* ASCE, Vol. 132(11): 1381-1392.
- DeJong, J.T., Mortensen, B.M., Martinez, B.C., Nelson, D.C. (2010). "Bio-mediated soil improvement." *Ecological Engineering*, Vol. 36: 197-210.
- Dhami, Navdeep Kaur, M. Sudhakara Reddy, and Abhijit Mukherjee. "Improvement in strength properties of ash bricks by bacterial calcite." *Ecological Engineering* 39 (2012): 31-35.
- Dionex application note 140, Dionex Corp., Sunnyvale, CA, USA.

- Dixon, N.E., Hinds, J.A., Fiheiy, A.K., Gazzola, C., Winzor, D.J., Blakeley, R.L. and Zerner, B. (1980). "Jack bean urease (EC 3.5.1.5). IV. The molecular size and the mechanism of inhibition by hydroxamic acids. Spectrophotometric titration of enzymes with reversible inhibitors." *Can. J. Biochem.*, Vol.58, pp 1323.
- Dixon, J.C., and McLaren, S.J. (2009). Duricrusts. *Geomorphology of Desert Environments*. 2nd Ed. Netherlands, Springer Netherlands.
- Ehrlich, H.L. (2002). *Geomicrobiology*. New York, Marcel Dekker.
- Fortin, D., Ferris, F.G., and Beveridge, T.J., (1997). Surface-mediated mineral development by bacteria. *Geomicrobiology: Interactions between Microbes and Minerals* (Rev Mineral, Vol.35), edited by J.F. Banfield and K.H. Nealson, Mineralogical Society of America, Washington D.C., pp. 161-180.
- Grasby, Stephen E. "Naturally precipitating vaterite (μ -CaCO₃) spheres: unusual carbonates formed in an extreme environment." *Geochimica et Cosmochimica Acta* 67, no. 9 (2003): 1659-1666.
- Gomez, M., DeJong, J.T., Martinez, B.C., Hunt, C.E., deVlaming, L.A., Major, D.W., and Dworatzek, S.M. (2013). "Bio-mediated Soil Improvement Field Study to Stabilize Mine Sands," *Proc. GeoMontreal2013*.
- Gustavsen, Öyvind, Katerina Kofina, Petros Koutsoukos, Tore Larsen, Marianna Lioliou, Terje Östvold, and Takis Paraskevas. "Method and composition for stabilizing earth and sand to prevent soil erosion." U.S. Patent 7,841,804, issued November 30, 2010.
- Gutierrez, A. (2013). "The Impact of Liquefaction on the Microstructure of Cohesionless Soils." M.S, Thesis, Department of Civil, Environmental, and Sustainable Engineering Arizona State University, Tempe, AZ.
- Hamdan, N., Kavazanjian, E., Jr., Rittmann, B.E., and Karatas, I. (2011) "Carbonate Mineral Precipitation for Soil Improvement through Microbial Denitrification," *Proc. GeoFrontiers 2011: Advances in Geotechnical Engineering*, ASCE Geotechnical Special Publication 211, pp. 3925 – 3934.
- Harkes, M. P., Van Paassen, L. A., Booster, J. L., Whiffin, V. S., and Van Loosdrecht, M. (2010) "Fixation and Distribution of Bacterial Activity in Sand to Induce Carbonate Precipitation for Ground Reinforcement," *Ecological Engineering*, 36(2), 112-117.

- Harris, Ralph Edmund, and Ian Donald McKay. "Method for treatment of underground reservoirs." U.S. Patent 6,763,888, issued July 20, 2004.
- He, J., Chu, J., and Ivanov, V. (2013). "Mitigation of Liquefaction of Saturated Sand using Biogas," *Geotechnique*, 63(4), 267-275.
- Hirayama, Chikara, Masahiro Sugimura, Hitoshi Saito, and Masatoshi Nakamura. "Purification and properties of urease from the leaf of mulberry, *Morus alba*." *Phytochemistry* 53, no. 3 (2000): 325-330.
- Hogan, Margaret E., Ian E. Swift, and James Done. "Urease assay and ammonia release from leaf tissues." *Phytochemistry* 22, no. 3 (1983): 663-667.
- Jabri, Evelyn, Mann H. Lee, Robert P. Hausinger, and P. Andrew Karplus. "Preliminary crystallographic studies of urease from jack bean and from *Klebsiella aerogenes*." *Journal of molecular biology* 227, no. 3 (1992): 934-937.
- Jones, R. D., and Mary A. Hood. "Effects of temperature, pH, salinity, and inorganic nitrogen on the rate of ammonium oxidation by nitrifiers isolated from wetland environments." *Microbial Ecology* 6, no. 4 (1980): 339-347.
- Jones, Bradley D., and H. L. Mobley. "Proteus mirabilis urease: nucleotide sequence determination and comparison with jack bean urease." *Journal of bacteriology* 171, no. 12 (1989): 6414-6422.
- Karatas, I. (2008). *Microbiological Improvement of the Physical Properties of Soils*. PhD. Dissertation, Department of Civil, Environmental, and Sustainable Engineering Arizona State University, Tempe, AZ.
- Kavazanjian Jr, E., and Karatas, I. (2008). "Microbiological improvement of the Physical Properties of Soil," in *Proc. 6th Int. Conf. on Case Histories in Geotech. Engineering, Rolla, MO (CD-ROM)*.
- Kayastha, Arvind M., and Nilanjana Das. "A simple laboratory experiment for teaching enzyme immobilization with urease and its application in blood urea estimation." *Biochemical Education* 27, no. 2 (1999): 114-117.
- Kile, D. E., D. D. Eberl, A. R. Hoch, and M. M. Reddy. "An assessment of calcite crystal growth mechanisms based on crystal size distributions." *Geochimica et Cosmochimica Acta* 64, no. 17 (2000): 2937-2950.

- Kotlar, H. K., F. Haavind, M. Springer, S. S. Bekkelund, and O. Torsaeter. "A new concept of chemical sand consolidation: From idea and laboratory qualification to field application." In SPE Annu. Tech. Conf. Exhib., SPE, vol. 95723, pp. 9-12. 2005.
- Krogmeier, Michael J., Gregory W. McCarty, and John M. Bremner. "Phytotoxicity of foliar-applied urea." Proceedings of the National Academy of Sciences 86, no. 21 (1989): 8189-8191.
- Marzadori, Claudio, Silvia Miletta, Carlo Gessa, and Stefano Ciurli. "Immobilization of jack bean urease on hydroxyapatite: urease immobilization in alkaline soils." Soil Biology and Biochemistry 30, no. 12 (1998): 1485-1490.
- Meyer, F. D., S. Bang, S. Min, L. D. Stetler, and S. S. Bang. "Microbiologically-Induced Soil Stabilization: Application of *Sporosarcina pasteurii* for Fugitive Dust Control." In Geo-Frontiers 2011@ sAdvances in Geotechnical Engineering, pp. 4002-4011. ASCE, 2011.
- Nemati, M., E. A. Greene, and G. Voordouw. "Permeability profile modification using bacterially formed calcium carbonate: comparison with enzymic option." Process biochemistry 40, no. 2 (2005): 925-933.
- Nemati, M., and G. Voordouw. "Modification of porous media permeability, using calcium carbonate produced enzymatically in situ." Enzyme and Microbial Technology 33, no. 5 (2003): 635-642.
- Neupane, Debendra, Hideaki Yasuhara, Naoki Kinoshita, and Toshiyasu Unno. "Applicability of Enzymatic Calcium Carbonate Precipitation as a Soil-Strengthening Technique." Journal of Geotechnical and Geoenvironmental Engineering 139, no. 12 (2013a): 2201-2211.
- Neupane, D., H. Yasuhara, and N. Kinoshita. "Soil Improvement through Enzymatic Calcite Precipitation Technique: Small to Large Scale Experiments." International Journal of Landslide and Environment 1, no. 1 (2013b).
- Pettit, N. M., A. R. J. Smith, R. B. Freedman, and R. G. Burns. "Soil urease: activity, stability and kinetic properties." Soil Biology and Biochemistry 8, no. 6 (1976): 479-484.

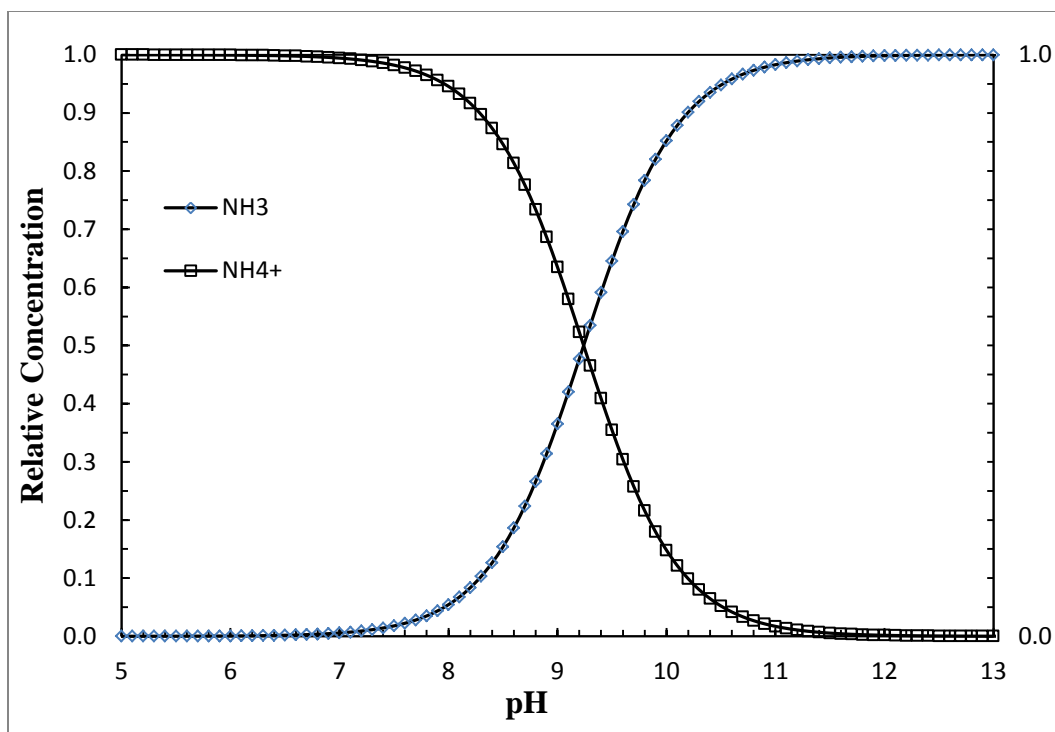
- Phoenix, V.R., Konhauser, K.O. (2008). "Benefits of bacterial biomineralization." *Geobiology*, Vol. 6: 303–308.
- Rebata-Landa, Veronica, and J. Carlos Santamarina. "Mechanical effects of biogenic nitrogen gas bubbles in soils." *Journal of Geotechnical and Geoenvironmental Engineering* 138, no. 2 (2012): 128-137.
- Rittmann, B. E. and P. L. McCarty (2001). *Environmental Biotechnology: Principles and Applications*. McGraw-Hill Book Co., New York.
- Rodriguez-Navarro, Carlos, Concepcion Jimenez-Lopez, Alejandro Rodriguez-Navarro, Maria Teresa Gonzalez-Muñoz, and Manuel Rodriguez-Gallego. "Bacterially mediated mineralization of vaterite." *Geochimica et Cosmochimica Acta* 71, no. 5 (2007): 1197-1213.
- Ruiz, G., D. Jeison, and R. Chamy. "Nitrification with high nitrite accumulation for the treatment of wastewater with high ammonia concentration." *Water Research* 37, no. 6 (2003): 1371-1377.
- Shimadzu Lab Note 42. Shimadzu Corporation. Kyoto, Japan
<http://www.shimadzu.com/an/hplc/support/lib/1ctalk/42lab.html>
- Shock, E.L. (2009). "Minerals as Energy Sources for Microorganisms." *Economic Geology*, Vol. 104, 1235–1248.
- Srivastava, Punit K., and Arvind M. Kayastha. "Characterization of gelatin-immobilized pigeonpea urease and preparation of a new urea biosensor." *Biotechnology and applied biochemistry* 34, no. 1 (2001): 55-62.
- Van Meurs, G., W. Van Der Zon, J. Lambert, D. Van Ree, V. S. Whiffin, and W. O. Molendijk. "The challenge to adapt soil properties." *Proceedings of the 5th ICEG: Environ. Geotechnics: Opportunities, Challenges and Responsibilities for Environmental Geotechnics* 2 (2006): 1192-1199.
- Van Oss, Hendrik, and Amy C. Padovani. "Cement manufacture and the environment." *Journal of Industrial Ecology* 6, no. 1 (2002): 89-106.
- van Paassen, L.A., Daza, C.M., Staal, M., Sorokin, D.Y., van Loosdrecht, M.C. (2008). In situ soil reinforcement by microbial denitrification. 1st Int. Conf. on Bio-Geo-Civil Engineering, Netherlands: 124-133, June 23-25.

- van Paassen, Leon A., Ranajit Ghose, Thomas JM van der Linden, Wouter RL van der Star, and Mark CM van Loosdrecht. "Quantifying biomediated ground improvement by ureolysis: large-scale biogROUT experiment." *Journal of geotechnical and geoenvironmental engineering* 136, no. 12 (2010): 1721-1728.
- Whiffin, V. (2004) *Microbial CaCO₃ precipitation for the production of biocement*, Ph.D. Dissertation, School of Biological Sciences and Biotechnology, Murdoch University, Australia, September.
- Whiffin, Victoria S., Leon A. van Paassen, and Marien P. Harkes. "Microbial carbonate precipitation as a soil improvement technique." *Geomicrobiology Journal* 24, no. 5 (2007): 417-423.
- Williams, D.A. Greely, Ronald. (2013) "NASA's Planetary Aeolian Laboratory: Exploring Aeolian Processes on Earth, Mars, and Titan." 44th Lunar and Planetary Science Conference.
- Yasuhara, Hideaki, Debendra Neupane, Kazuyuki Hayashi, and Mitsu Okamura. "Experiments and predictions of physical properties of sand cemented by enzymatically-induced carbonate precipitation." *Soils and Foundations* 52, no. 3 (2012): 539-549.
- Yasuhara, Hideaki and Hayashi, Kazuyuki. "Soil Improving Method." Japan Patent JP2011157700, issued August 2011.
- <http://www.sumobrain.com/patents/JP2011157700A.html>
- Warthmann, R., van Lith, Y., Vasconcelos, C., McKenzie, J.A., and Karpoff A.M. (2000). "Bacterially induced dolomite precipitation in anoxic culture experiments." *Geology*, Vol. 28(12):1091-1094.
- Zambelli, Barbara, Francesco Musiani, Stefano Benini, and Stefano Ciurli. "Chemistry of Ni²⁺ in urease: sensing, trafficking, and catalysis." *Accounts of chemical research* 44, no. 7 (2011): 520-530.
- Zhang, Yuping, and Richard Dawe. "The kinetics of calcite precipitation from a high salinity water." *Applied Geochemistry* 13, no. 2 (1998): 177-184.
- Zorlu, K., and Kasapoglu, K.E. (2009). "Determination of geomechanical properties and collapse potential of a caliche by in situ and laboratory tests." *Environmental Geology*, Vol. 56: 1449-1459.

Zuddas, Pierpaolo, and Alfonso Mucci. "Kinetics of calcite precipitation from seawater: II. The influence of the ionic strength." *Geochimica et Cosmochimica Acta* 62, no. 5 (1998): 757-766.

APPENDIX A

RELATIVE CONCENTRATIONS AND pH IN THE $\text{NH}_3\text{-NH}_4^+$ SYSTEM



pH	Fraction as NH ₃	Fraction as NH ₄ ⁺	pH	Fraction as NH ₃	Fraction as NH ₄ ⁺	pH	Fraction as NH ₃	Fraction as NH ₄ ⁺
0	5.754E-10	1.000E+00	2.7	2.884E-07	1.000E+00	5.4	1.445E-04	9.999E-01
0.1	7.244E-10	1.000E+00	2.8	3.631E-07	1.000E+00	5.5	1.819E-04	9.998E-01
0.2	9.120E-10	1.000E+00	2.9	4.571E-07	1.000E+00	5.6	2.290E-04	9.998E-01
0.3	1.148E-09	1.000E+00	3	5.754E-07	1.000E+00	5.7	2.883E-04	9.997E-01
0.4	1.445E-09	1.000E+00	3.1	7.244E-07	1.000E+00	5.8	3.629E-04	9.996E-01
0.5	1.820E-09	1.000E+00	3.2	9.120E-07	1.000E+00	5.9	4.569E-04	9.995E-01
0.6	2.291E-09	1.000E+00	3.3	1.148E-06	1.000E+00	6	5.751E-04	9.994E-01
0.7	2.884E-09	1.000E+00	3.4	1.445E-06	1.000E+00	6.1	7.239E-04	9.993E-01
0.8	3.631E-09	1.000E+00	3.5	1.820E-06	1.000E+00	6.2	9.112E-04	9.991E-01
0.9	4.571E-09	1.000E+00	3.6	2.291E-06	1.000E+00	6.3	1.147E-03	9.989E-01
1	5.754E-09	1.000E+00	3.7	2.884E-06	1.000E+00	6.4	1.443E-03	9.986E-01
1.1	7.244E-09	1.000E+00	3.8	3.631E-06	1.000E+00	6.5	1.816E-03	9.982E-01
1.2	9.120E-09	1.000E+00	3.9	4.571E-06	1.000E+00	6.6	2.286E-03	9.977E-01
1.3	1.148E-08	1.000E+00	4	5.754E-06	1.000E+00	6.7	2.876E-03	9.971E-01
1.4	1.445E-08	1.000E+00	4.1	7.244E-06	1.000E+00	6.8	3.618E-03	9.964E-01
1.5	1.820E-08	1.000E+00	4.2	9.120E-06	1.000E+00	6.9	4.550E-03	9.954E-01
1.6	2.291E-08	1.000E+00	4.3	1.148E-05	1.000E+00	7	5.721E-03	9.943E-01
1.7	2.884E-08	1.000E+00	4.4	1.445E-05	1.000E+00	7.1	7.192E-03	9.928E-01

1.8	3.631E-08	1.000E+00	4.5	1.820E-05	1.000E+00	7.2	9.038E-03	9.910E-01
1.9	4.571E-08	1.000E+00	4.6	2.291E-05	1.000E+00	7.3	1.135E-02	9.886E-01
2	5.754E-08	1.000E+00	4.7	2.884E-05	1.000E+00	7.4	1.425E-02	9.858E-01
2.1	7.244E-08	1.000E+00	4.8	3.631E-05	1.000E+00	7.5	1.787E-02	9.821E-01
2.2	9.120E-08	1.000E+00	4.9	4.571E-05	1.000E+00	7.6	2.240E-02	9.776E-01
2.3	1.148E-07	1.000E+00	5	5.754E-05	9.999E-01	7.7	2.803E-02	9.720E-01
2.4	1.445E-07	1.000E+00	5.1	7.244E-05	9.999E-01	7.8	3.504E-02	9.650E-01
2.5	1.820E-07	1.000E+00	5.2	9.119E-05	9.999E-01	7.9	4.371E-02	9.563E-01
2.6	2.291E-07	1.000E+00	5.3	1.148E-04	9.999E-01	8	5.441E-02	9.456E-01

pH	Fraction as NH3	Fraction as NH ₄ ⁺	pH	Fraction as NH3	Fraction as NH ₄ ⁺	pH	Fraction as NH3	Fraction as NH ₄ ⁺
8.1	6.755E-02	9.324E-01	10.8	9.732E-01	2.680E-02	13.5	9.999E-01	5.495E-05
8.2	8.358E-02	9.164E-01	10.9	9.786E-01	2.141E-02	13.6	1.000E+00	4.365E-05
8.3	1.030E-01	8.970E-01	11	9.829E-01	1.708E-02	13.7	1.000E+00	3.467E-05
8.4	1.263E-01	8.737E-01	11.1	9.864E-01	1.362E-02	13.8	1.000E+00	2.754E-05
8.5	1.540E-01	8.460E-01	11.2	9.892E-01	1.085E-02	13.9	1.000E+00	2.188E-05
8.6	1.864E-01	8.136E-01	11.3	9.914E-01	8.634E-03	14	1.000E+00	1.738E-05
8.7	2.238E-01	7.762E-01	11.4	9.931E-01	6.871E-03			
8.8	2.664E-01	7.336E-01	11.5	9.945E-01	5.465E-03			
8.9	3.137E-01	6.863E-01	11.6	9.957E-01	4.346E-03			
9	3.653E-01	6.347E-01	11.7	9.965E-01	3.455E-03			
9.1	4.201E-01	5.799E-01	11.8	9.973E-01	2.747E-03			
9.2	4.770E-01	5.230E-01	11.9	9.978E-01	2.183E-03			
9.3	5.345E-01	4.655E-01	12	9.983E-01	1.735E-03			
9.4	5.911E-01	4.089E-01	12.1	9.986E-01	1.378E-03			
9.5	6.454E-01	3.546E-01	12.2	9.989E-01	1.095E-03			
9.6	6.961E-01	3.039E-01	12.3	9.991E-01	8.702E-04			
9.7	7.425E-01	2.575E-01	12.4	9.993E-01	6.914E-04			
9.8	7.841E-01	2.159E-01	12.5	9.995E-01	5.492E-04			
9.9	8.205E-01	1.795E-01	12.6	9.996E-01	4.363E-04			
10	8.519E-01	1.481E-01	12.7	9.997E-01	3.466E-04			
10.1	8.787E-01	1.213E-01	12.8	9.997E-01	2.753E-04			
10.2	9.012E-01	9.881E-02	12.9	9.998E-01	2.187E-04			
10.3	9.199E-01	8.012E-02	13	9.998E-01	1.737E-04			
10.4	9.353E-01	6.471E-02	13.1	9.999E-01	1.380E-04			
10.5	9.479E-01	5.209E-02	13.2	9.999E-01	1.096E-04			
10.6	9.582E-01	4.183E-02	13.3	9.999E-01	8.709E-05			
10.7	9.665E-01	3.351E-02	13.4	9.999E-01	6.918E-05			

APPENDIX B

SOIL PROPERTIES FOR F-60 SAND

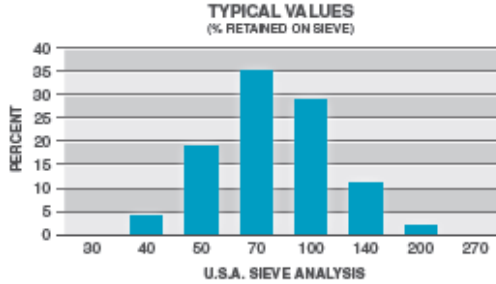
Product Data



F-60

UNGROUND SILICA

PLANT: OTTAWA, ILLINOIS



USA STD SIEVE SIZE		TYPICAL VALUES		
MESH	MILLIMETERS	% RETAINED		% PASSING
		INDIVIDUAL	CUMULATIVE	CUMULATIVE
30	0.600	0.0	0.0	100.0
40	0.425	4.0	4.0	96.0
50	0.300	19.0	23.0	77.0
70	0.212	35.0	58.0	42.0
100	0.150	29.0	87.0	13.0
140	0.106	11.0	98.0	2.0
200	0.075	2.0	100.0	0.0
270	0.053	0.0		

TYPICAL PHYSICAL PROPERTIES	
AFS TM Acid Demand (@pH 7)	<1.0
AFS TM Grain Fineness	60
Color	White
Grain Shape	Round
Hardness (Mohs)	7
Melting Point (Degrees F)	3100
Mineral	Quartz
Moisture Content (%)	<0.05
pH	7
Specific Gravity	2.65

(1) American Foundrymen's Society

TYPICAL CHEMICAL ANALYSIS, %	
SiO ₂ (Silicon Dioxide)	99.8
Fe ₂ O ₃ (Iron Oxide)	0.020
Al ₂ O ₃ (Aluminum Oxide)	0.06
TiO ₂ (Titanium Dioxide)	0.01
CaO (Calcium Oxide)	<0.01
MgO (Magnesium Oxide)	<0.01
Na ₂ O (Sodium Oxide)	<0.01
K ₂ O (Potassium Oxide)	<0.01
LOI (Loss On Ignition)	0.1

December 15, 1997

U.S. Silica Company
8490 Progress Drive, Suite 300
Frederick, MD 21701
(301) 682-0600 (phone)
(800) 249-7500 (toll-free)
ussilica.com

DISCLAIMER: The information set forth in this Product Data Sheet represents typical properties of the product described; the information and the typical values are not specifications. U.S. Silica Company makes no representation or warranty concerning the Products, expressed or implied, by this Product Data Sheet.

WARNING: The product contains crystalline silica – quartz, which can cause silicosis (an occupational lung disease) and lung cancer. For detailed information on the potential health effect of crystalline silica - quartz, see the U.S. Silica Company Material Safety Data Sheet.



APPENDIX C

SOIL PROPERTIES FOR 20-30 SAND



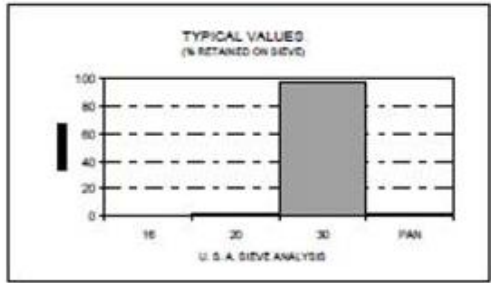
PRODUCT DATA

ASTM⁽¹⁾ 20/30

UNGROUND SILICA

PLANT: OTTAWA, ILLINOIS

(1) AMERICAN SOCIETY FOR TESTING AND MATERIALS



USA STD SIEVE SIZE		TYPICAL VALUES		
MESH	MILLIMETERS	% RETAINED		% PASSING
		INDIVIDUAL	CUMULATIVE	CUMULATIVE
16	1.180	0.0	0.0	100.0
20	0.850	1.0	1.0	99.0
30	0.600	97.0	98.0	2.0
PAN		2.0	100.0	0.0

TYPICAL PROPERTIES

COLOR WHITE
 GRAIN SHAPE ROUND
 HARDNESS (Mohs) 7
 MELTING POINT (Degrees F) 3100
 MINERAL QUARTZ
 pH 7
 SPECIFIC GRAVITY 2.65

TYPICAL CHEMICAL ANALYSIS, %

SiO₂ (Silicon Dioxide) 99.8
 Fe₂O₃ (Iron Oxide) 0.020
 Al₂O₃ (Aluminum Oxide) 0.06
 TiO₂ (Titanium Dioxide) 0.01
 CaO (Calcium Oxide) <0.01
 MgO (Magnesium Oxide) <0.01
 Na₂O (Sodium Oxide) <0.01
 K₂O (Potassium Oxide) <0.01
 LOI (Loss On Ignition) 0.1

CONFORMS TO ASTM C778

December 15, 1997

DISCLAIMER: The information set forth in this Product Data Sheet represents typical properties of the product described; the information and the typical values are not specifications. U.S. Silica Company makes no representation or warranty concerning the Products, expressed or implied, by this Product Data Sheet.

WARNING: The product contains crystalline silica - quartz, which can cause silicosis (an occupational lung disease) and lung cancer. For detailed information on the potential health effect of crystalline silica - quartz, see the U.S. Silica Company Material Safety Data Sheet.

U.S. Silica Company

P.O. Box 187, Berkeley Springs, WV 25411-0187

(304) 258-2500